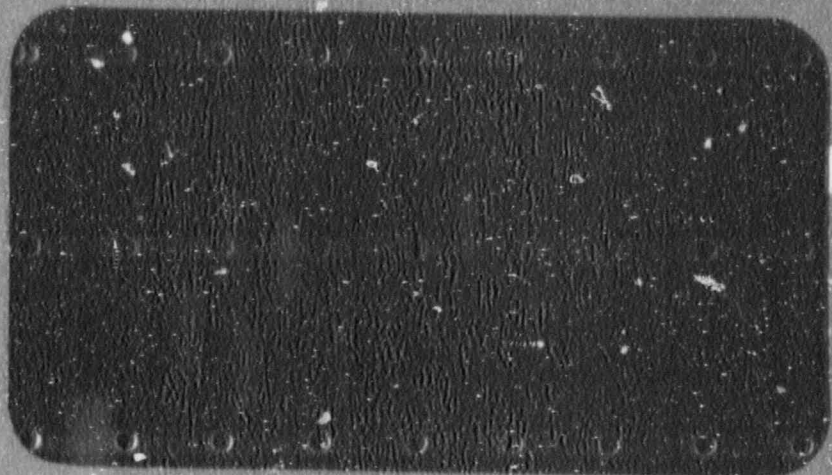


FOR UNRESTRICTED DISTRIBUTION
DATE _____ WEC



Westinghouse Energy Systems



9101290168 910118
FDR. ADOCK 05000334
01/11/11 PDR

Westinghouse Energy Systems



9101290168 710118
PDR ADOCK 05000334
Q PIR

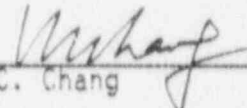
WCAP 12728

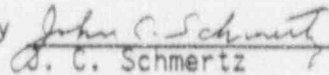
EVALUATION OF THERMAL STRATIFICATION
FOR THE BEAVER VALLEY UNIT 1
PRESSURIZER SURGE LINE

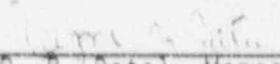
NOVEMBER 1990

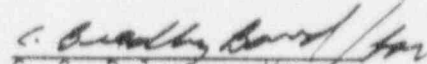
T. H. Liu
L. M. Valasek
E. L. Cranford

F. J. Witt
S. Tandon
J. F. Petsche

Verified by 
K. C. Chang

Verified by 
D. C. Schmertz

Approved by 
R. B. Patel, Manager
System Structural Analysis

Approved by 
S. S. Palusamy, Manager
Diagnostics and Monitoring
Technology

WESTINGHOUSE ELECTRIC CORPORATION
Nuclear and Advanced Technology Division
P.O. Box 2728
Pittsburgh, Pennsylvania 15230-2728

© 1990 Westinghouse Electric Corp.

TABLE OF CONTENTS

Section	Title	Page
	EXECUTIVE SUMMARY	xvii
1.0	INTRODUCTION AND UPDATE OF DESIGN TRANSIENTS	1-1
1.1	Introduction	1-1
1.1.1	System Description	1-1
1.1.2	Thermal Stratification in the Surge Line	1-2
1.1.3	Surge Line Stratification Program	1-3
1.2	Update of Design Transients	1-4
1.2.1	System Design Information	1-4
1.2.2	Stratification Effects Criteria	1-5
1.2.3	Plant Monitoring	1-5
1.2.4	Heat Transfer and Stress Analysis	1-6
1.2.5	Stratification Profiles	1-7
1.2.6	Development of Conservative Normal and Upset Transients	1-7
1.2.7	Temperature Limitations During Heatup and Cooldown	1-8
1.2.8	Historical Data	1-8
1.2.9	Development of Heatup and Cooldown Design Transients With Stratification	1-9
1.2.9.1	[] ^{a,c,e} Transients	1-10
1.2.9.2	Fluctuation Transients	1-14
1.2.9.3	Transient Basis Exceedances	1-14
1.2.10	Striping Transients	1-14
1.3	Conclusions	1-15
2.0	STRESS ANALYSES	2-1
2.1	Piping System Structural Analysis	2-1
2.1.1	Introduction	2-1
2.1.2	Discussion	2-2

TABLE OF CONTENTS (cont.)

Section	Title	Page
	2.1.3 Results from Beaver Valley Unit 1 Analysis	2-5
	2.1.4 Conclusions	2-5
2.2	Local Stress Due to Non-Linear Thermal Gradient	2-6
	2.2.1 Explanation of Local Stress	2-6
	2.2.2 Superposition of Local and Structural Stresses	2-6
	2.2.3 Finite Element Model of Pipe for Local Stress	2-7
	2.2.4 Pipe Local Stress Results	2-7
	2.2.5 Unit Structural Load Analyses For Pipe	2-8
	2.2.6 RCL Hot Leg Nozzle Analysis	2-8
	2.2.7 Conservatism	2-9
2.3	Thermal Striping	2-9
	2.3.1 Background	2-9
	2.3.2 Thermal Striping Stresses	2-9
	2.3.3 Factors Which Affect Striping Stress	2-10
	2.3.4 Conservatism	2-12
3.0	ASME SECTION III FATIGUE USAGE FACTOR EVALUATION	3-1
3.1	Code and Criteria	3-1
3.2	Analysis for Thermal Stratification	3-1
	3.2.1 Stress Input	3-1
	3.2.2 Classification and Combination of Stresses	3-2
	3.2.3 Cumulative Fatigue Usage Factor Evaluation	3-2
	3.2.4 Simplified Elastic-Plastic Analysis	3-3
	3.2.5 Fatigue Usage Results	3-4
3.3	Conservatism in Fatigue Usage Calculation	3-4
3.4	References	3-5

TABLE OF CONTENTS (cont.)

Section	Title	Page
4.0	FATIGUE CRACK GROWTH EVALUATION	4-1
4.1	Introduction	4-1
4.2	Initial Flaw Size	4-2
4.3	Critical Locations for FCG	4-2
4.4	Results of FCG Analysis	4-3
4.5	References	4-3
5.0	ASSESSMENT OF LEAK-BEFORE-BREAK	5-1
5.1	Background	5-1
5.2	Methodology	5-1
5.3	Material and Fracture Toughness Properties	5-1
5.4	Loading Conditions	5-2
5.5	Results	5-3
5.6	Conclusions	5-4
5.7	References	5-4
6.0	CONCLUSIONS	6-1
	APPENDIX A - LIST OF COMPUTER PROGRAMS	A-1
	APPENDIX B - FATIGUE CYCLE APPROACH VS. DESIGN TRANSIENTS	B-1

LIST OF TABLES

Table	Title	Page
1-1	IMPORTANT DIMENSIONLESS GROUPS FOR SIMILITUDE IN HYDRODYNAMIC TESTING	1-16
1-2	STRATIFICATION POTENTIAL BASED ON RICHARDSON NUMBER	1-17
1-3	NOTES FOR TRANSIENT DEVELOPMENT FLOW CHART	1-18
1-4	SURGE LINE TRANSIENTS WITH STRATIFICATION HEATUP (H) AND COOLDOWN (C) - 200 CYCLES TOTAL	1-21
1-5	SURGE LINE TRANSIENTS WITH STRATIFICATION NORMAL AND UPSET TRANSIENT LIST	1-23
1-6	STRATIFICATION PROFILES	1-25
1-7	HEATUP - COOLDOWN TRANSIENTS	1-26
1-8	DESIGN TRANSIENTS WITH STRATIFICATION	1-27
1-9	PLANT OPERATIONAL CONSTRAINTS	1-28
1-10	OPERATIONS SURVEY	1-29
1-11	HEATUP DATA SUMMARY (PZR - HOT LEG) TEMP. DIFFERENCE AND TIME DURATION FOR EACH PHASE	1-30
1-12	COOLDOWN DATA SUMMARY (PZR - HOT LEG) TEMP. DIFFERENCE AND TIME DURATION FOR EACH PHASE	1-31
1-13	TRANSIENT TYPES	1-32
1-14	SUMMARY OF FATIGUE CYCLES FROM [] ^{a,c,e}	1-33
1-15	SUMMARY OF PLANT MONITORING TRANSIENTS WITH STRENGTH OF STRATIFICATION (RSS)	1-34
1-16	SUMMARY OF MONITORED TRANSIENT CYCLES (ONE HEATUP)	1-36
1-17	SUMMARY OF % TIMES AT MAXIMUM TEMPERATURE POTENTIAL $RMTP_K$	1-37
1-18	SURGE LINE TRANSIENTS - STRIPING LOADS FOR HEATUP (H) AND COOLDOWN (C)	1-38

LIST OF TABLES (cont.)

Table	Title	Page
2-1	COMPARISON OF WECAN AND ANSYS RESULTS FOR LINEAR STRATIFICATION - Case 2	2-13
2-2	COMPARISON OF WECAN [] ^{a,c,e} AND ANSYS [] ^{a,c,e} RESULTS FOR CASE 3	2-14
2-3	TEMPERATURE PROFILES IN PRESSURIZER SURGE LINE	2-15
2-4	BEAVER VALLEY SURGE LINE MAXIMUM LOCAL AXIAL STRESSES AT [] ^{a,c,e}	2-16
2-5	SUMMARY OF LOCAL STRATIFICATION STRESSES IN THE SURGE LINE RCL NOZZLE	2-17
2-6	SUMMARY OF PRESSURE AND BENDING INDUCED STRESSES IN THE SURGE LINE RCL NOZZLE FOR UNIT LOAD CASES	2-18
2-7	STRIPING FREQUENCY AT 2 MAXIMUM LOCATIONS FROM 15 TEST RUNS	2-19
3-1	CODE/CRITERIA	3-6
4-1	FATIGUE CRACK GROWTH RESULTS FOR 10% WALL INITIAL FLAW SIZE	4-4
5-1	STEPS IN A LEAK-BEFORE-BREAK ANALYSIS	5-6
5-2	LBB CONSERVATISMS	5-7
5-3	ROOM TEMPERATURE MECHANICAL PROPERTIES OF THE PRESSURIZER SURGE LINE MATERIALS AND WELDS OF THE BEAVER VALLEY UNIT 1 PLANT	5-8
5-4	TENSILE PROPERTIES FOR THE SURGE LINE MATERIAL AT 135°F AND 653°F	5-9
5-5	FRACTURE TOUGHNESS PROPERTIES FOR 316 STAINLESS STEELS AND WELDS	5-10
5-6	TYPES OF LOADINGS	5-11
5-7	NORMAL AND FAULTED LOADING CASES FOR LBB EVALUATIONS	5-12
5-8	ASSOCIATED LOAD CASES FOR ANALYSES	5-13
5-9	SUMMARY OF LOADS AND STRESSES AT THE CRITICAL LOCATIONS	5-14
5-10	LOAD CASES, LOCATION AND TEMPERATURES CONSIDERED FOR LEAK-BEFORE-BREAK EVALUATIONS	5-15

LIST OF TABLES (cont.)

Table	Title	Page
5-11	LEAKAGE FLAWS FOR THE LEAK-BEFORE-BREAK ANALYSES	5-16
5-12	RESULTS OF STABILITY EVALUATION	5-17

LIST OF FIGURES

Figure	Title	Page
1	Determination of the Effects of Thermal Stratification	xxii
1-1	Simplified Diagram of the NSSS	1-39
1-2	Reactor Coolant System Flow Diagram (Typical Loop)	1-40
1-3	RCS Pressurizer	1-41
1-4	Estimate of Flow Stratification Pattern in Elbow Under Pressurizer	1-42
1-5	Transient Development Flow Chart	1-43
1-6	Beaver Valley Pressurizer Surge Line Monitoring Locations	1-44
1-7	Plant A Pressurizer Surge Line Monitoring Locations	1-45
1-8	Plant B Pressurizer Surge Line Monitoring Locations	1-46
1-9	Plant C Pressurizer Surge Line Monitoring Locations	1-47
1-10	Temperature Profile (6.5-inch ID Pipe)	1-48
1-11	Dimensionless Temperature Profile (14.3-inch ID Pipe)	1-49
1-12	Surge Line Stratification	1-50
1-13	Surge Line Hot-Cold Interface Locations	1-51
1-14	Hot-Cold Interface Location From Temperature Measurements	1-52
1-15	Inadvertant RCS Depressurization ($\Delta T = 260^\circ F$ in Surge Line)	1-53
1-16	Steam Bubble Mode Heatup	1-54
1-17	Steam Bubble Mode Cooldown	1-55
1-18	Heatup [] ^{a,c,e}	1-56
1-19	Cooldown [] ^{a,c,e}	1-57
1-20	Heatup [] ^{a,c,e}	1-58
1-21	Cooldown [] ^{a,c,e}	1-59
1-22	Heatup [] ^{a,c,e}	1-60

LIST OF FIGURES (cont.)

Figure	Title	Page
1-23	Cooldown [] ^{a,c,e}	1-61
1-24	Heatup [] ^{a,c,e}	1-62
1-25	Cooldown [] ^{a,c,e}	1-63
1-26	Heatup [] ^{a,c,e}	1-64
1-27	Cooldown [] ^{a,c,e}	1-65
1-28	[] ^{a,c,e} Location 1 - Heatup (4 days)	1-66
1-29	[] ^{a,c,e} Location 2 - Heatup (11 Days)	1-67
1-30	[] ^{a,c,e} Location 1 - Heatup (7 Days)	1-68
1-31	[] ^{a,c,e} Location 1 Fatigue Cycles - Heatup (11 Days)	1-69
1-32	Plant C Location #1 (3 Days)	1-70
1-33	Comparison of Design to Monitored Transients	1-71
1-34	Comparison of Design to Monitored Transients	1-72
2-1	Determination of the Effects of Thermal Stratification	2-20
2-2	Stress Analysis	2-21
2-3	Typical Pressurizer Surge Line Layout	2-22
2-4	Cases 1 to 4: Radial Temperature Profiles	2-23
2-5	Case 5: Radial and Axial Temperature Profile	2-24
2-6	Finite Element Model of the Pressurizer Surge Line Piping General View	2-25
2-7	Finite Element Model of the Pressurizer Surge Line Piping Hot Leg Nozzle Detail	2-26
2-8	Thermal Expansion of the Pressurizer Surge Line Under Uniform Temperature	2-27
2-9	Case 2 (linear) Temperature Profile at Hot Leg Nozzle	2-28
2-10	Case 2 (linear) Temperature Profile at Pressurizer Elbow	2-29

LIST OF FIGURES (cont.)

Figure	Title	Page
2-11	Thermal Expansion of Pressurizer Surge Line Under Linear Temperature Gradient	2-30
2-12	Bowing of Beams Subject to Top-to-Bottom Temperature Gradient	2-31
2-13	Case 3 (Mid-Plane Step): Temperature Profile at Hot Leg Nozzle	2-32
2-14	Case 3 (Mid-Plane Step): Temperature Profile at Pressurizer Nozzle	2-33
2-15	Case 4 (Top Half Step): Temperature Profile at Hot Leg Nozzle	2-34
2-16	Case 4 (Top Half Step): Temperature Profile at Pressurizer Elbow	2-35
2-17	Case 5: Axial and Radial Temperature Profile	2-36
2-18	Case 5: Axial and Radial Temperature Profile at Hot Leg Nozzle	2-37
2-19	Case 5: Axial and Radial Temperature Profile at Pipe Bend	2-38
2-20	Case 5: Axial and Radial Temperature Profile at Pressurizer Elbow	2-39
2-21	[] ^{a,c,e} Profile	2-40
2-22	Beaver Valley Unit 1 Pressurizer Surge Line	2-41
2-23	Conclusions - Global Stress Analysis	2-42
2-24	Local Stress in Piping Due to Thermal Stratification	2-43
2-25	Independence of Local and Structural Thermal Stratification Stresses Permits Combination by Superposition	2-44
2-26	Test Case for Superposition of Local and Structural Stresses	2-45
2-27	Local Stress - Finite Element Models/Loading	2-46
2-28	Piping Local Stress Model and Thermal Boundary Conditions	2-47
2-29	Surge Line Temperature Distribution at [] ^{a,c,e} Axial Locations	2-48
2-30	Surge Line Local Axial Stress Distribution at [] ^{a,c,e} Axial Locations	2-49

LIST OF FIGURES (cont.)

Figure	Title	Page
2-31	Surge Line Local Axial Stress on Inside Surface at [] ^{a,c,e} Axial Locations	2-50
2-32	Surge Line Local Axial Stress on Outside Surface at [] ^{a,c,e} Axial Locations	2-51
2-33	Surge Line Temperature Distribution at Location [] ^{a,c,e}	2-52
2-34	Surge Line Local Axial Stress Distribution at Location [] ^{a,c,e}	2-53
2-35	Surge Line Temperature Distribution at Location [] ^{a,c,e}	2-54
2-36	Surge Line Local Axial Stress Distribution at Location [] ^{a,c,e}	2-55
2-37	Surge Line Temperature Distribution at Location [] ^{a,c,e}	2-56
2-38	Surge Line Local Axial Stress Distribution at Location [] ^{a,c,e}	2-57
2-39	Surge Line Temperature Distribution at Location [] ^{a,c,e}	2-58
2-40	Surge Line Local Axial Stress Distribution at Location [] ^{a,c,e}	2-59
2-41	Surge Line Temperature Distribution at Location [] ^{a,c,e}	2-60
2-42	Surge Line Local Axial Stress Distribution at Location [] ^{a,c,e}	2-61
2-43	Surge Line RCL Nozzle 3-D WECAN Model #1	2-62
2-44	Surge Line RCL Nozzle 3-D WECAN Model #2	2-63
2-45	Hot Leg Nozzle Stress Analysis	2-64
2-46	Surge Line Nozzle Temperature Profile Due to Thermal Stratification	2-65
2-47	Surge Line Nozzle Stress Intensity Due to Thermal Stratification	2-66
2-48	Surge Line Nozzle Stress in Direction Axial to Surge Line Due to Thermal Stratification	2-67

LIST OF FIGURES (cont.)

Figure	Title	Page
2-49	Surge Line Nozzle Stress Intensity Due to Pressure	2-68
2-50	Surge Line Nozzle Stress Intensity Due to Pressure	2-69
2-51	Surge Line Nozzle Stress Intensity Due to Bending	2-70
2-52	Surge Line Nozzle Stress in Direction Axial to Surge Line Due to Bending Showing Magnified Displacement	2-71
2-53	Surge Line Nozzle Stress Intensity Due to Bending Showing Magnified Displacement	2-72
2-54	Surge Line Nozzle Stress Intensity Due to Bending	2-73
2-55	Results	2-74
2-56	Local Stress Conservatism	2-75
2-57	Background - Thermal Striping Analysis	2-76
2-58	Thermal Striping Fluctuation	2-77
2-59	Stratification and Striping Test Models	2-78
2-60	Thermal Striping Temperature Distribution	2-79
2-61	Striping Finite Element Model	2-80
2-62	Thermal Striping Stresses	2-81
2-63	Factors Affecting Thermal Striping Stress	2-82
2-64	Attenuation of Thermal Striping Potential by Molecular Conduction (Interface Wave Height of [$\lambda_{a,c,e}$])	2-83
2-65	Conservatisms in Thermal Striping Analysis	2-84
4-1	Determination of the Effects of Thermal Stratification on Fatigue Crack Growth	4-5
4-2	Fatigue Crack Growth Methodology	4-6
4-3	Aspects of the Fatigue Crack Growth Evaluation	4-7
4-4	Fatigue Crack Growth Rate Curve for Austenitic Stainless Steel	4-8
4-5	Fatigue Crack Growth Equation for Austenitic Stainless Steel	4-9
4-6	Fatigue Crack Growth Critical Locations	4-10

LIST OF FIGURES (cont.)

Figure	Title	Page
4-7	Fatigue Crack Growth Controlling Positions at Each Location	4-11
4-8	Fatigue Crack Growth Conservatism	4-12
5-1	Minimum True Stress-True Strain Curve for 316 Stainless Steel at 653°F	5-18
5-2	Minimum True Stress-True Strain Curve for 316 Stainless Steel at 135°F	5-19
5-3	Sketch of Analysis Model for Beaver Valley Unit 1 Pressurizer Surge Line Showing Node Points, Critical Locations, Weld Locations and Type of Welds	5-20
B-1	[] ^{a,c,e} , Location 1, Observed Transients	B-2
B-2	Typical Heatup Design Transient Distribution Applied To One Heatup Cycle	B-3
B-3	[] ^{a,c,e}	B-4

EXECUTIVE SUMMARY

The pressurizer of a Westinghouse type pressurized water reactor maintains and controls pressure in the reactor coolant system (RCS) via the pressurizer surge line which connects to a hot leg of the primary loop. The pressure is maintained such that boiling is suppressed and departure from nucleate boiling is prevented.

The flow path for a typical reactor coolant loop is from the reactor vessel to the inlet plenum of the steam generator. High temperature reactor coolant flows through the U-tubes in the steam generator, transferring heat to the secondary water, out of the tubes into the outlet plenum to the suction of the reactor coolant pump. The reactor coolant pump increases the pressure head of the reactor coolant which flows back to the reactor vessel.

The pressurizer vessel contains steam and water at saturated conditions with the steam-water interface level between 25 and 60% depending on the plant operating conditions. From the time the steam bubble is initially drawn during the heatup operation to hot standby conditions, the level is maintained at approximately 25%. During power ascension, the level is increased to approximately 60%.

Investigations of primary coolant water flow into and out of the pressurizer have shown that significant temperature differences may exist in the surge line from end-to-end and from top-to-bottom during heatup or cooldown. Unanticipated large surge line pipe displacements have been experienced and temperature differences exceeding 250°F in a pipe cross section have been noted. Thermal stratification (layering of different temperature water) has been measured over significant time periods. The unexpected magnitudes of the pipe displacements and temperature differences exceed those defined in the design transients, suggesting that thermal design transients should be updated to incorporate the effects of the stratification. Such an update is performed for Beaver Valley Unit 1 in this report and the structural response is evaluated. A similar evaluation has been performed for Beaver Valley Unit 2 as documented in WCAP-12093 and WCAP-12093 Supplements 1, 2 and 3.

Of particular significance to surge line stratification are the normal charging and letdown function provided by the Chemical and Volume Control System and the suction and return lines associated with the Residual Heat Removal System (RHRS). The former directly controls the RCS mass inventory and therefore affects flow in the surge line. The RHRS is used to remove heat from the RCS and thereby influences coolant temperature and consequently coolant volume through thermal expansion and contraction.

Other systems which affect surge line flow conditions are main spray flow supplied to the pressurizer from one or two cold legs and the pressurizer electric heaters. Spray operation does not significantly alter the total RCS mass inventory but does reduce system pressure by condensing some of the steam in the pressurizer. The pressurizer heaters, when energized, generate steam and, as a result, increase RCS pressure.

Thermal stratification in the pressurizer surge line is the direct result of the difference in densities between the pressurizer water and the generally cooler hot leg water. The lighter pressurizer water tends to float on the cooler heavier hot leg water. The potential for stratification is increased as the difference in temperature between the pressurizer and the hot leg increases and as the insurge or outsurge flow rates decrease.

At power, when the difference in temperature between pressurizer and hot leg is relatively small (less than 50°F) the extent and effects of stratification have been observed to be small. However, during certain modes of plant heatup and cooldown, this difference in temperature can be relatively large end-to-end, in which case the effects of stratification must be accounted for. A diagram of the approach taken to evaluate significant stratification is given in figure 1.

A rather extensive data base has been obtained by pressurizer surge line transient monitoring including results from the Beaver Valley Unit 1 plant. The data consist of pressures, displacements, operational status and temperature monitored along the surge line. The most relevant data are those associated with heatup and cooldown.

An extensive study was made of the available data base. From this study a set of conservative design transients was developed which incorporated the characteristics of thermal stratification in the pressurizer surge line. This set formed the basis for the stress and fatigue analyses and the leak-before-break evaluation summarized below.

The stress analyses were performed in three steps. Finite element structural or system stress analyses were made to determine pipe displacements, support reaction loads and force and moment loads. These loads were used as input to the fatigue, fatigue crack growth and leak-before-break evaluations. Both axial and radial variations in the pipe metal temperatures were included as appropriate. Specifically, eleven cases of thermal stratification were analyzed reflecting temperature differences in the surge line up to 335°F. Stratification at operating temperatures as well as heatup and cooldown temperatures was analyzed consistent with the observed thermal stratification data. The loads were found to be acceptable for all design conditions including the updated transients to account for thermal stratification.

Local stresses were calculated for the top-to-bottom non-linear thermal gradients in the surge line at the most critical locations which represent a bounding of hot-to-cold interface levels as implied from the test observations. Three-dimensional finite element models of both pipe and nozzles were used.

The total stress is required for the fatigue analyses. Such stresses were found by superposition of the structural stresses and the local stresses.

Thermal striping due to the oscillation of the hot and cold stratified boundary was also evaluated. The concern is with the stresses due to the differences between the pipe inside surface wall temperatures and the average through wall temperature. Finite element analyses were also made for this case. The ASME Section III fatigue usage factor due to thermal striping alone was found to be well below the ASME Section III code criterion of 1.

Fatigue usage factors were evaluated based on Section III of the ASME Code for the total stresses using the updated design cycles which includes the effect of stratification. Due to the non-axisymmetric nature of the stratification loading, stresses due to all loadings were obtained from finite element analysis and then combined on a stress component basis. Peak stresses were calculated for each transient. The combined usage factor was less than the ASME Section III code criterion of 1. Five events exceeding a system ΔT of 320°F were included in the analysis.

The above usage factors do not include the effects of striping. Because the nature of striping damage is at a much higher frequency, varies in location due to fluid level changes and is maximized at a different location than the ASME usage factor, it was assumed to be more appropriate to determine a total usage factor by conservatively adding the above calculated usage factors and the striping usage factors. This gave a maximum total usage factor which is still less than the ASME Code allowable of 1.0.

To determine the sensitivity of the pressurizer surge line to the presence of small cracks when subjected to the updated transients, fatigue crack growth analyses were performed. Various initial surface flaws were assumed to exist. The flaws were assumed to be semi-elliptical with a six-to-one aspect ratio. The largest initial flaw assumed to exist was one with a depth equal to 10% of the wall thickness, the maximum flaw size that could be found acceptable by Section XI of the ASME code. There is currently no fatigue crack growth rate curve in the ASME Code for austenitic stainless steels in a water environment. However, the fatigue crack growth curve for austenitic stainless steel used in the analyses is the one currently in the 1989 Edition of Section XI of the ASME Code for an air environment.

The locations, representative of all cross-sections of the surge line where thermal stratification could occur, were evaluated for fatigue crack growth. The transients exceeding a system ΔT of 320°F were included in the analysis. The maximum growth of a flaw assumed initially to have a depth of 10% of the wall was seen to remain well below one-half the wall for full service life.

A leak-before-break analysis was performed for the surge line of Beaver Valley Unit 1. Particular attention was given to thermal stratification which changes the operating loads somewhat and imposes large bending stresses during the lower temperature heatup and cooldown conditions.

Seven separate leak-before-break evaluations were performed to envelop the stress states due to thermal stratification. The temperature for the evaluations ranged from 135°F to 653°F with top-to-bottom temperature differences up to 320°F considered. A forced cooldown situation through a shutdown stratification due to unidentified leakage at operating temperature was evaluated. Long term maximum stratification situations were also evaluated. Leak-before-break was demonstrated at operating temperature with and without stratification. Leak-before-break was also demonstrated for the forced cooldown situation and for long term maximum stratification.

Based on the current understanding of the thermal stratification phenomenon, it is concluded that thermal stratification has very limited impact on the integrity of the pressurizer surge line of the Beaver Valley Unit 1 nuclear power plant. The forty year design life is not impacted.

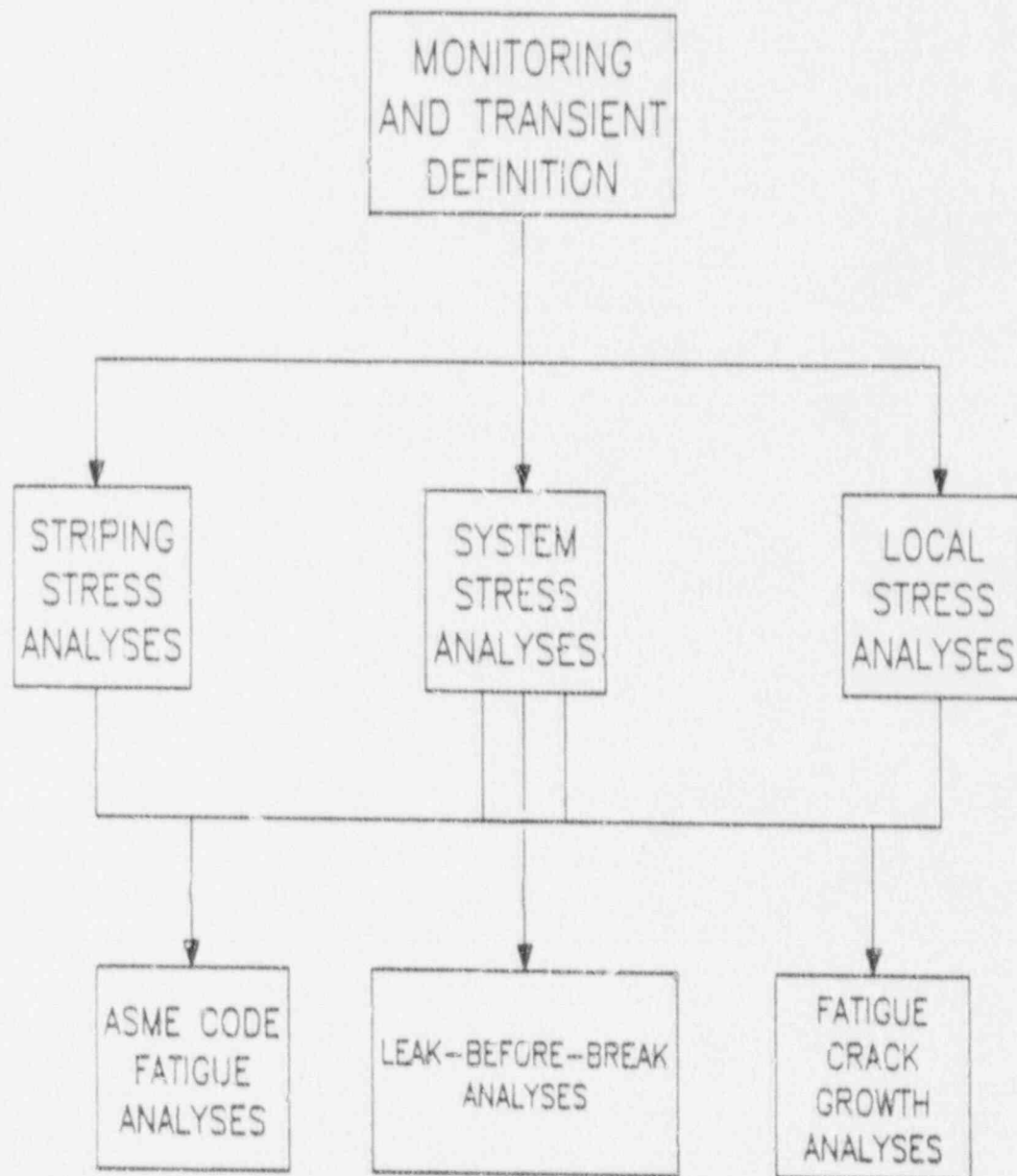


Figure 1. Determination of the Effects of Thermal Stratification

SECTION 1.0
INTRODUCTION AND UPDATE OF DESIGN TRANSIENTS

1.1 Introduction

1.1.1 System Description

The primary function of the reactor coolant system (RCS) is to transport heat from the reactor core to the steam generators for the production of steam (figure 1-1). The system pressure is maintained and controlled by the pressurizer, such that boiling is suppressed and departure from nucleate boiling (DNB) is prevented. The RCS integrity is insured by the overpressure protection of the pressurizer safety and relief valves.

The Beaver Valley Unit 1 RCS consists of three similar heat transfer loops connected to the reactor vessel. Each loop contains a reactor coolant pump (RCP) and a steam generator. The system also includes a pressurizer, connecting piping, pressurizer safety and relief valves, and a relief tank.

The flow path for a typical reactor coolant loop is from the reactor vessel to the inlet plenum of the steam generator (figure 1-2). High temperature reactor coolant flows through the U-tubes in the steam generator, transferring heat to the secondary water, out of the tubes into the outlet plenum to the suction of the reactor coolant pump. The reactor coolant pump increases the pressure head of the reactor coolant which flows back to the reactor vessel.

The pressurizer vessel (figure 1-3) contains steam and water at saturated conditions with the steam-water interface between 25 and 60% depending on the plant operating conditions. From the time the steam bubble is initially drawn during the heatup operation to hot standby conditions, the level is maintained at approximately 25%. During power ascension, the level is increased to approximately 60%.

As illustrated in figure 1-2, the bottom of the pressurizer vessel is connected to the hot leg of one of the coolant loops by the surge line, a 14 inch schedule 160 stainless steel pipe, a portion of which is almost horizontal, that is, slightly pitched down toward the hot leg.

The simplified diagram shown in figure 1-2 indicates the auxiliary systems that interface with the RCS. Of particular significance to surge line stratification are the normal charging and letdown function provided by the Chemical and Volume Control System (CVCS), and the suction and return lines associated with the Residual Heat Removal System (RHRS). The former directly controls the RCS mass inventory and therefore affects flow in the surge line. The RHRS is used to remove heat from the RCS and thereby influences coolant temperature and consequently coolant volume through thermal expansion and contraction.

Other systems which affect surge line flow conditions are main spray flow supplied to the pressurizer from one or two cold legs and the pressurizer electric heaters. Spray operation does not significantly alter the total RCS mass inventory, but does reduce system pressure by condensing some of the steam in the pressurizer. The pressurizer heaters when energized generate steam and as a result increase RCS pressure.

1.1.2 Thermal Stratification In the Surge Line

Thermal stratification in the pressurizer surge line is the direct result of the difference in densities between the pressurizer water and the generally cooler hot leg water. The lighter pressurizer water tends to float on the cooler heavier hot leg water. The potential for stratification is increased as the difference in temperature between the pressurizer and the hot leg increases and as the insurge or outsurge flow rates decrease.

At power, when the difference in temperature between pressurizer and hot leg is relatively small (less than 50°F) the extent and effects of stratification have been observed to be small. However, during certain modes of plant heatup

and cooldown, this difference in temperature can be large, in which case the effects of stratification must be accounted for.

A common approach for assessing the potential for stratification is to evaluate the Richardson Number (tables 1-1 and 1-2) which is the ratio of the thermal density head diametrically across the pipe to the fluid flow dynamic head, or

$$Ri = \frac{g\beta D\Delta T}{U^2}$$

where

- Ri = Richardson number
- g = gravitation constant
- U = hot fluid velocity
- ΔT = hot-to-cold fluid temperature difference
- D = pipe inside diameter
- β = water temperature coefficient of thermal expansion

For a range of surge line flow rates from approximately 700 gpm down to a bypass flow of approximately 1 to 5 gpm and $\Delta T = 320^\circ\text{F}$, the Richardson number is greater than the value of 1 which is required to initiate stratification. Thus under this range of conditions, the flow has the potential to be stratified due to the relatively large hot-to-cold fluid temperature difference combined with the low hot fluid velocity. To eliminate stratification (i.e., Ri smaller than 1) a flow velocity of over 2.4 fps (approximately 700 gpm) is needed (figure 1-4).

1.1.3 Surge Line Stratification Program

The surge line stratification program for Beaver Valley Unit 1 consist of two major parts:

- (a) Plant monitoring and update of design transients

- (b) ASME III stress, fatigue cumulative usage factor (CUF), fatigue crack growth (FCG) and leak-before-break (LBB) analyses

1.2 Update of Design Transients

Because the Beaver Valley Unit 1 and Unit 2 plants are similar in geometry, and because both units have similar operational guidelines, the transients generated in the Beaver Valley Unit 2 analysis (WCAP-12093) will be used as a baseline for creating Beaver Valley Unit 1 transients. First, the development of these baseline transients is demonstrated. Next, Beaver Valley Unit 1 historical records are used to modify the transient set to account for pressurizer/hot leg temperature differences of greater than 320°F (as illustrated later, this temperature difference was a limit defined in the generation of the Unit 2 transients, see Supplement 3 of WCAP-12093). Finally, monitoring information from one actual heatup is used to ensure that the baseline transients envelope Beaver Valley 1 transient activity.

1.2.1 System Design Information (table 1-3)

The thermal design transients used for the Beaver Valley Unit 1 Reactor Coolant System, including the pressurizer surge line, are defined in Westinghouse Systems Standard Design Criteria (SSDC) documents SSDC 1.3.

The design transients for the surge line consist of two major categories:

- (a) Heatup and Cooldown transients - table 1-4
- (b) Normal and Upset operation transient - table 1-5. By definition, the emergency and faulted transients are not considered in the ASME III Section NB fatigue life assessment of components.

In the evaluation of surge line stratification, the current definition of normal and upset design events and the number of occurrences of the design events remains unchanged ("Label", "Type", and "Cycles" columns of table 1-5).

The total number of current heatup-cooldown cycles (200) remains unchanged (table 1-4). The definition of heatup-cooldown events and the number of

occurrences ("Label", "Type" and "Cycle" columns of table 1-4) is updated to reflect monitoring data, as described later.

In all cases, the definition of surge line flow temperature is modified to replace the original uniform temperature by a maximum stratification temperature differential ("MAX ΔT_{strat} " and "Nominal" columns on tables 1-4 and 1-5).

1.2.2 Stratification Effects Criteria (table 1-3)

To determine the normal and upset pipe top-to-bottom temperature difference, " ΔT_{strat} " (tables 1-4 and 1-5), the following conservatism is introduced.

For a given event, the ΔT_{strat} in the pipe will be the difference between the maximum pressurizer temperature and minimum hot leg temperature, even when they do not occur simultaneously.

[

] ^{a,c,e}

1.2.3 Plant Monitoring (table 1-3)

Surge line stratification data from [] ^{a,c,e} Westinghouse plants, including Beaver Valley Unit 2 (figures 1-6 to 1-9) has been utilized in this analysis in developing the baseline transients. The data was obtained by continuous monitoring of the piping OD temperature, displacements and plant parameters.

The data is sufficient to characterize stratification temperatures in the pipe during critical operating transients and heatup-cooldown operation. Also, the data is sufficient to verify that the pipe movements are consistent with analytical predictions, within an accuracy normally expected from hot functional tests, as discussed in section 2.1.

The monitoring of plant parameters is sufficient to correlate measured temperature fluctuations to changes in operation. In particular, it is apparent that temperature fluctuations are due to flow insurge (into the pressurizer) and outsurge (out of the pressurizer) which in turn are due to differential pressure in the system. While a simple and definite mechanistic relationship between plant operation and insurge and outsurge has not been achieved, the data indicate that a steady state stratified condition can be altered by any of the following events:

- (a) Expansion of the pressurizer bubble
- (b) RCP trip in the surge line loop
- (c) Safety injection
- (d) Large charging - letdown mismatch
- (e) Large spray rates

In light of these observations, the update of design transients is based on plant monitoring results, operational experience and plant operational procedures. Conservatism has been incorporated throughout the process in the definition of transients (cycles, ΔT) and in the analysis, as described in the report.

1.2.4 Heat Transfer and Stress Analysis (table 1-3)

The correlation of measured pipe OD temperature to ID temperature distribution is achieved by heat transfer analysis as well as previous experience with flow at large Richardson numbers ($Ri > 1$) (figures 1-10 and 1-11).

These analyses and test data available to date show that a stratified flow condition, [

] ^{a,c,e} is a proper and conservative depiction of the flow condition inside the pipe at large ΔT and low flow rates ($Ri > 1$).

An additional conclusion from the heat transfer and stress analyses is that [

] ^{a,c,e}

1.2.5 Stratification Profiles

Table 1-6 summarizes the major stratification profile characteristics. The monitored data shows a consistent axial temperature profile along the horizontal portions of the [] ^{a,c,e} surge lines monitored (figures 1-12, 1-13 & 1-14).

For purposes of analysis, this temperature profile was divided in [] ^{a,c,e} regions or "locations" along the pipe axis (figure 1-14).

1.2.6 Development of Conservative Normal and Upset Transients (table 1-3)

Several conservatisms are introduced in the definition of the normal and upset thermal transients (tables 1-4, 1-5, 1-7 and 1-8).

[

] ^{a,c,e}

...] a, c, e

The normal and upset transients are listed in tables 1-4 and 1-5.

1.2.7 Temperature Limitations During Heatup and Cooldown (tables 1-3 and 1-9)

The maximum expected temperature difference between the pressurizer and the hot leg expected for Beaver Valley is 320°F, therefore, this limit is used in creating the baseline transients. However, based on a review of historical records, this temperature difference was exceeded during five of the heatups and cooldowns. These exceedances have been incorporated into the transient set as described later.

With the RCL cold, the pressurizer pressure (and therefore temperature) is limited by the cold overpressure mitigation system (COMS).

Practically, plants operate to minimize downtime and heatup-cooldown time, when power is not being generated. The times at large ΔT are therefore reasonably limited, as discussed later.

1.2.8 Historical Data (table 1-3)

Since not all heatup and cooldown parameters affecting stratification are formally limited by Technical Specification or Administrative controls, it is necessary to consider plant operational procedures and heatup-cooldown practices to update the original heatup and cooldown design transient curves of SSDC 1.3 (figures 1-16 and 1-17).

To this end, a review of procedures, operational data, operators experience, and historical records was conducted for []^{a,c,e} Westinghouse PWR plants, including Beaver Valley Unit 1 (table 1-10).

The heatup and cooldown operations information acquired from this review is summarized in tables 1-11 and 1-12, []^{a,c,e}

The information is divided into heatup and cooldown tables and diagrams. The diagram presents the pressurizer water and hot leg temperature profiles versus time. The various phases of the process are identified by letters along the diagrams' abscissa and in tables 1-11 and 1-12.

1.2.9 Development of Heatup and Cooldown Design Transients With Stratification

As described above, the database of information used to update the heatup and cooldown transients, included the following:

- a) Typical heatup and cooldown curves, as developed from review of procedures, operational data and operators experience.
- b) Transients as monitored at []^{a,c,e} plants
- c) Historical records of critical heatup and cooldown temperatures

The heatup and cooldown transients are presented in the following sections as []^{a,c,e} and in similar fashion to the normal and upset transients. Table 1-13 gives the general characteristics of the two types of transients observed.

1.2.9.1 []^{a,c,e} Transients

A) Monitoring Transient Summary

For a given monitored location, plots of temperature difference versus time were generated (figures 1-28, 1-29, 1-30, and 1-31). Two parameters were plotted, the pipe top to bottom temperature difference (labeled "surge line") and the pressurizer to hot leg temperature difference (labeled "system"). Only heatup data was available, discussion of cooldown transients follows in section G.

It is clear from the curves (figures 1-28, 1-29, 1-30, and 1-31) that for the observed heatups, []^{a,c,e} while the Beaver Valley Plants, Units 1 and 2 (figures 1-28 and 1-29, respectively) had moderate thermal transient activity.

For conservatism, the envelope from measured transients in all plants is applied to define the transients, even though there was only a moderate level of these transients observed at both Beaver Valley plants.

B) Fatigue Cycles

The fatigue cycles were obtained using the technique illustrated on figure 1-31, [

] ^{a,c,e}.

C) Strength of Stratification

Plant monitoring data indicate that for the various transients observed the ΔT in the pipe (top to bottom) is not as large as the ΔT in the system

(pressurizer to hot leg). The ratio of ΔT in the pipe to ΔT in the system will be referred to as "strength of stratification".

[

] ^{a,c,e} It should also be noted that the maximum strength of stratification observed was 0.95.

D) Number of Stratification Cycles (table 1-16)

Plant monitoring data indicated the significant events which could occur during a given heatup. [

] ^{a,c,e}

E) Maximum Temperature Potential

The key factor in thermal stratification of the surge line is the temperature difference between the pressurizer and hot leg (section 1.2). This temperature difference is clearly maximized during the heatup and cooldown, when the plant is in mode 5 cold shutdown (hot leg less than 200°F) and the pressurizer bubble has been drawn with the reactor coolant pump running (pressurizer temperature larger than 425°F). [

]a,c,e

F) Final Cycles and Stratification Ranges

[

]a,c,e

[

j^{a,c,e}

For Heatup: $i = 1$ to 24, $j = 1$ to 6, $k = 1$ to 4

The 24 transients produced are conservatively summed, based on ΔT_i range, into 9 transients (H1 to H9).

For cooldown $i = 1$ to 30, $j = 1$ to 6, $k = 1$ to 5

The 30 transients produced are conservatively summed, based on ΔT_i range, into 7 transients (C1 to C7).

G) Cooldown Transients

The procedure used in heatup is applied to develop transients for plant cooldown. [

j^{a,c,e}

1.2.9.2 []^{a,c,e} Transients

[

] ^{a,c,e}

1.2.9.3 Transient Basis Exceedances

As indicated previously, based on a review of the Beaver Valley 1 operating records, there were five events which had a system delta T greater than the transient basis assumed upper limit of 320°F. Since none of these system delta temperatures were greater than [

] ^{a,c,e}

Therefore, the addition of these cycles conservatively accounts for the events in which the system delta temperature exceeded 320°F.

1.2.10 Striping Transients

Because of the nature of thermal striping stresses, the maximum stratification value rather than the fatigue range is to be used. This results in larger values of stratification temperature. [

] ^{a,c,e}

1.3 Conclusions

Design transients were updated to incorporate stratification. The transients were developed to conservatively represent the cyclic effects of stratification at the Beaver Valley Plants. Additionally, the Beaver Valley 1 monitoring data for one heatup was examined relative to the transients used in the fatigue analysis. Based on this comparison, it was determined that the transients used in the analysis envelope Beaver Valley 1 cyclic activity. To further illustrate the margin included in the development of these heatup transients, a simplified fatigue factor calculation is provided in figures 1-33 and 1-34. This comparison indicates that the design transients have a factor of conservatism of approximately [

]a,c,e

TABLE 1-1

IMPORTANT DIMENSIONLESS GROUPS FOR SIMILITUDE
IN HYDRODYNAMIC TESTING

Parameter	Symbol	Definition	Significance
1. Weibach friction factor	f	$\frac{D \Delta p}{2 \rho V^2 L}$	Pressure force/inertia force
2. Cavitation number	σ	$\frac{P_1 - P_v}{\rho V^2}$	Pressure difference/inertia force
3. Reynolds number	Re	$\frac{\rho V D}{\mu}$	inertia force/viscous force
4. Strouhal number	St	$\frac{f D}{V}$	Vortex shedding frequency/inertia force
5. Weber number	We	$\frac{\rho V^2 D}{\sigma}$	inertia force/surface-tension force
6. Froude number	Fr	$\frac{V^2}{g D}$	inertia force/gravity force
7. Richardson number (Modified Froude number)	Ri	$\frac{g D \Delta \rho}{\rho V^2}$	Buoyancy force/inertia force
8. Euler number	Eu	$\frac{\Delta p}{\rho V^2}$	Pressure force/inertia force
9. Prandtl number	Pr	$\frac{\mu C_p}{k}$	Momentum diffusivity/thermal diffusivity
10. Peclet number	Pe	$\frac{\rho V D C_p k}{\mu}$ ($Re \times Pr$)	Convective heat transfer/ conductive heat transfer
11. Grashof number	Gr	$\frac{L^3 \rho^2 g \beta \Delta T}{\mu^2}$	Buoyancy force/viscous force
12. Rayleigh number	Ra	$\frac{L^3 \rho^2 C g \beta \Delta T}{\mu k}$ ($Gr \times Pr$)	—

NOMENCLATURE:

C = specific heat	g = acceleration of gravity
ρ = density	P = pressure
σ = surface tension	P_1 = static fluid pressure
k = thermal conductivity	P_v = fluid vapor pressure
β = volumetric expansion coefficient	L, D = characteristic dimensions
ΔT = fluid temperature change	V = fluid velocity
f = vortex shedding frequency	μ = viscosity

TABLE 1-2
STRATIFICATION POTENTIAL BASED ON
RICHARDSON NUMBER

• Stratification potential exists if $R_i > 1$



a,c,e

TABLE 1-3
NOTES FOR TRANSIENT DEVELOPMENT FLOW CHART
(See Figure 1-5)

(1) System Design Information: This includes the Following Documents.

- System Standard Design Criteria 1.3F, 1.3X, 1.3 Rev. 2 etc. (Cycles, Press, T_{press} , T_{RCS} , Surge Rate)

SSDC Were Reviewed to Obtain Events and Cycles. Design Events and Cycles Were Not Altered.

(2) Criteria was Established to Determine Effects of a Design Event on the Surge Line. The Following Conservative Criteria was Established.

[

j^{a,c,e}

(3) Plant Monitored Data Reviewed from the Following:

- o Beaver Valley
- o Plants [j^{a,c,e}

TABLE 1-3 (Cont'd.)
NOTES FOR TRANSIENT DEVELOPMENT FLOW CHART

Pipe Temperatures Obtained From RTD's and System Parameters Obtained from
Plant Computer.

[

]a,c,e

TABLE 1-3 (Cont'd.)
NOTES FOR TRANSIENT DEVELOPMENT FLOW CHART

[

] a,c,e

(10) Design transients developed for stratification and striping affects in surge line

TABLE 1-4
SURGELINE TRANSIENTS WITH STRATIFICATION
HEATUP (H) AND COOLDOWN (C) - 200 CYCLES TOTAL

TEMPERATURES (*F)

a.c.e



TABLE 1-4 (Cont'd)
SURGELINE TRANSIENTS WITH STRATIFICATION
HEATUP (H) AND COOLDOWN (C) - 200 CYCLES TOTAL

TEMPERATURES (°F)

a.c.e



*Input for maximizing moment range only

I/O = Insurge - Outsurge

F = Fluctuation

WESTINGHOUSE PROPRIETARY CLASS 2

TABLE 1-5
 SURGE LINE TRANSIENTS WITH STRATIFICATION
 NORMAL AND UPSET TRANSIENT LIST

LABEL	TYPE	CYCLES	ΔT Strat	TEMPERATURES ($^{\circ}F$)		a, c, e
				MAX	NOMINAL	
				PRZ T	RCS T	

TABLE 1-5 (Cont'd.)
 SURGE LINE TRANSIENTS WITH STRATIFICATION
 NORMAL AND UPSET TRANSIENT LIST

LABEL	TYPE	CYCLES	ΔT_{Strat}	TEMPERATURES ($^{\circ}F$)		a, c, e
				MAX	NOMINAL	
				PRZ T	RCS T	

TABLE 1-6
STRATIFICATION PROFILES

[

a,c,e

TABLE 1-7
HEATUP - COOLDOWN TRANSIENTS

o Transients Were Developed Based On:

- Typical Heatup Cooldown Curves
- Envelope (Plus Margin) of Events (Transients) Monitored
- Historical Data on Temperature Plateaus

[

j a, c, e

TABLE 1-8
DESIGN TRANSIENTS WITH STRATIFICATION

- o Heatup and Cooldown Combined With Other Events
- o Design Transient Criteria

[

a,c,e

- o Input for Local and Structural Analysis Defined - Plus Nozzle
- o Striping Transients Defined to Consider Maximum Stratification Cycles Regardless of Range

TABLE 1-9
PLANT OPERATIONAL CONSTRAINTS

- o Tech Spec or Administrative Limit of []^{a,c,e} Between Pressurizer and Spray Temperatures
- o Reactor Coolant System Pressure of []^{a,c,e} required for RCP operation []^{a,c,e}
- o Cold Overpressure Mitigation Requires - Minimize Pressure at Low RCS Temperatures (Appendix G Curves) - Steam Bubble Beneficial for Minimizing LTOP.
- o Overall Goal to Maximize Time at Power
- o Recent Administrative Limits on Minimum RCS Temperature Prior to Pressurizer Heatup

TABLE 1-10
OPERATIONS SURVEY

- o Summary of Plants Surveyed

PLANT	NO. OF LOOPS	YEARS OF OPERATION (MAXIMUM)
-------	-----------------	---------------------------------

ja,c,e

- o Reviewed Typical Heatup Cooldown Process
- o Reviewed Administrative/Tech Spec Limitations
- o Reviewed Historical Events and Time Durations
- o Developed Heatup - Cooldown Profiles

TABLE 1-11
HEATUP DATA SUMMARY
(PZR - HOT LEG) TEMP. DIFFERENCE AND TIME DURATION FOR EACH PHASE

a.c.c.e

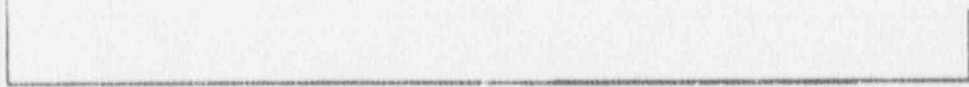
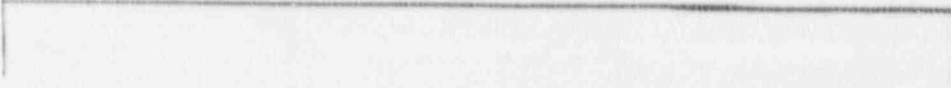


TABLE 1-12
COOLDOWN DATA SUMMARY
(PZR - HOT LEG) TEMP. DIFFERENCE AND TIME DURATION FOR EACH PHASE

a.c.e

1-31

TABLE 1-13
TRANSIENT TYPES

j a, c, e

TABLE 1-14

SUMMARY OF FATIGUE CYCLES FROM [

] a.c.e

Cycle	Delta Range (°F)	Cycle	Delta Range (°F)
] a.c.e			

NOTE:

The delta range represents the relative severity (ΔT) of each transient following the fatigue cycle approach.

TABLE 1-15
 SUMMARY OF PLANT MONITORING TRANSIENTS
 WITH STRENGTH OF STRATIFICATION (RSS)

[] ^{a,c,e}		[] ^{a,c,e}		Beaver Valley Unit 1		Beaver Valley Unit 2	
Observed Cycles	RSS (1)	Observed Cycles	RSS (1)	Observed Cycles	RSS (1)	Observed Cycles	RSS (1)

								a,c,e
--	--	--	--	--	--	--	--	-------

OBSERVED TRANSIENTS GROUPED
 BY STRENGTH OF STRATIFICATION
 (RSS) INTERVALS

RSS	No. Observed Cycles	% of Total
-----	------------------------	---------------

			a,c,e
--	--	--	-------

TABLE 1-15 (cont.)
 SUMMARY OF PLANT MONITORING TRANSIENTS
 WITH STRENGTH OF STRATIFICATION (RSS)

<u>RSS</u>	<u>J</u>	<u>% of Transients</u>

a,c,e

RELATIVE NUMBER OF CYCLES OF
 STRENGTH OF STRATIFICATION (RNSSj)
 AFTER GROUPING

<u>RNSSj</u> <u>% Transients (2)</u>	<u>j</u>	<u>RSSj</u> <u>Strength of</u> <u>Stratification (1)</u>

a,c,e

Nomenclature:

- (1) Strength of Stratification (RSS)
- (2) Relative Number of Cycles of Strength of Stratification (RNSS)

TABLE 1-16
 SUMMARY OF MONITORED TRANSIENT CYCLES (ONE HEATUP)

Plant	No. of Cycles
[]	

a,c,e

Avg. Monitored Cycles: 15.75 = x;

Selected No. of Design Cycles: 36.5 (added 30% to observed maximum number of cycles, plant A)

DESIGN DISTRIBUTION APPLIED TO MAX NUMBER OF
 TRANSIENTS EXCEPTED MULTIPLIED BY 200
 HEATUP OR COOLDOWN CYCLES

No. of Transients	RSS
[]	

a,c,e

TABLE 1-17
SUMMARY OF % TIMES AT
MAXIMUM TEMPERATURE POTENTIAL

RTMP_K

HEATUP

a,c,e

Note: Recorded Range of Systems ΔT and RTMP_K from
Plant A (9 heatups, 7 cooldowns)
Plant B (8 heatups, 7 cooldowns)

TABLE 1-18
SURGE LINE TRANSIENTS - STRIPING LOADS
FOR HEATUP (H) and COOLDOWN (C)

a,c,e

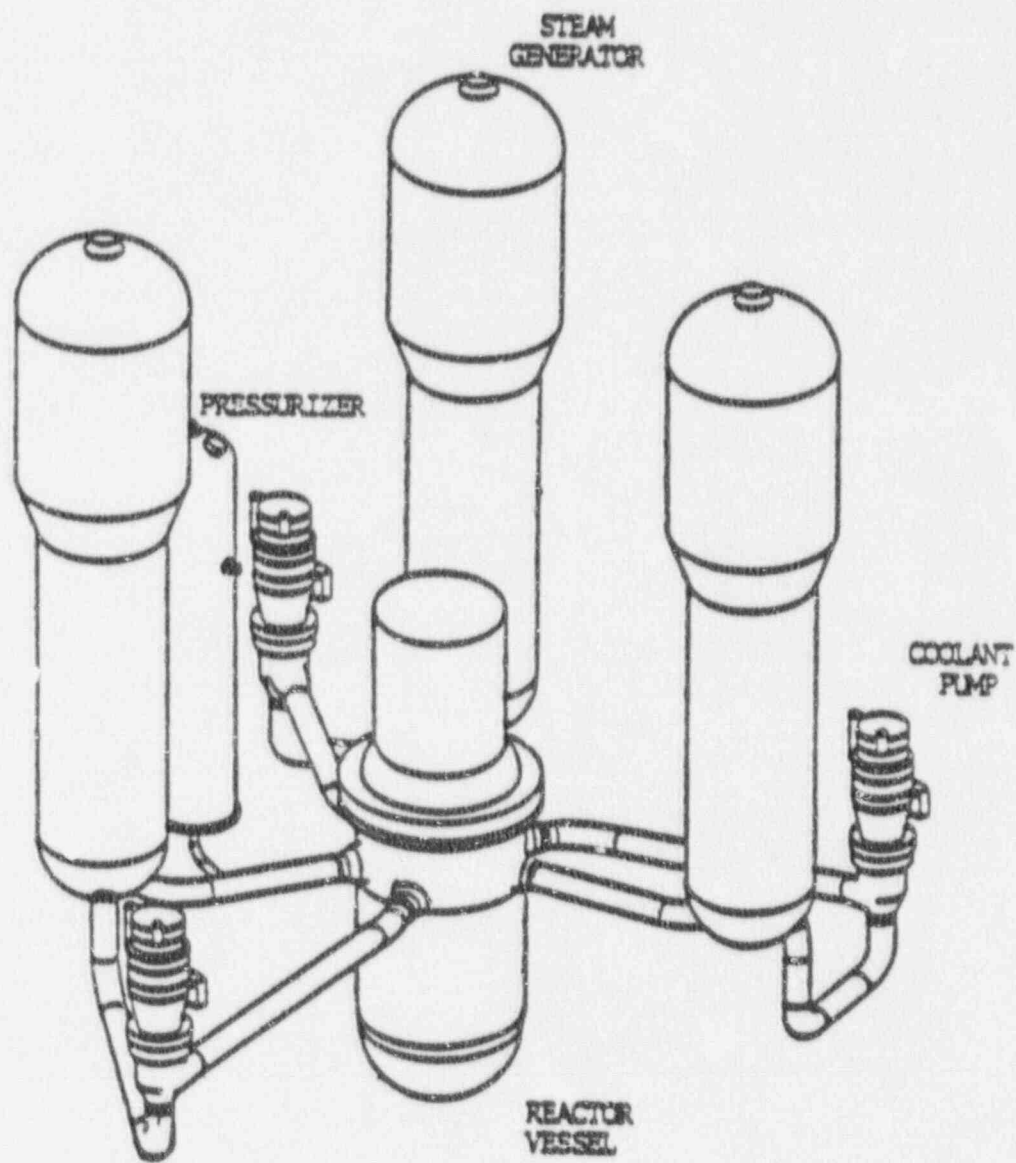


Figure 1-1. Simplified Diagram of the NSSS

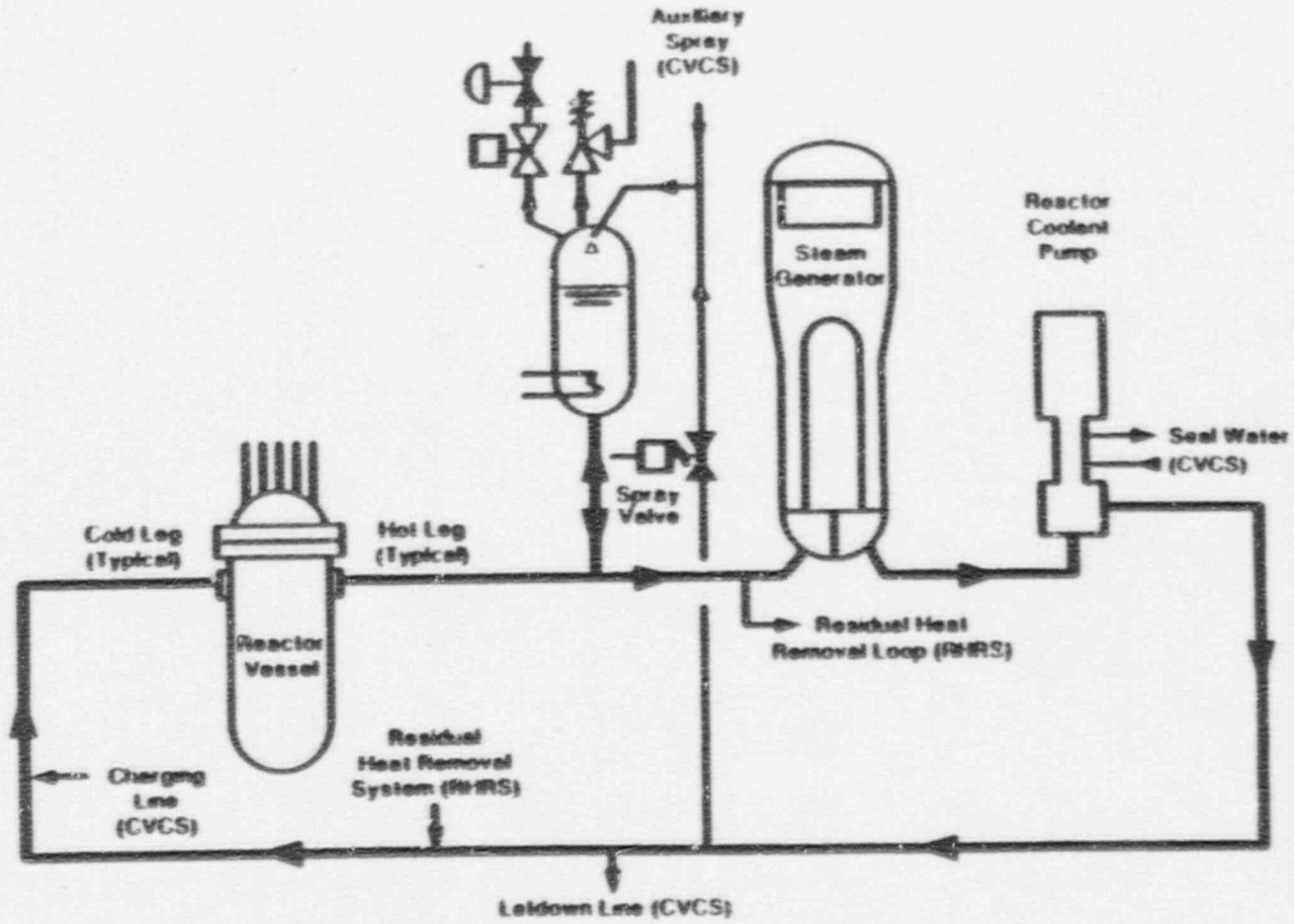


Figure 1-2. Reactor Coolant System Flow Diagram (Typical Loop)

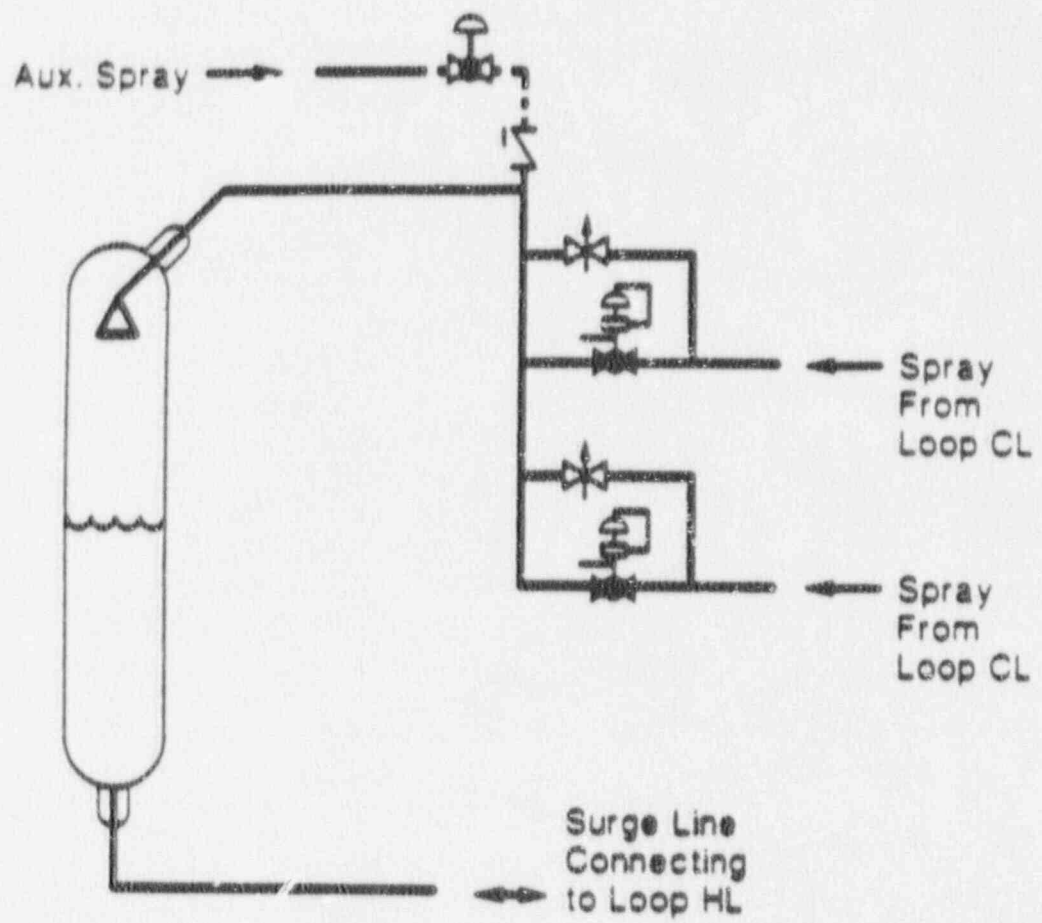


Figure 1-3. RCS Pressurizer

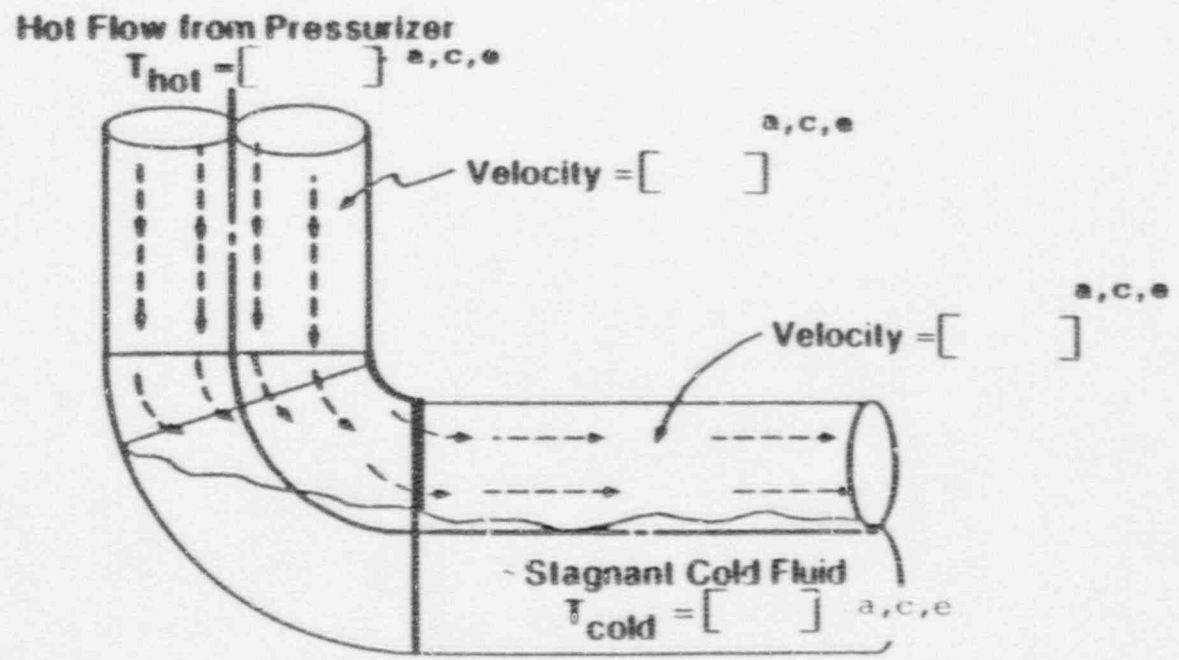


Figure 1-4. Estimate of Flow Stratification Pattern in Elbow Under Pressurizer

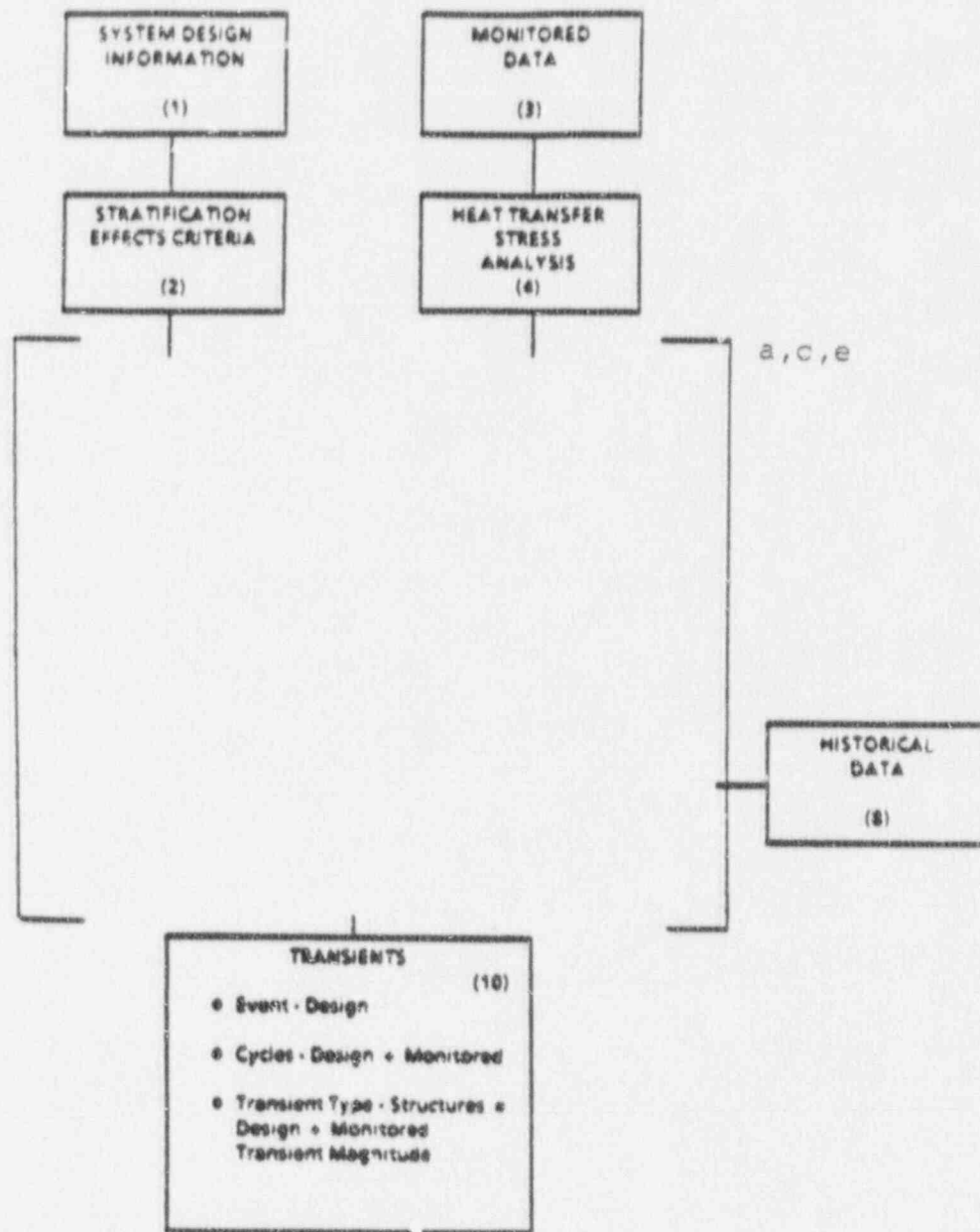


Figure 1-5. Transient Development Flow Chart

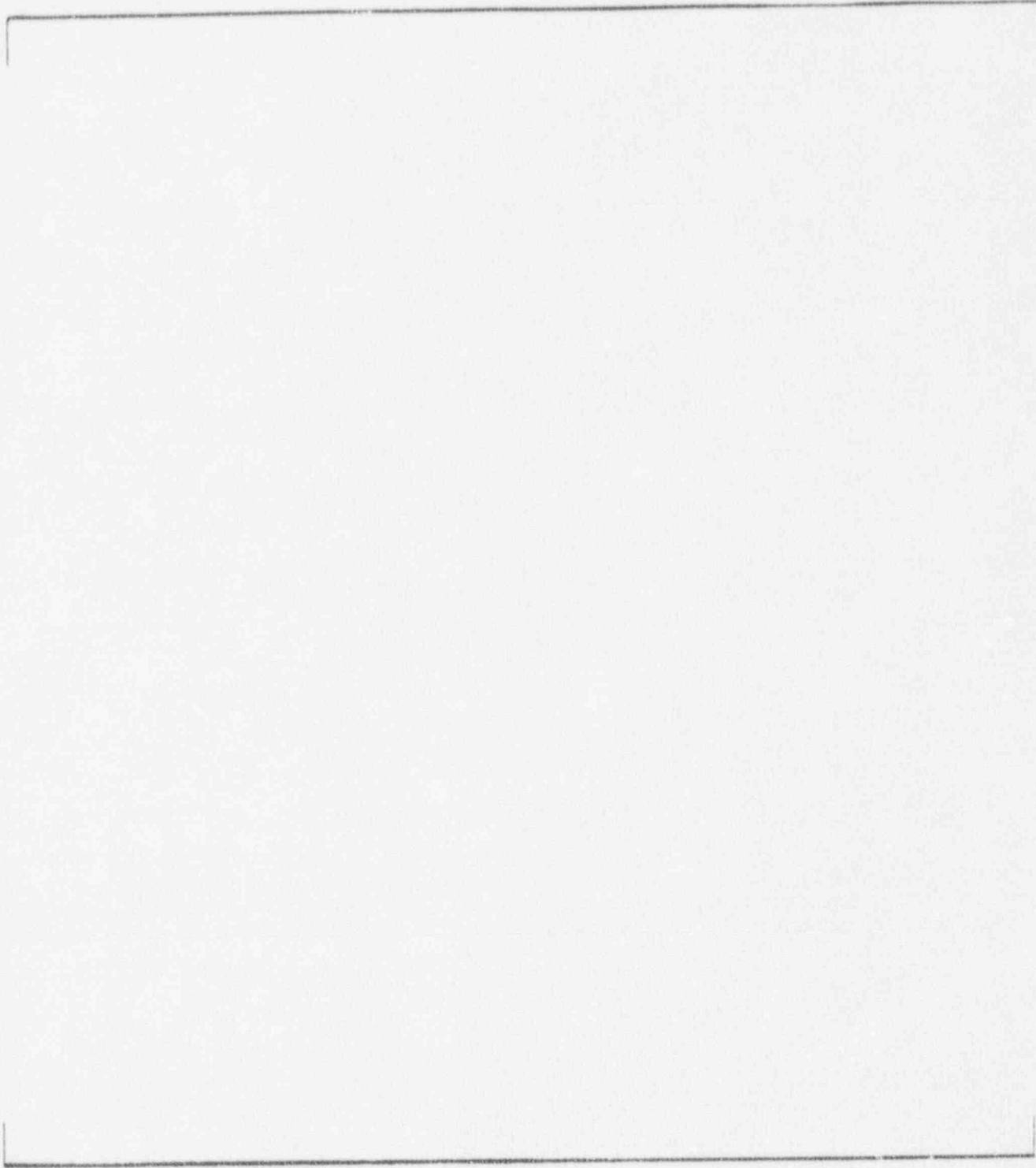


Figure 1-6. Beaver Valley Pressurizer Surge Line Monitoring Locations

4700s-092890 10

1-45

a,c,e

Figure 1-7. Plant A Pressurizer Surge Line Monitoring Locations

a, C, e



Figure 1-8. Plant B Pressurizer Surge Line Monitoring Locations

47005 (09/88) 10



Figure 1-9. Plant C Pressurizer Surge Line Monitoring Locations

Temperature (°F)



a,c,e

Angle β (Degrees)

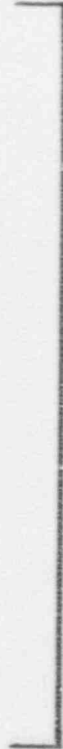
1-48

Figure 1-10. Temperature Profile (6.5-inch ID Pipe)

Angle, (degrees)



a,c,e



Dimensionless Temperature, 0

Figure 1-11. Dimensionless Temperature Profile (14.3-inch ID Pipe)

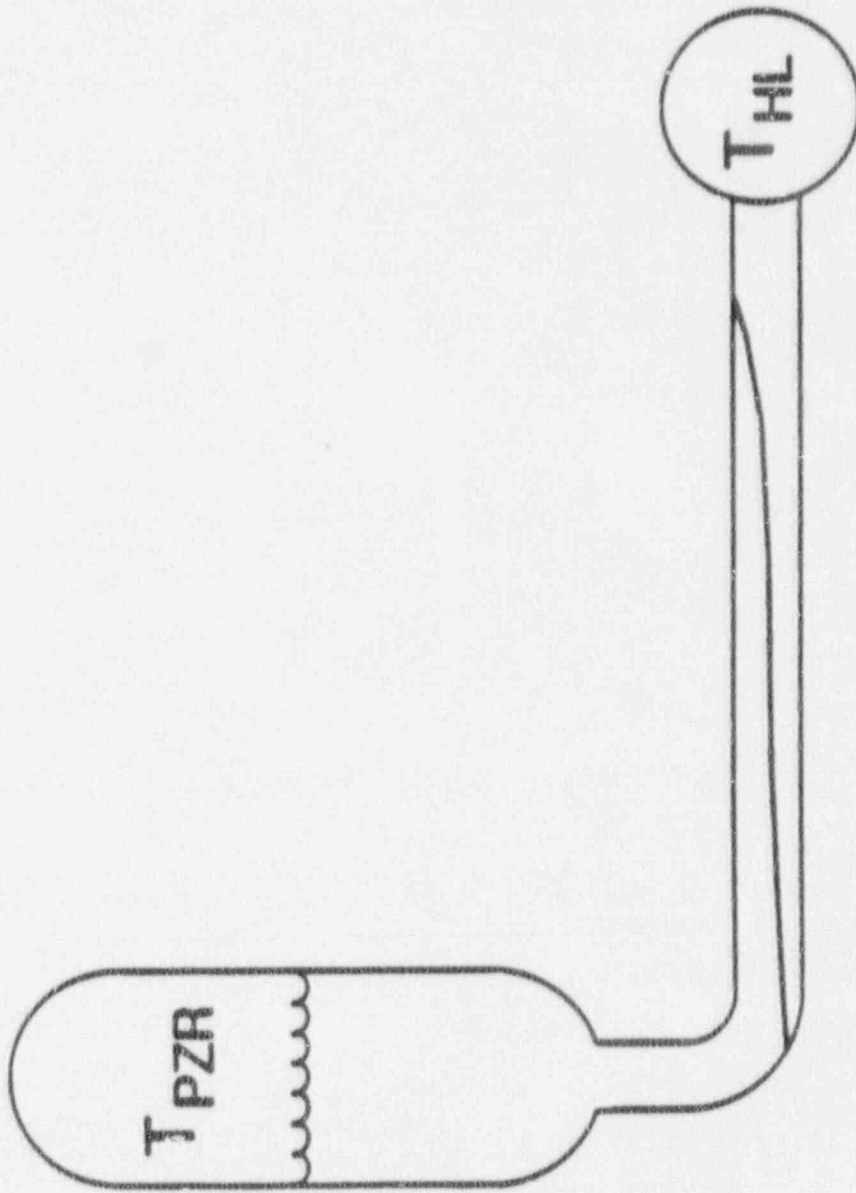


Figure 1-12. Surge Line Stratification



Figure 1-13. Surge Line Hot-Cold Interface Locations



Figure 1-14. Hot-Cold Interface Location From Temperature Measurements

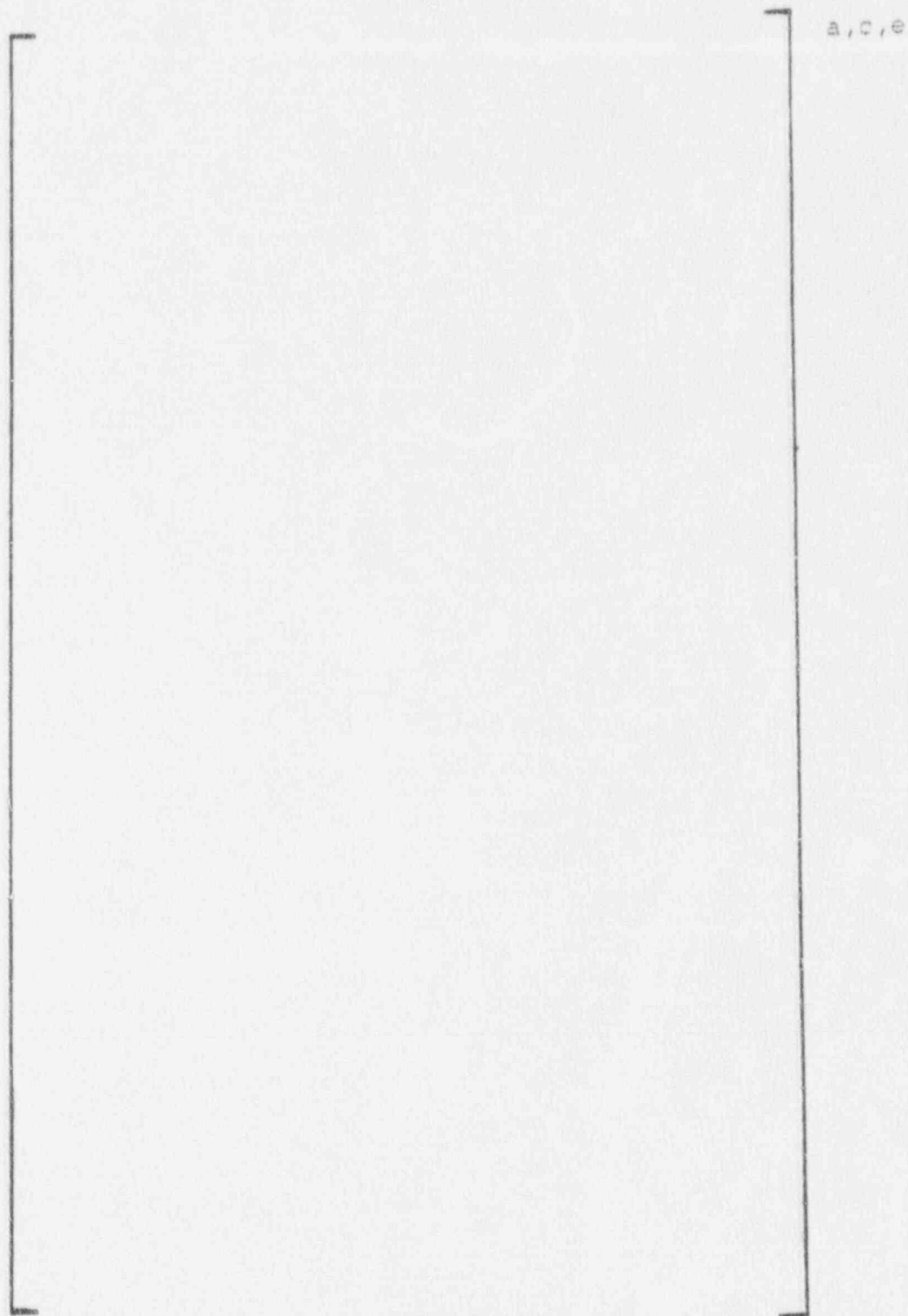


Figure 1-15. Inadvertant RCS Depressurization ($\Delta T = 260^\circ\text{F}$ in Surge Line)

1-54

Temperature (°F)



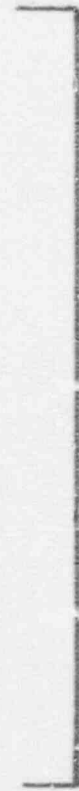
a,c,e

Time (Hours)

Figure 1-16. Steam Bubble Mode Heatup

1-55

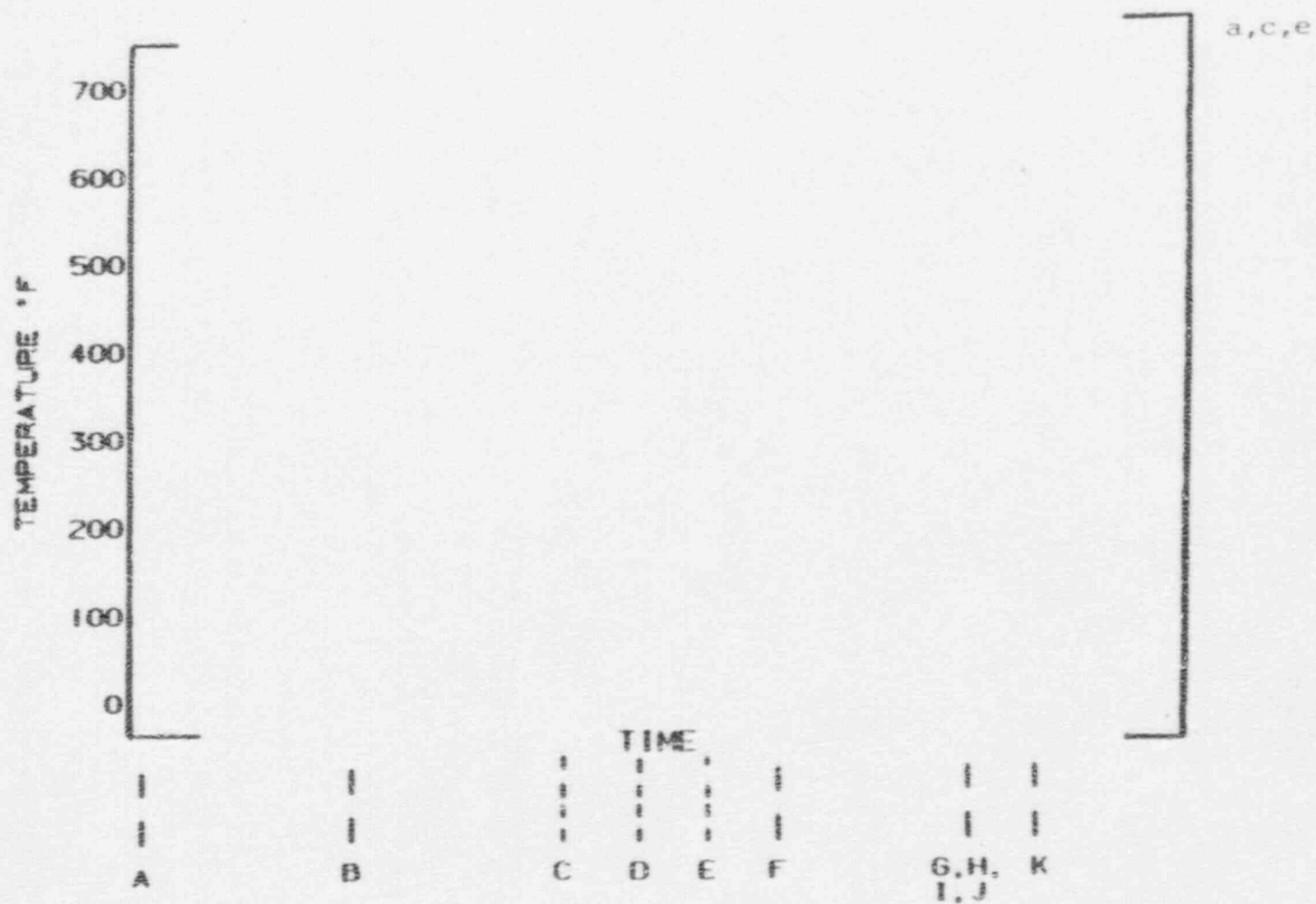
Temperature (°F)



a, c, e

Time (Hours)

Figure 1-17. Steam Bubble Mode Cooldown

Figure 1-18. Heatup []^{a,c,e}

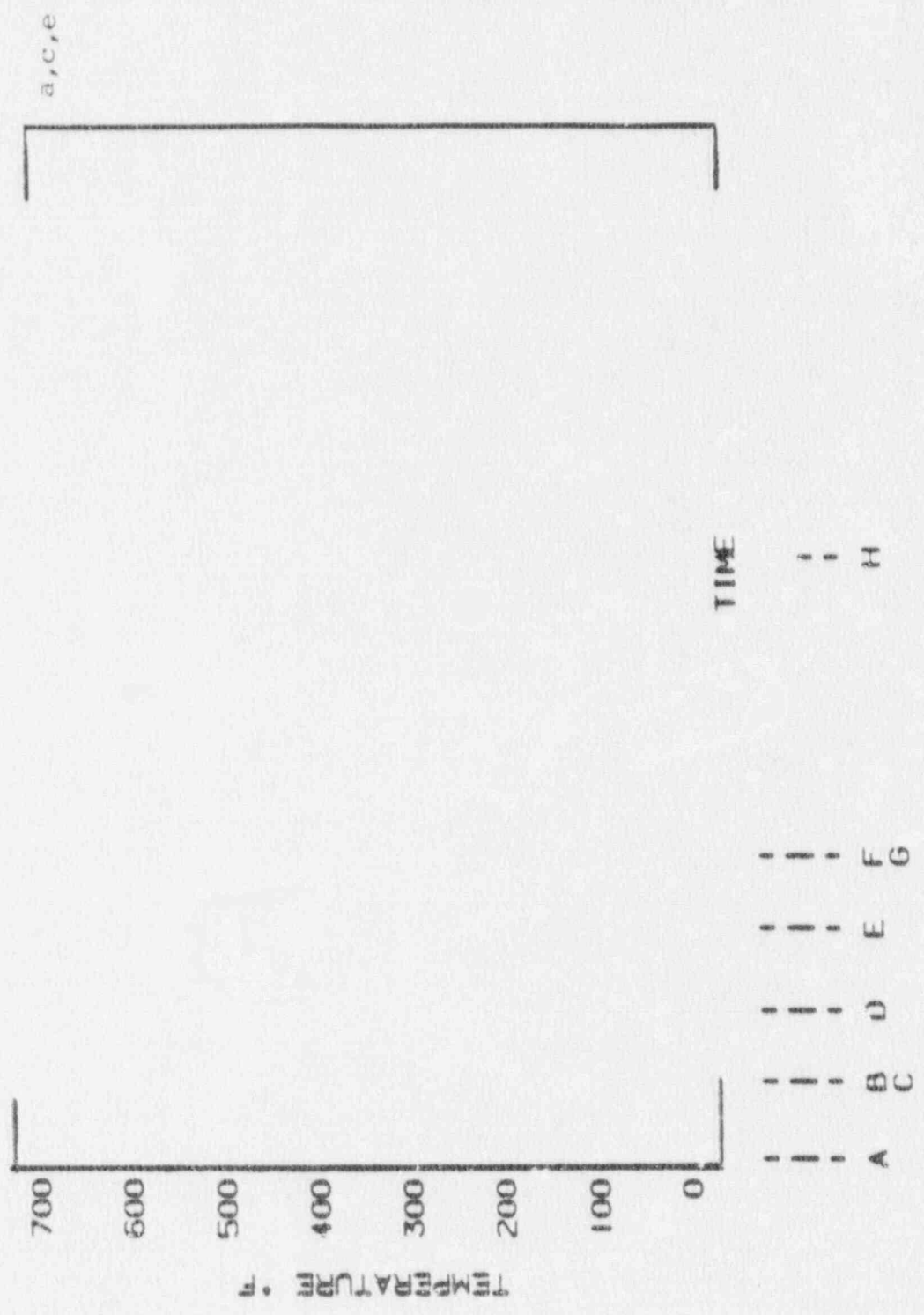


Figure 1-19. Cooldown [a.c.e]

4700s/092830 10

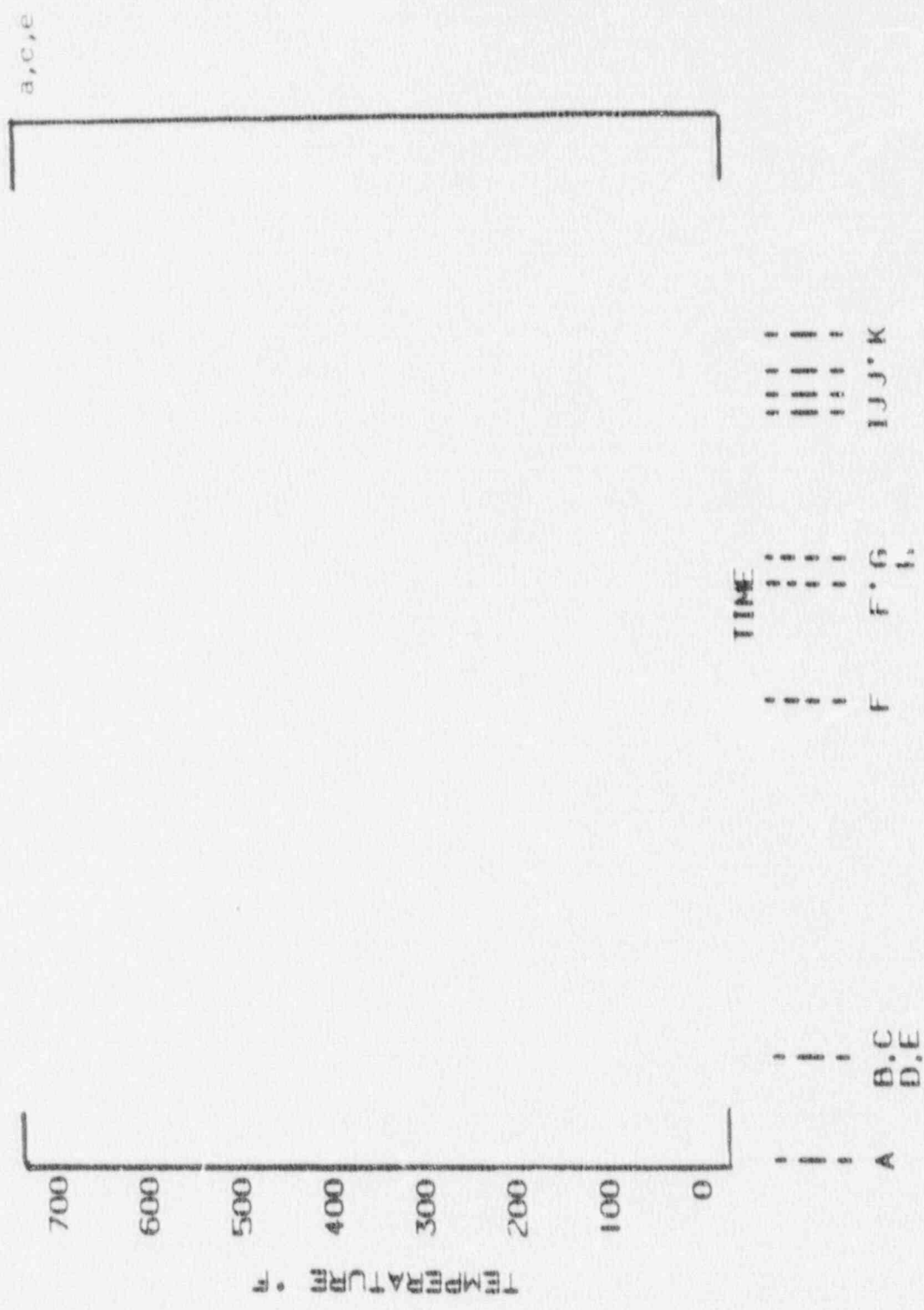


Figure 1-20. Heatup []^{a,c,e}

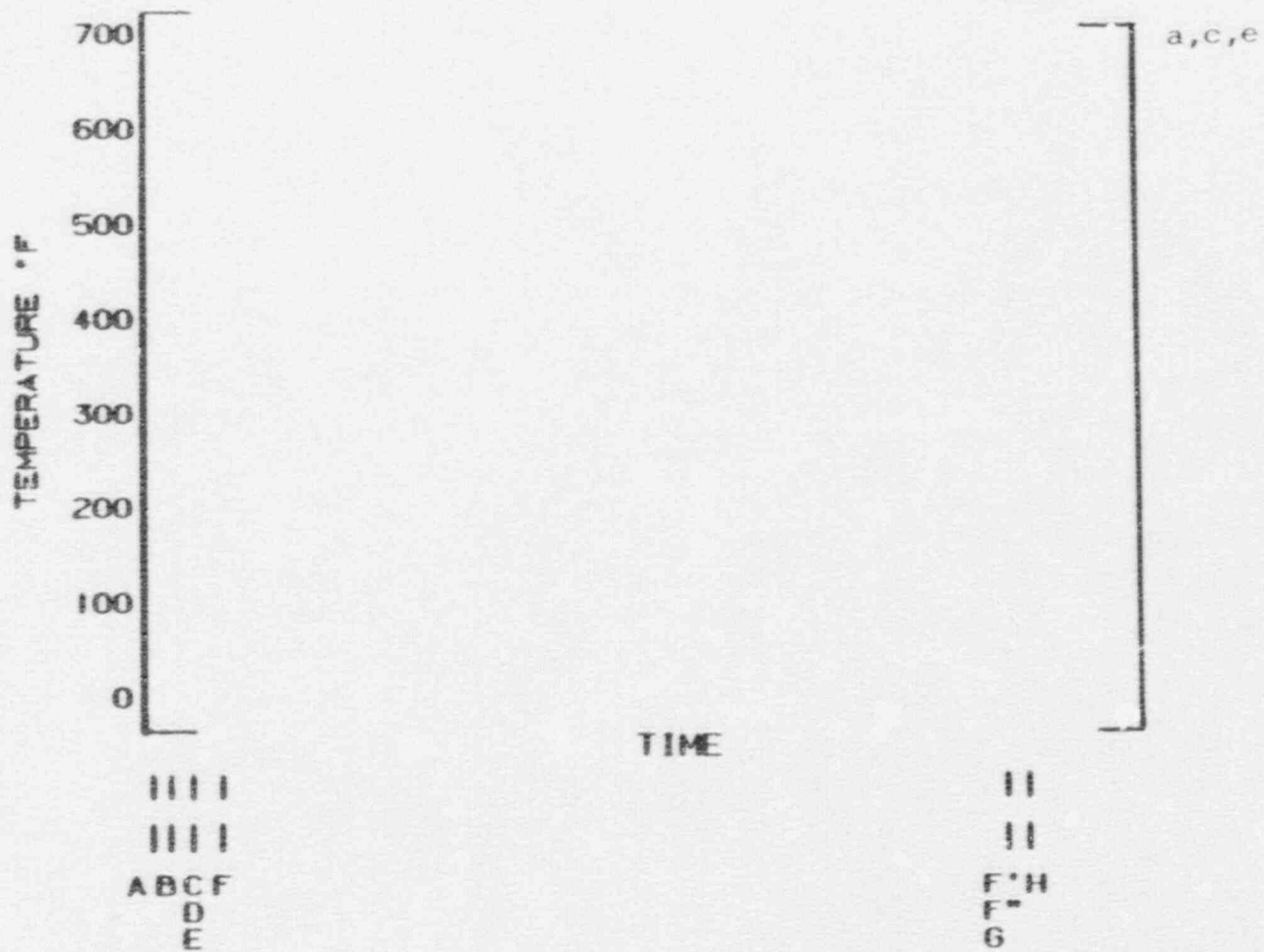


Figure 1-21. Cooldown []^{a,c,e}

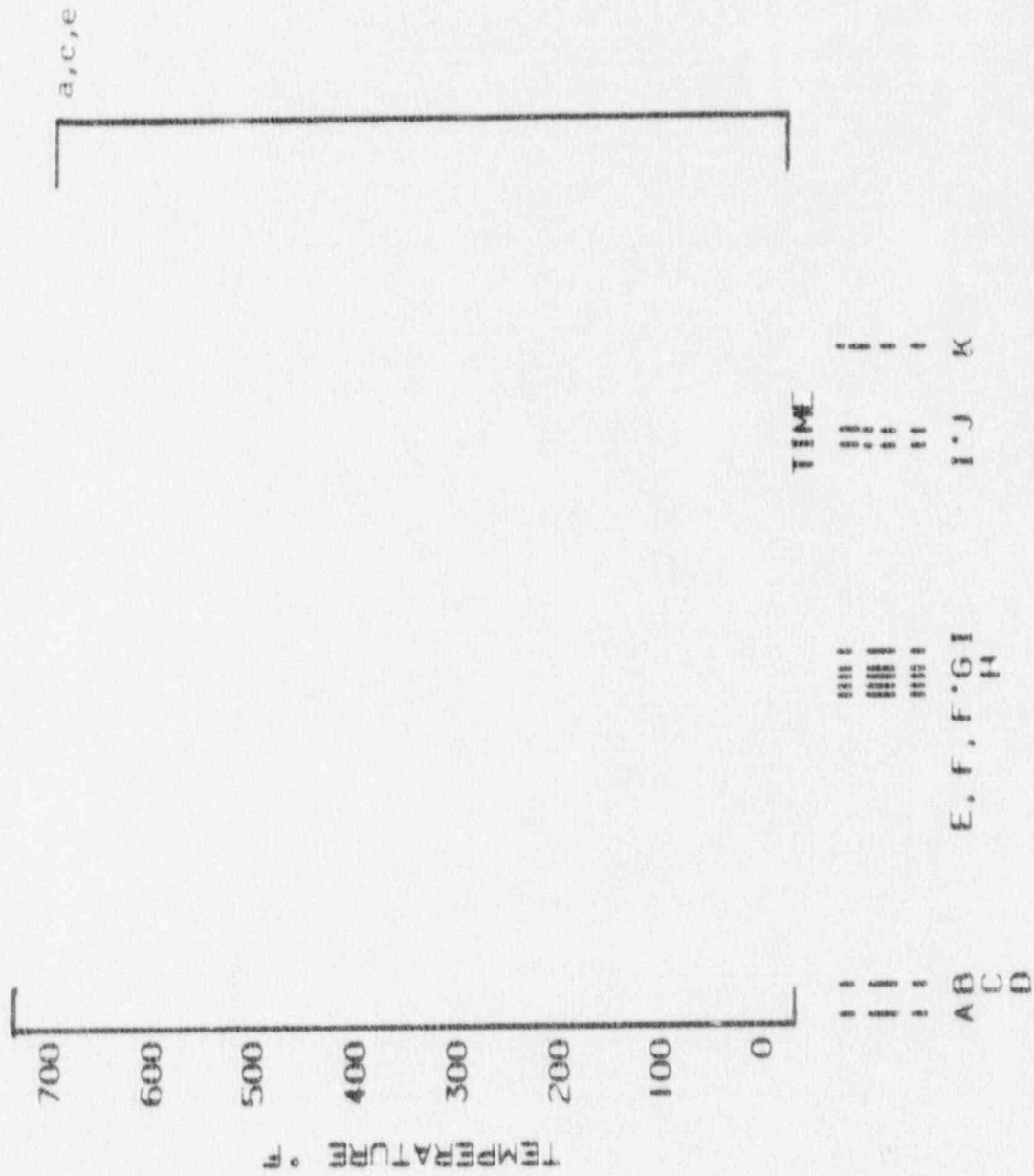


Figure 1-22. Heatup I]^{a, c, e}

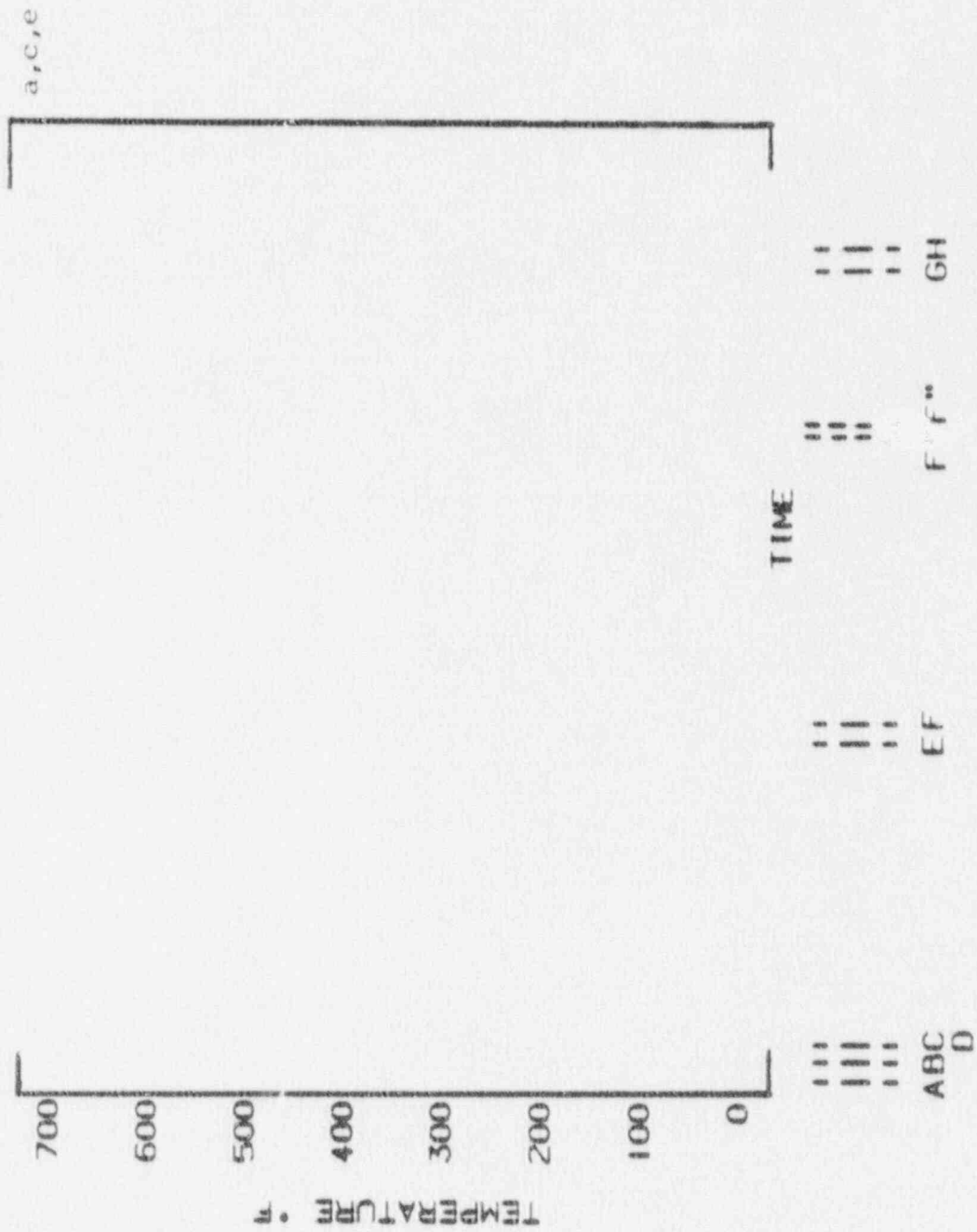


Figure 1-23. Cooldown []^{a, c, e}

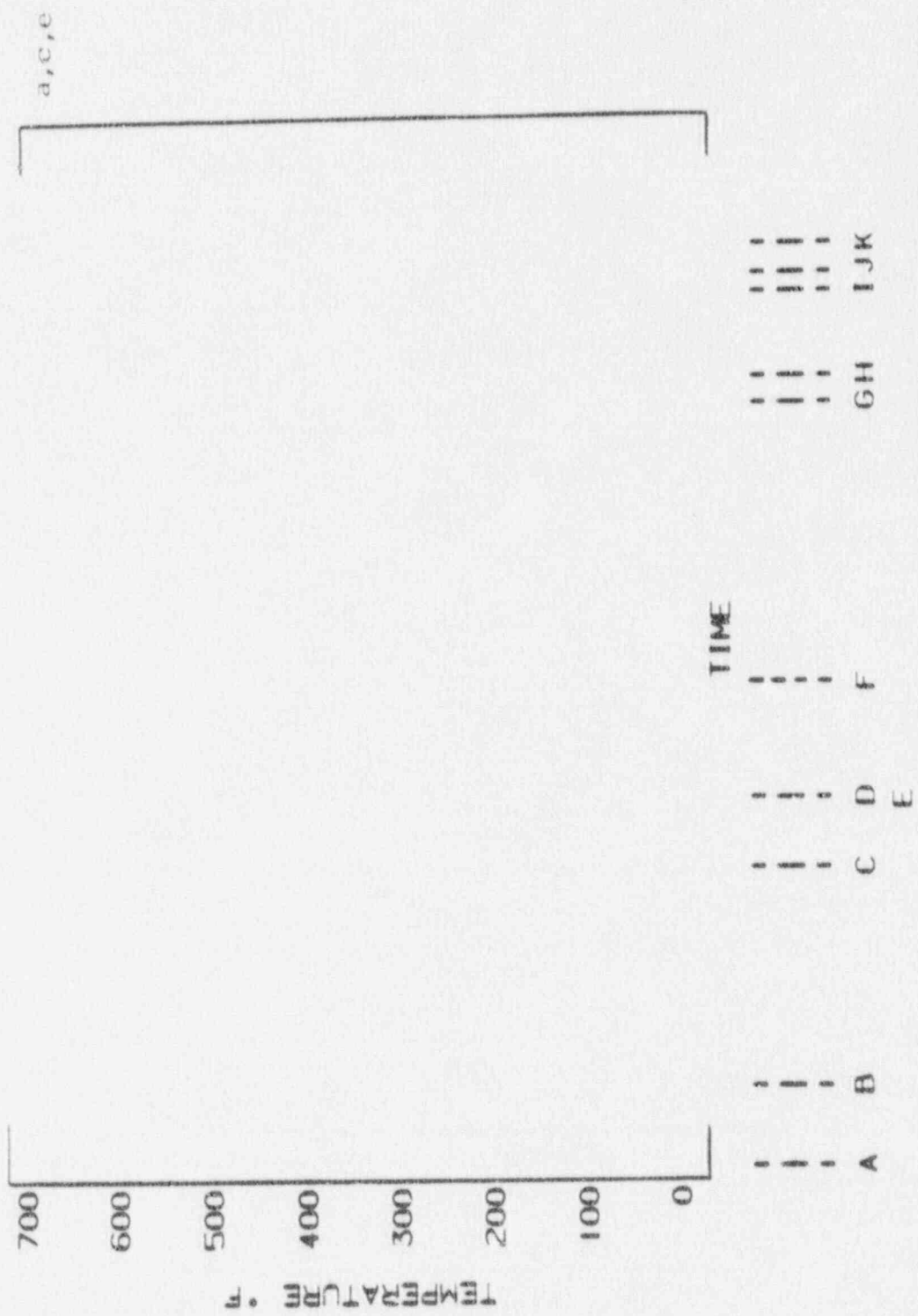


Figure 1-24. Heatup []^{a,c,e}

47004/09/2890 10

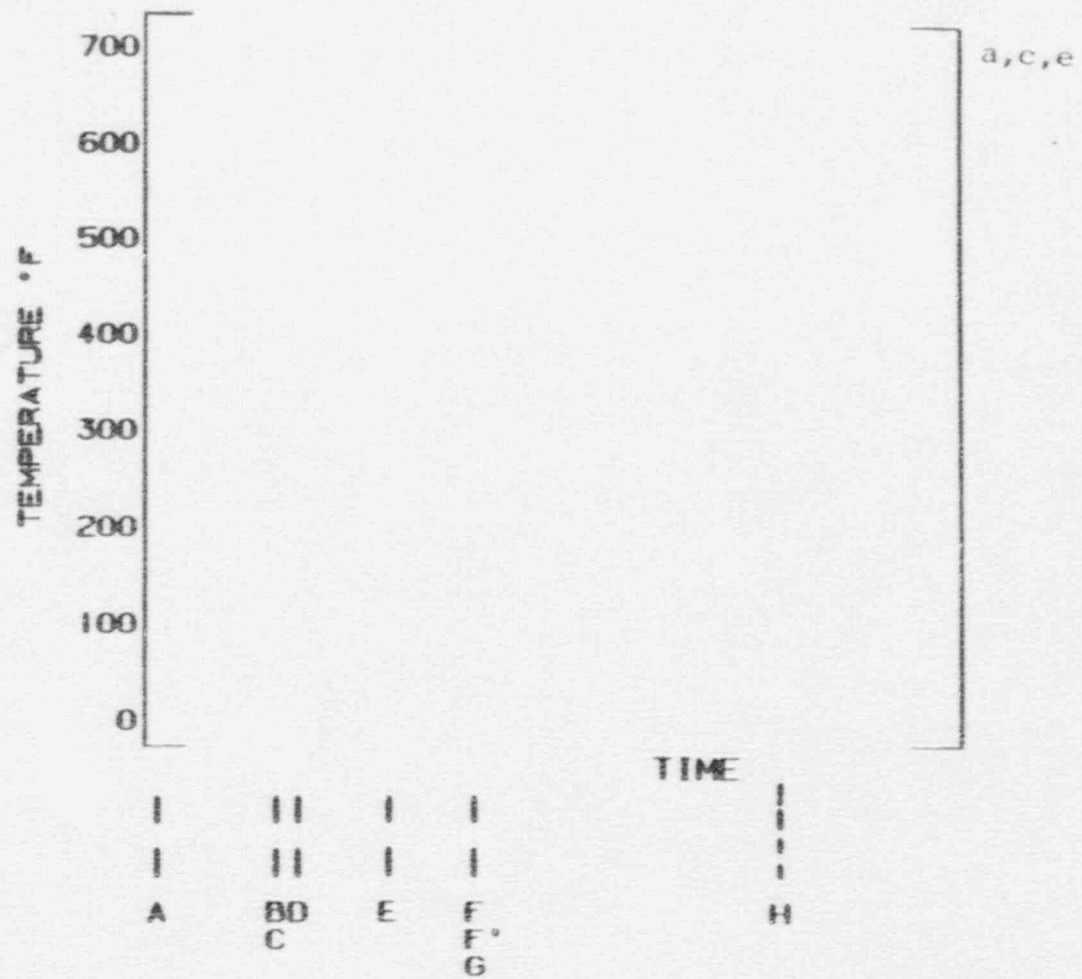


Figure 1-25. Cooldown []^{a,c,e}

1-64

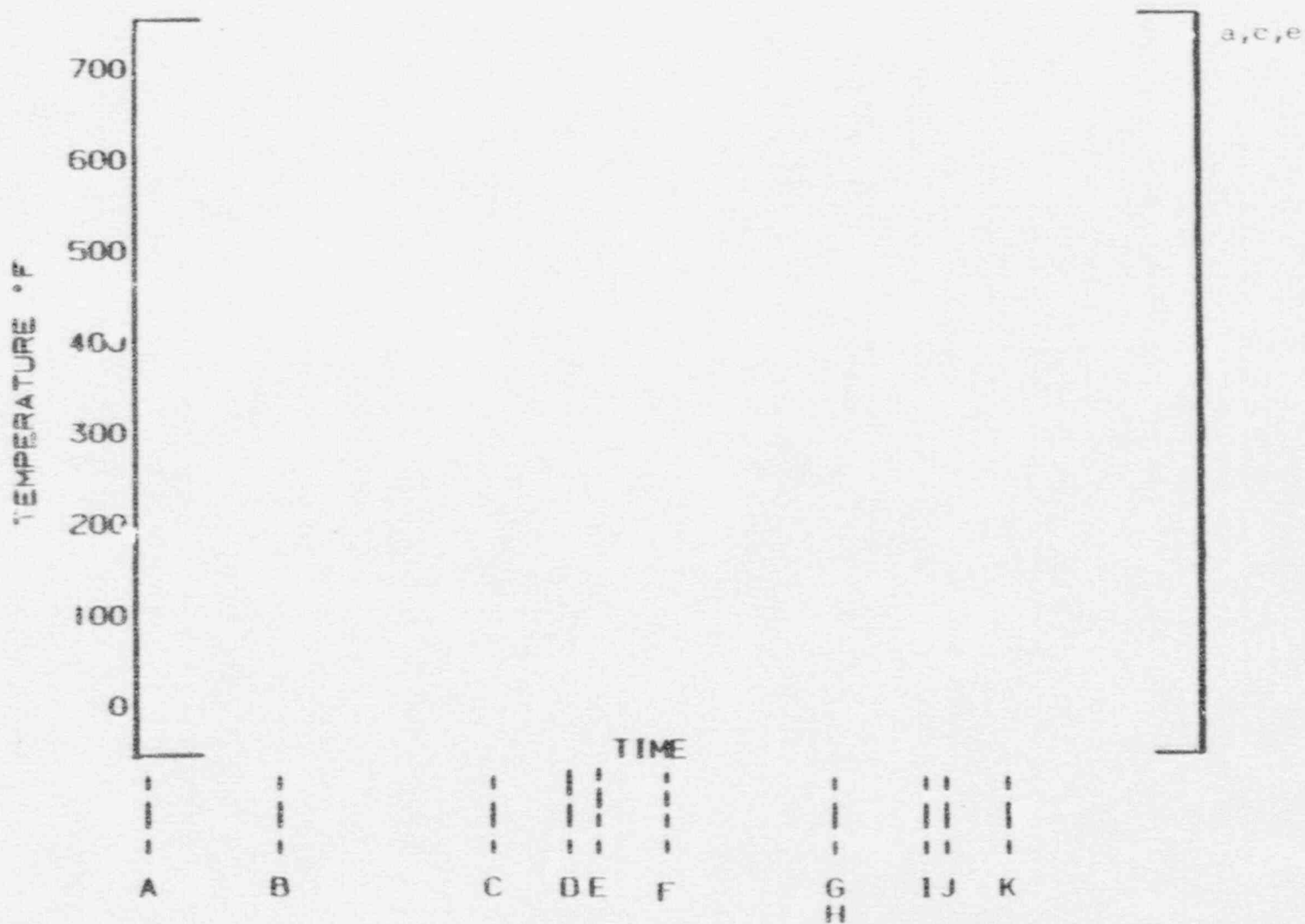


Figure 1-26. Heatup []^{a,c,e}

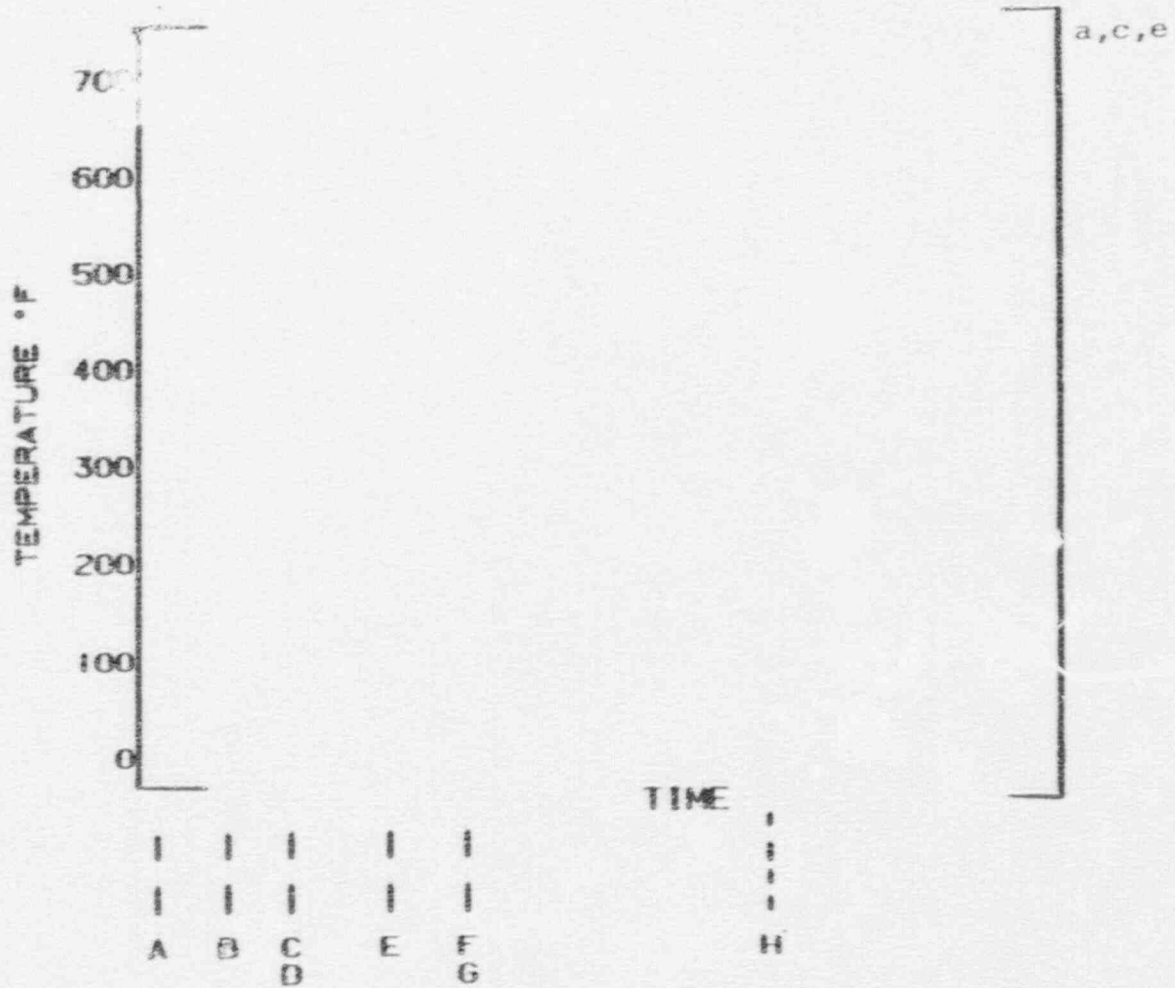


Figure 1-27. Cooldown []^{a,c,e}

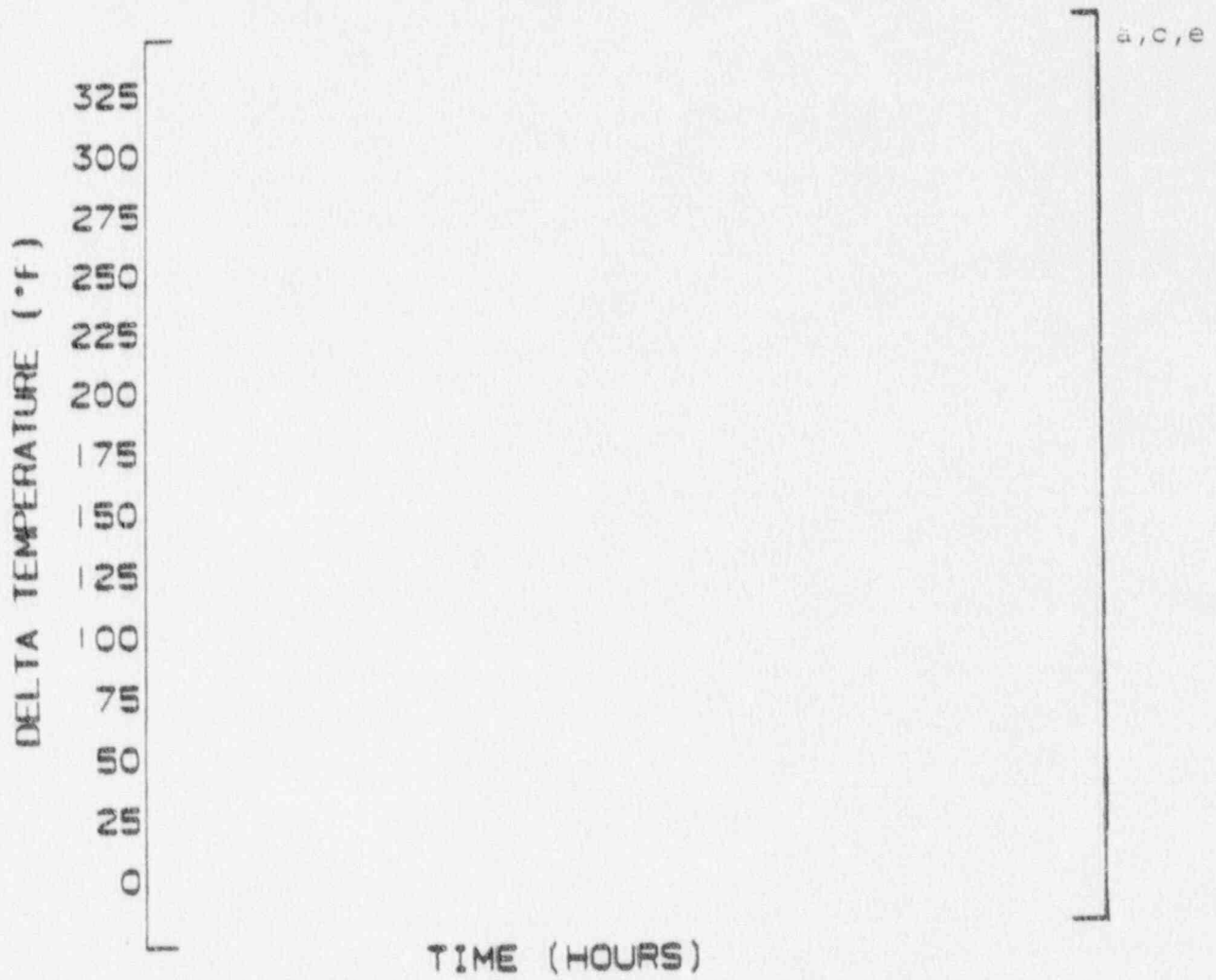


Figure 1-28. [

] ^{a,c,e} Location 1 - Heatup (4 days)



a,c,e

Figure 1-29 [

] ^{a,c,e} Location 2 - Heatup (11 Days)

89-1

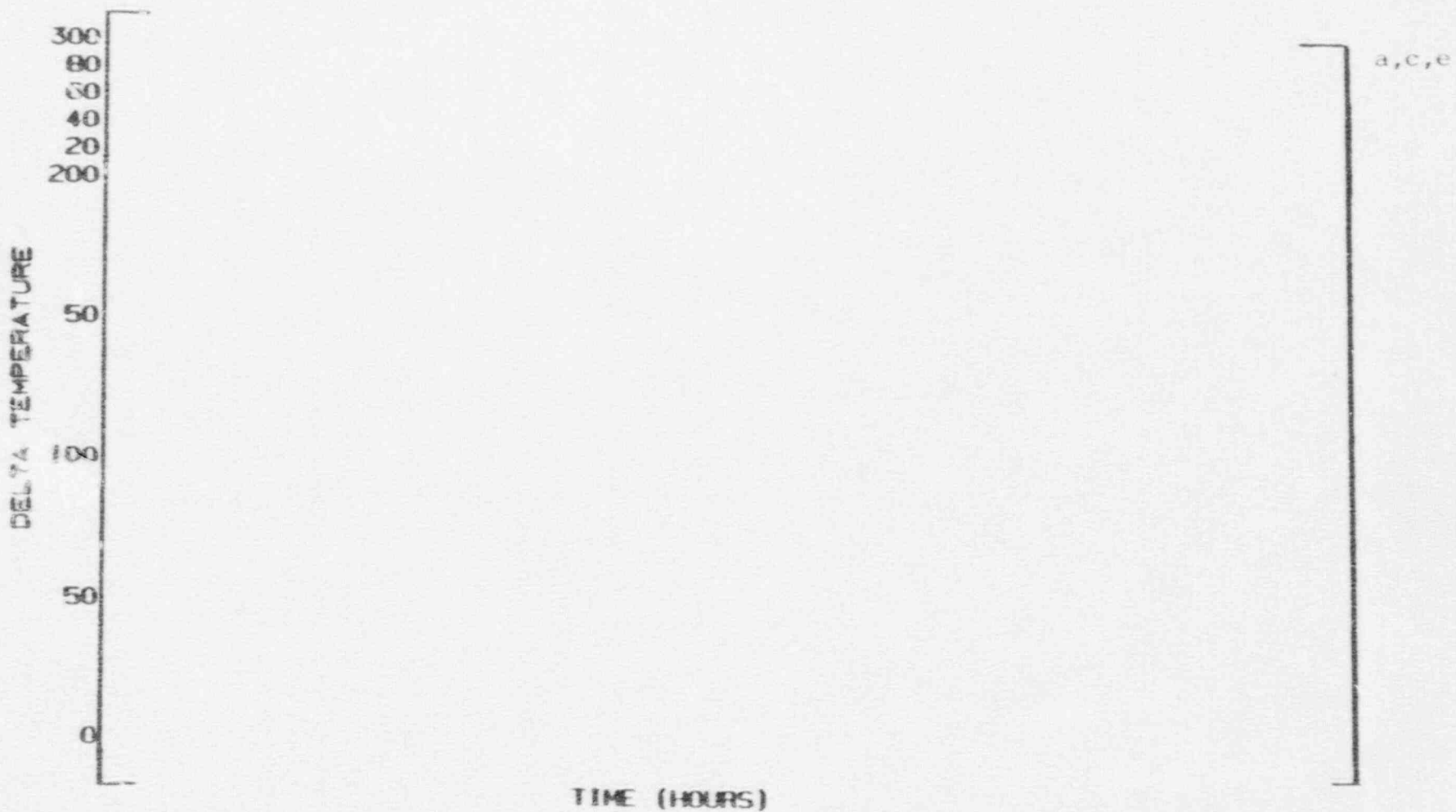


Figure 1-30. []^{a,c,e} Location 1 - Heatup (7 Days)

69-1

DELTA TEMPERATURE (°F)

EVENT NUMBER

a,c,e

Figure 31. []^{a,c,e} Location 1 Fatigue Cycles - Heatup (11 Days)

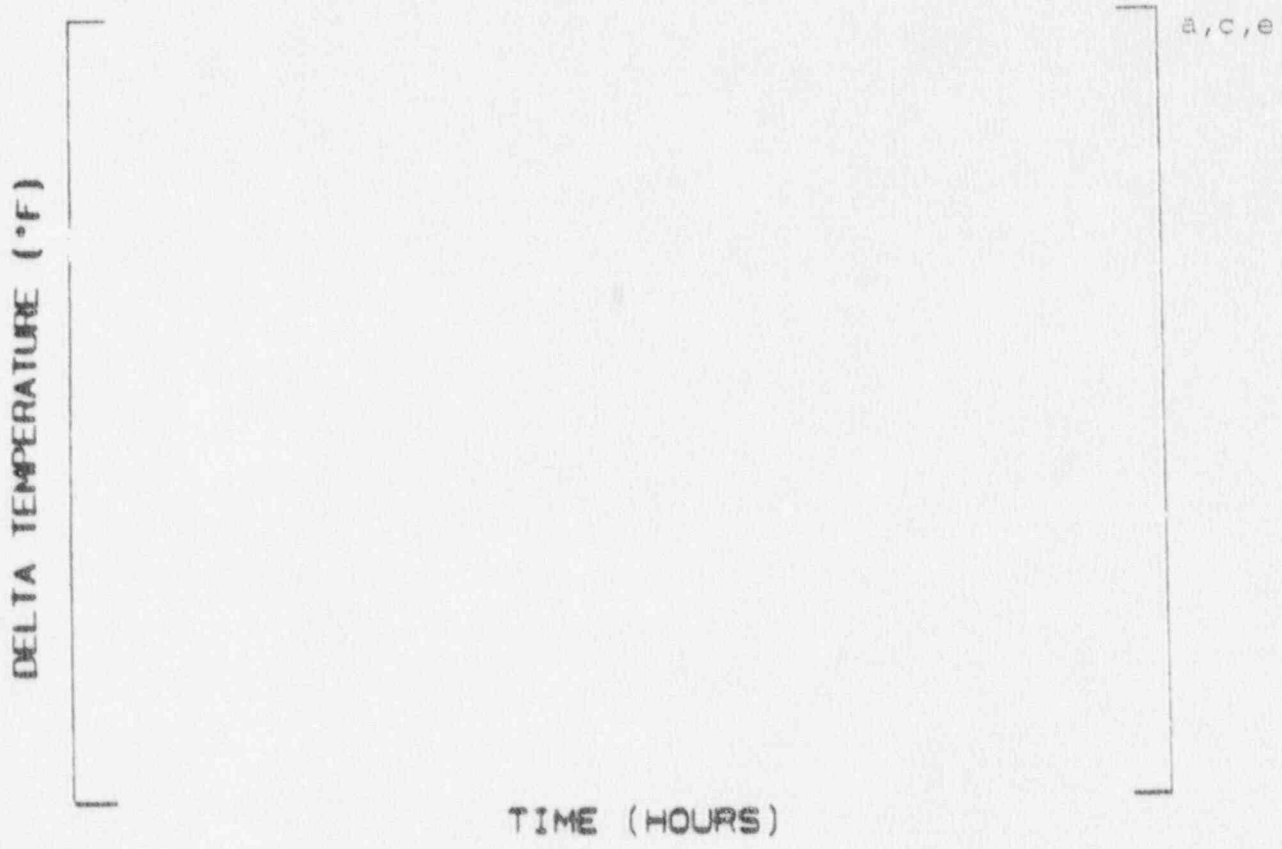


Figure 1-32. Plant C Location #1 (3 Days)

CYCLES (ONE HEATUP)

a, c, e

Figure 1-33. Comparison of Design to Monitored Transients



Figure 1-34. Comparison of Design to Monitored Transients

SECTION 2.0 STRESS ANALYSES

Flow diagram figure 2-1 describes the procedure to determine the effects of thermal stratification on the pressurizer surge line based on transients developed in section 1.0. [

]a,c,e

Section 2.1 Addresses the structural or global effect of stratification

Section 2.2 Addresses the local stress effects due to the nonlinear portion of the temperature profile

Section 2.3 Addresses the total stress effects due to the oscillation of the hot-to-cold boundary layer (striping) plus the thermal stratification stress

2.1 Piping System Structural Analysis

2.1.1 Introduction

The thermal stratification computer analysis of the piping system to determine the pipe displacement, support reaction loads as well as moment and force loads in the piping is referred to as the piping system structural analysis. These loads are used as input to the leak-before-break, fatigue, and fatigue crack growth evaluations. The thermal stratification condition consists of both axial and radial variations in the pipe metal temperature, as described in section 1.0. The model consists of straight pipe and elbow elements for the ANSYS computer code. [

]a,c,e These studies verified the suitability of the ANSYS computer code for the thermal stratification analysis. [

]a,c,e

j a, c, e

2.1.2 Discussion

The piping layout for a typical surgeline is shown in figure 2-3. The rigid support, R11, originally installed to reduce deadweight and seismic loads provides resistance to the displacements caused by thermal stratification.

[

j a, c, e

[

j a, c, e

[

]a,c,e

2.1.3 Results from Beaver Valley Unit 1 Analysis

The pressurizer surge line of Beaver Valley Unit 1 was structurally analyzed based on both a no pipe whip restraint contact configuration and the existing gaped configuration. During this period, the pipe whip restraint gaps were shimmed to a set of design values. On the last heat-up, the monitoring data obtained showed no whip restraint was in contact because of the imposed operating procedure. On the cooldown cycle, however, a conservative assumption was made in the fatigue analysis to reflect a potential of contact for the configuration even though the same imposed operating procedure remain effective. After this cycle, the pipe whip restraint gaps will be enlarged to allow for all thermal movement.

During one past plant specific heat-up under the non-contact configuration, the measured displacement of 1.90 inches in the vertical direction at whip restraint SLR-4 (Node 184) compares well with the calculated displacement of 1.97 inches at a pipe ΔT of 160°F. In the analysis, the calculated piping stress due to thermal stratification was reviewed to ensure that the system will not collapse in a "hinge-moment" mechanism. The primary plus secondary stress limit for this piping stress is given by ASME III, Section NB 3600, Equation 12 as $3.0 S_m$. The calculated stress intensity range was determined from the methodology in ASME III, Section NB-3685. The maximum Equation 12 stress intensity range, which occurs at the hot leg nozzle, is 49.9 ksi. This is less than the Code allowable value of 53.0 ksi. This corresponds to a bounding thermal stratification case with the system $\Delta T = 320^\circ\text{F}$. The maximum Equation 13 stress intensity range is 36.4 ksi as compared to the Code allowable of 50.1 ksi.

For the case where the system $\Delta T = 320^\circ\text{F}$ was exceeded from Section 1.2.9, the higher system $\Delta T = 335^\circ\text{F}$ was considered in the structural analysis. The maximum equation (12) stress intensity range is 52.0 ksi for the non-contract configuration, which is also smaller than the allowable 53.0 ksi.

2.1.4 Conclusions

Analytical studies with the ANSYS and WECAN computer codes have confirmed the validity of using an equivalent linear radial temperature profile to represent

the thermal stratification for displacement and loads. Good agreement was obtained between the ANSYS results and the measured displacements with thermal stratification. Eleven cases of thermal stratification were analyzed using the ANSYS code for the Beaver Valley Unit 1 surge line. Results for all other cases of stratification were obtained by interpolation. The resulting loads on the pressurizer and hot leg nozzles are acceptable. The surge line pipe stress satisfies the ASME III NB-3600 Code Equation 12 limits. Pipe movements will be reviewed for clearance considerations. The above conclusions are summarized in figure 2-23.

2.2 Local Stress Due to Non-Linear Thermal Gradient

2.2.1 Explanation of Local Stress

Figure 2-24 depicts the local axial stress components in a beam with a sharply nonlinear metal temperature gradient. Local axial stresses develop due to the restraint of axial expansion or contraction. This restraint is provided by the material in the adjacent beam cross section. For a linear top-to-bottom temperature gradient, the local axial stress would not exist. [1]

]a,c,e

2.2.2 Superposition of Local and Structural Stresses

For the purpose of this discussion, the stress resulting from the global structural analysis (section 2.1) will be referred to as "structural stress."

[
]a,c,e Local and structural stresses may be superimposed to obtain the total stress. This is true because linear elastic analyses are performed and the two stresses are independent of one another as summarized in figure 2-25.

Figure 2-26 presents the results of a test case that was performed to demonstrate the validity of superposition. As shown in the figure, the superposition of local and structural stress is valid. [

]a,c,e

2.2.3 Finite Element Model of Pipe for Local Stress

A short description of the pipe finite element model is shown in figure 2-27. The model with thermal boundary conditions is shown in figure 2-28. Due to symmetry of the geometry and thermal loading, only half of the cross section was required for modeling and analysis. [

]a,c,e

2.2.4 Pipe Local Stress Results

Figure 2-29 shows the temperature distributions through the pipe wall [

]a,c,e

]a,c,e

2.2.5 Unit Structural Load Analyses For Pipe

In order to accurately superimpose local and structural stresses, several additional stress analyses were performed using the 2-D pipe model. [

]a,c,e

2.2.6 RCL Hot Leg Nozzle Analysis

Two RCL surge line nozzle models were developed to evaluate the effects of thermal stratification. These two models are shown in figures 2-43 and 2-44. [

]a,c,e

Figures 2-46 thru 2-54 present color contour plots of temperature and stress distributions in the surge line RCL nozzle. A summary of local stresses in the RCL nozzle due to thermal stratification is given in table 2-5. A summary of pressure and bending stresses for unit loading is shown in table 2-6.

Results of the local stress analysis are summarized in figure 2-55.

2.2.7 Conservatism

Conservatism in the local stress analysis are listed on figure 2-56. [

]a,c,e

2.3 Thermal Striping

2.3.1 Background (figure 2-57)

At the time when the feedwater line cracking problems in PWR's were first discovered, it was postulated that thermal oscillations (striping) may significantly contribute to the fatigue cracking problems. These oscillations were thought to be due to either mixing of hot and cold fluid, or turbulence in the hot-to-cold stratification layer from strong buoyancy forces during low flow rate conditions. (See figure 2-58 which shows the thermal striping fluctuation in a pipe). Thermal striping was verified to occur during subsequent flow model tests. Results of the flow model tests were used to establish boundary conditions for the stratification analysis and to provide striping oscillation data for evaluating high cycle fatigue.

Thermal striping was also examined during water model flow tests performed for the Liquid Metal Fast Breeder Reactor primary pipe loop. The stratified flow was observed to have a dynamic interface region which oscillated in a wave pattern. (See figure 2-59 for test pipe sizes, thermocouple locations, and table 2-7 for typical frequency of striping oscillations.) These dynamic oscillations were shown to produce significant fatigue damage (primary crack initiation). The same interface oscillations were observed in experimental studies of thermal striping which were performed in Japan by Mitsubishi Heavy Industries.

2.3.2 Thermal Striping Stresses

Thermal striping stresses are a result of differences between the pipe inside surface wall and the average through wall temperatures which occur with time, due to the oscillation of the hot and cold stratified boundary. (See figure 2-60 which shows the typical temperature distribution through the pipe wall).

[

$\sigma_{a,c,e}$

The peak stress range and stress intensity is calculated from a 2-D finite element analysis. (See figure 2-61 for a description of the model.) [

$\sigma_{a,c,f}$ The methods used to determine alternating stress intensity are defined in the ASME code. Several locations were evaluated in order to determine the location where stress intensity was a maximum.

Stresses were intensified by K_3 to account for the worst stress concentration for all piping element in the surge line. The worst piping element was the butt weld.

[

$\sigma_{a,c,e}$

2.3.3 Factors Which Affect Striping Stress

The factors which affect striping are listed in figure 2-63:

[

$\sigma_{a,c,e}$

[

]a,c,e

[

]a,c,e

2.3.4 Conservatism

The conservatisms in the striping analysis are listed in figure 2-65. The major conservatism involves the combination of maximum striping usage factor with fatigue usage factor from all other stratification considerations. The

[

]a,c,e

TABLE 2-1
COMPARISON OF WECAN AND ANSYS RESULTS FOR
LINEAR STRATIFICATION - Case 2
(Displacements in Inches)

(JOBANSF) WECAN	(AGJAQLM) ANSYS	ANSYS/WECAN (PERCENTAGE)
-----------------	-----------------	-----------------------------

a,c,e

TABLE 2-2
 COMPARISON OF WECAN []^{a,c,e} A
 ANSYS []^{a,c,e} RESULTS FOR () E 3

Location	Direction	WECAN Case 3	ANSYS Case 3L	Case 3L/Case 3 (Percentage)
----------	-----------	--------------	---------------	--------------------------------

				a,c,e

Case 3L ANSYS: DC1SKXY, 11/12/88

TABLE 2-3
TEMPERATURE PROFILES IN PRESSURIZER SURGE LINE

a, c, e

TABLE 2-4
 BEAVER VALLEY SURGE LINE
 MAXIMUM LOCAL AXIAL STRESSES AT []^{a,c,e}

Location	Surface	Local Axial Stress (psi)	
		Maximum Tensile	Maximum Compressive
[]			
[]			

TABLE 2-5
 SUMMARY OF LOCAL STRATIFICATION STRESSES
 IN THE SURGE LINE RCL NOZZLE

Location	Diametral Location	<u>Linearized Stress Intensity Range (psi)</u>		<u>Peak Stress Intensity Range (psi)</u>	
		Inside	Outside	Inside	Outside
<div style="position: absolute; top: 5px; right: 5px;">a,c,e</div>					

TABLE 2-6
SUMMARY OF PRESSURE AND BENDING INDUCED STRESSES
IN THE SURGE LINE RCL NOZZLE FOR UNIT LOAD CASES

Location	Diametral Location	Unit Loading Condition	All Stress in psi			
			Linearized Stress Intensity Range		Peak Stress Intensity Range	
			Inside	Outside	Inside	Outside
[Empty table body]						

a,c,e

TABLE 2-7
STRIPING FREQUENCY AT 2 MAXIMUM LOCATIONS FROM 15 TEST RUNS



a,c,e

DETERMINATION OF THE EFFECTS OF THERMAL STRATIFICATION

a, c, e

Figure 2-1. Determination of the Effects of Thermal Stratification



Figure 2-2. Stress Analysis

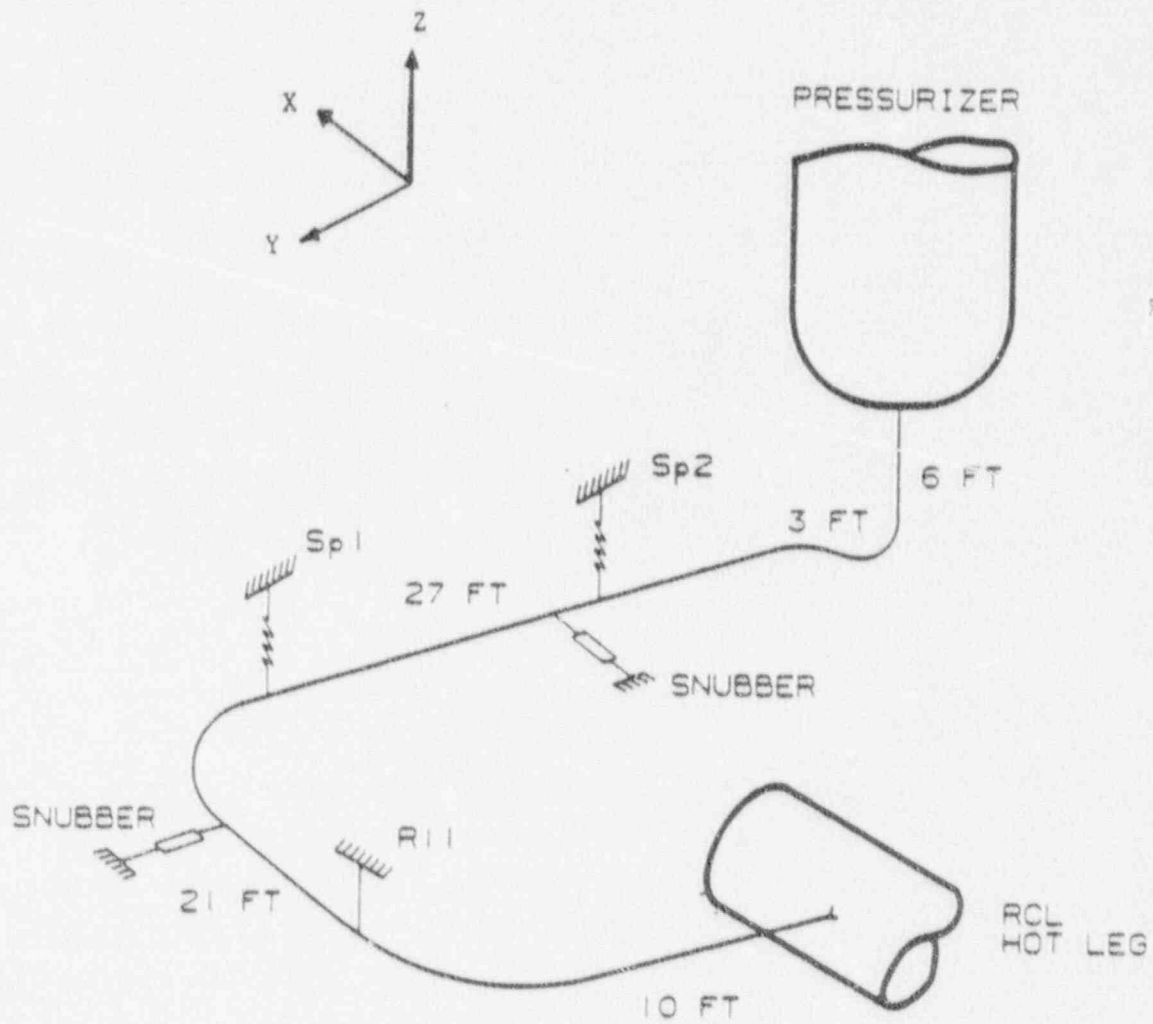


Figure 2-3. Typical Pressurizer Surge Line Layout



Figure 2-4. Cases 1 to 4: Radial Temperature Profiles

a, c, e



Figure 2-5. Case 5: Radial and Axial Temperature Profile



Figure 2-6. Finite Element Model of the Pressurizer Surge Line Piping
General View

a, c, e

Figure 2-7. Finite Element Model of the Pressurizer Surge Line Piping Hot Leg Nozzle Detail

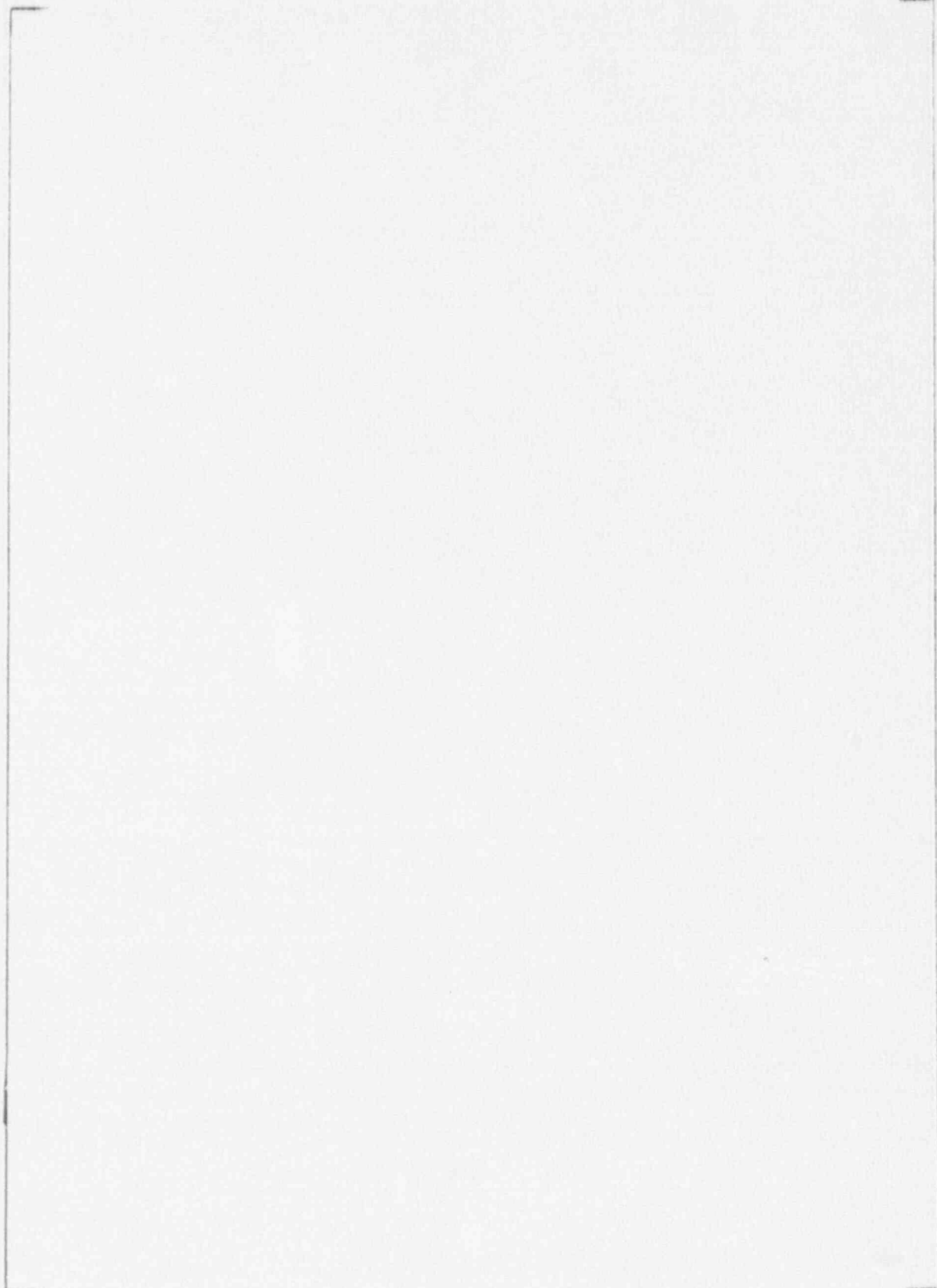


Figure 2-8. Thermal Expansion of the Pressurizer Surge Line Under Uniform Temperature

a, c, e

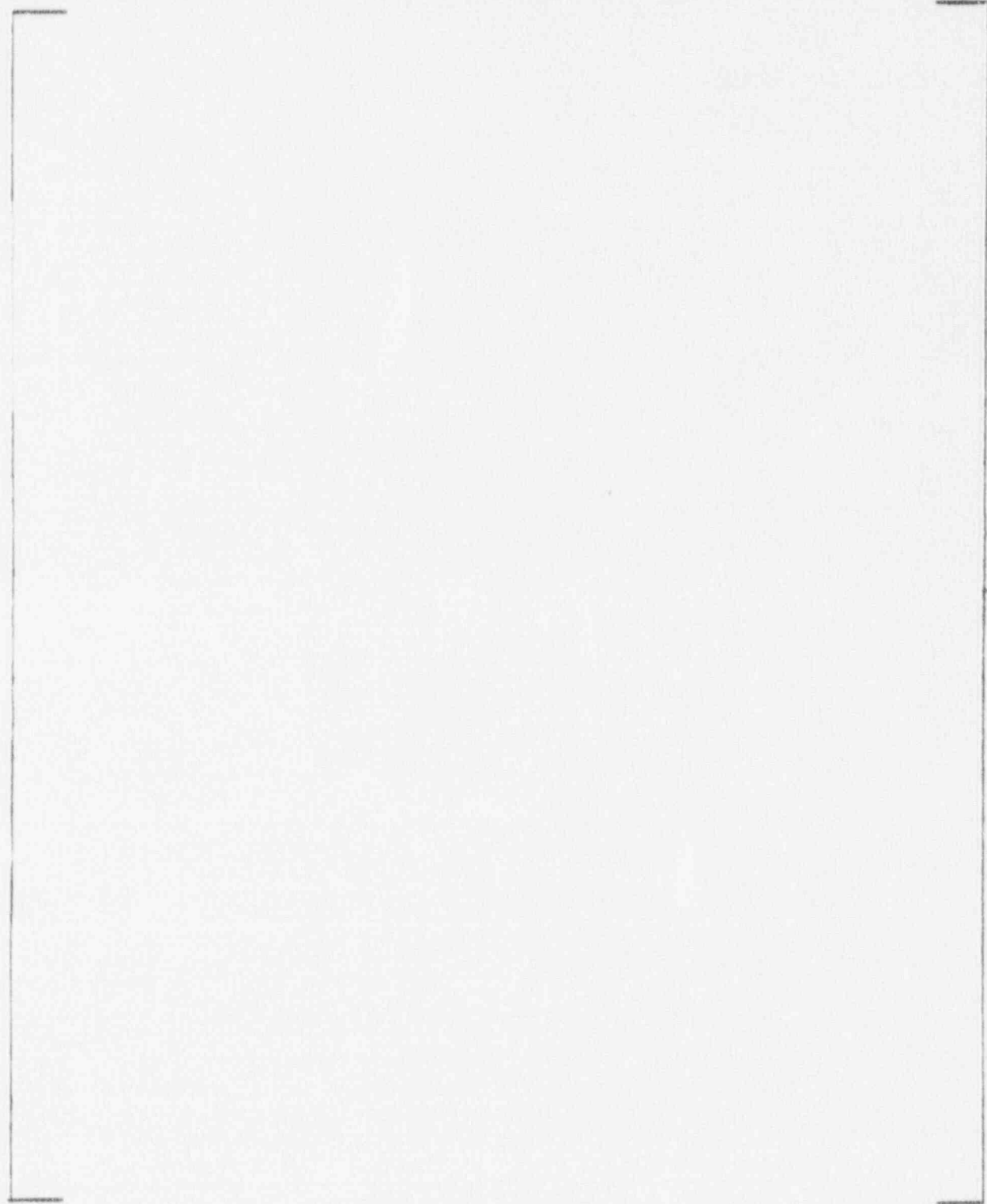


Figure 2-9. Case 2 (linear) Temperature Profile at Hot Leg Nozzle

a.c., 2

Figure 2-10. Case 2 (linear) Temperature Profile at Pressurizer Elbow

Figure 2-11. Thermal Expansion of Pressurizer Surge Line Under Linear Temperature Gradient



Figure 2-12. Bowing of Beams Subject to Top-to-Bottom Temperature Gradient

2-32

$a_3 C_3 t$

Figure 2-13. Case 3 (Mid-Plane Step): Temperature Profile at Hot Leg Nozzle

2-33



Figure 2-14. Case 3 (Mid-Plane Step): Temperature Profile at Pressurizer Nozzle



Figure 2-15. Case 4 (Top Half Step): Temperature Profile at Hot Leg Nozzle

2-35

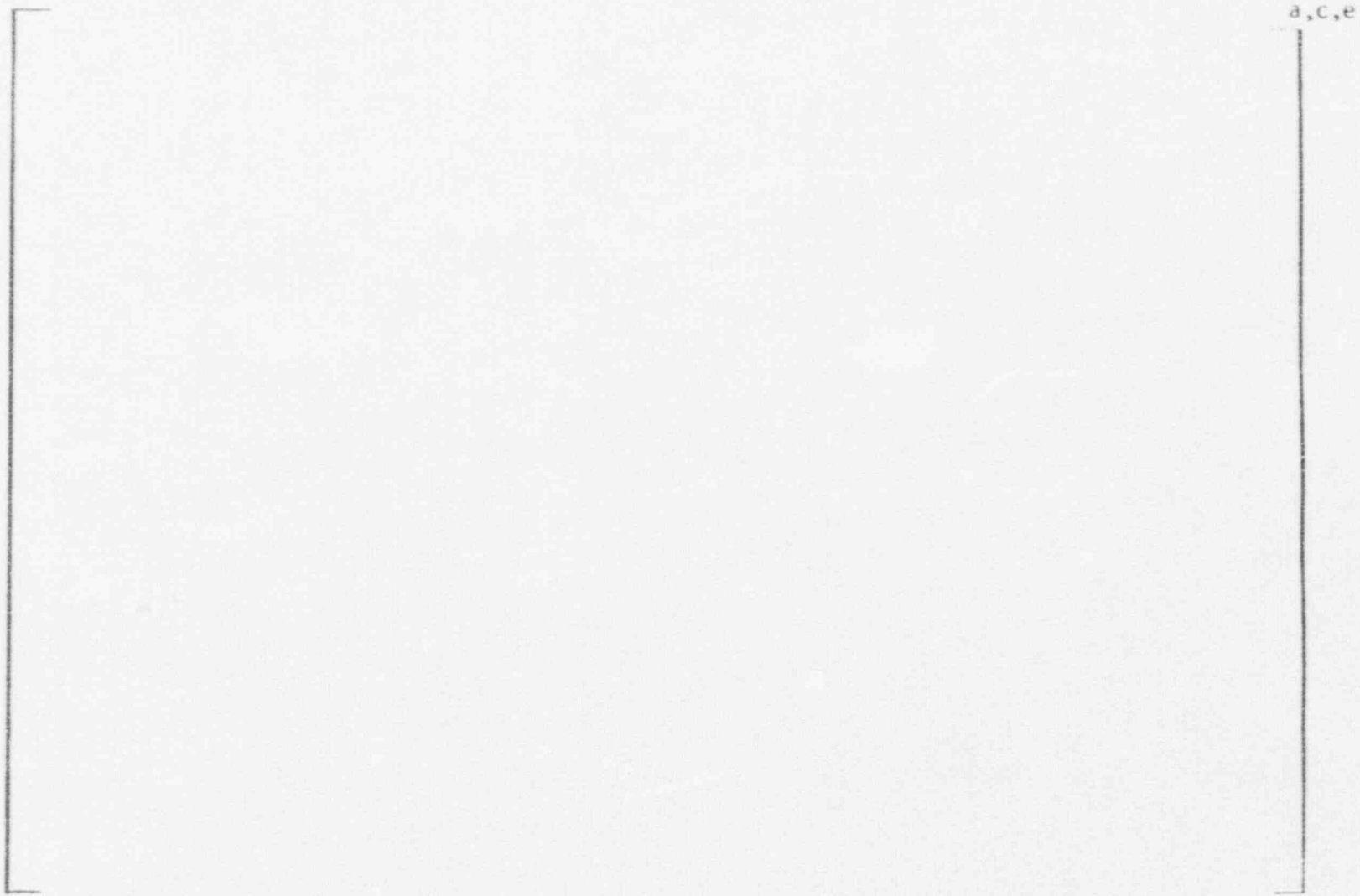


Figure 2-16. Case 4 (Top Half Step): Temperature Profile at Pressurizer Elbow



Figure 2-17. Case 5: Axial and Radial Temperature Profile

2-37

a,c,e



Figure 2-18. Case 5: Axial and Radial Temperature Profile at Hot Leg Nozzle



Figure 2-19. Case 5: Axial and Radial Temperature Profile at Pipe Bend



Figure 2-20. Case 5: Axial and Radial Temperature Profile at Pressurizer Elbow

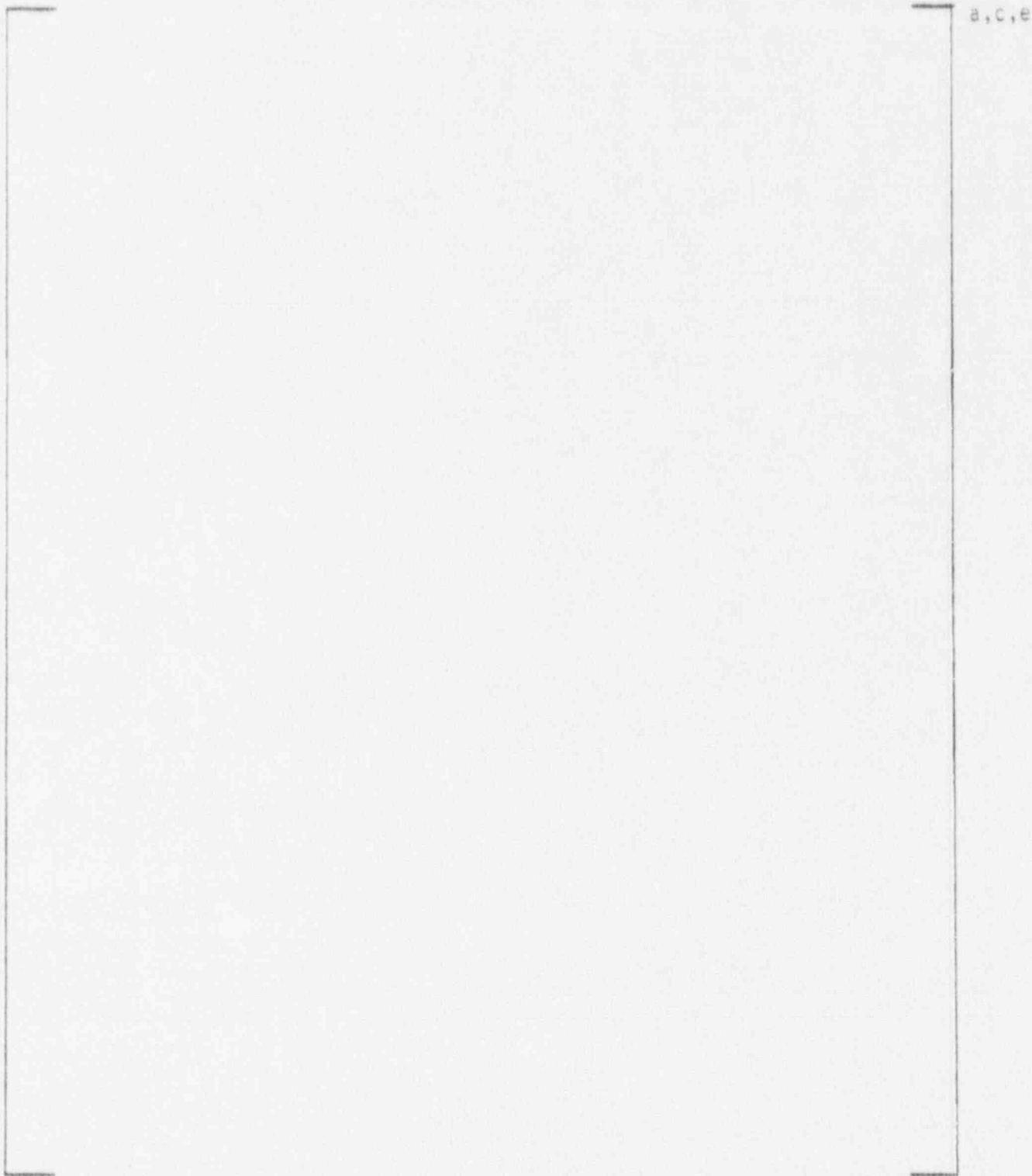


Figure 2-21. [

]a,c,e Profile

- ▲ FIELD WELDS
- ⊗ SHOP WELDS

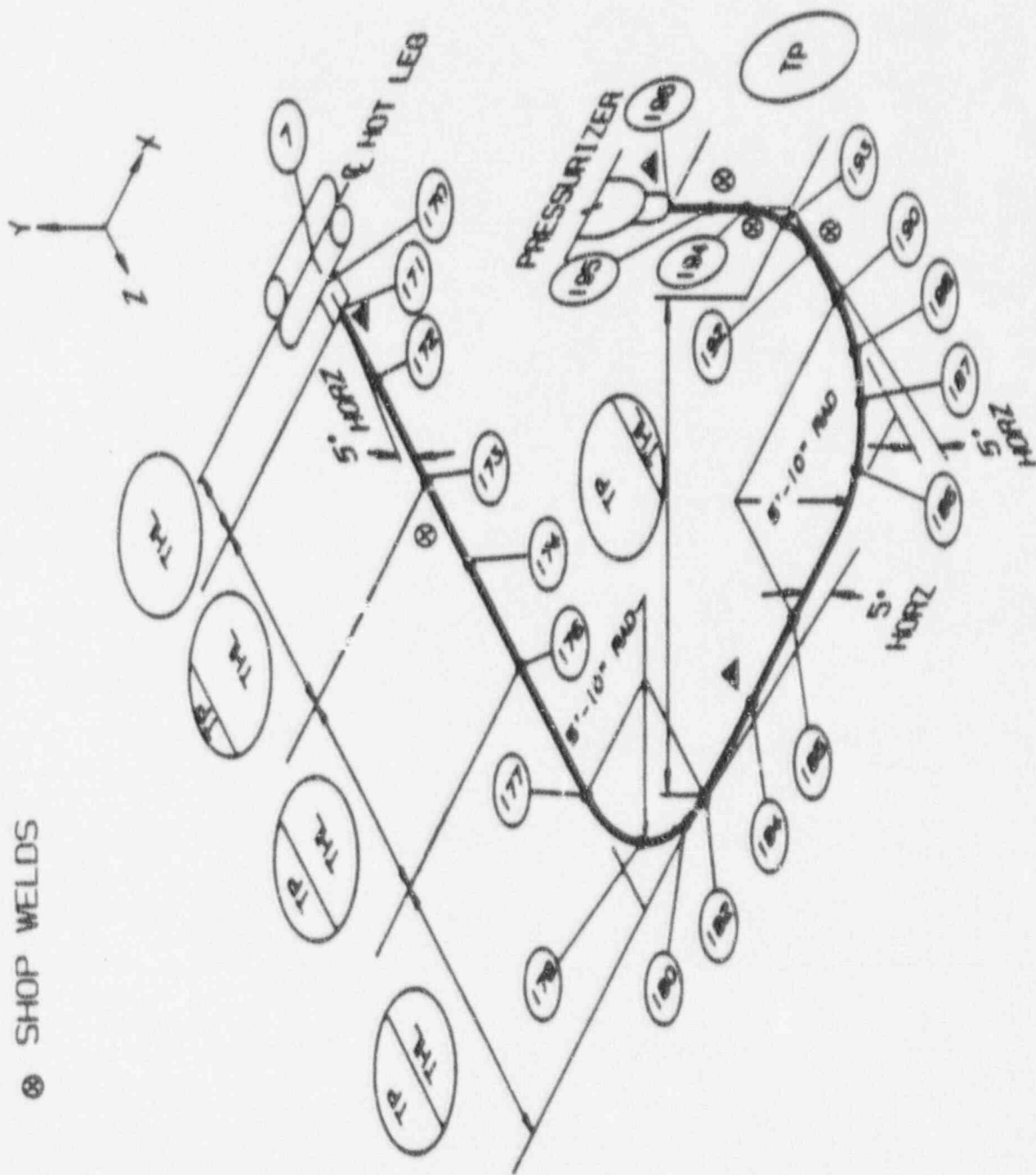


Figure 2-22. Beaver Valley Unit 1 Pressurizer Surge Line

- o Temperature Profiles Established Through Parametric Study
- o Good Agreements on Measured and Calculated Displacements at Node 182
- o Eleven (11) Cases Analyzed to Calculate All Required Loading Conditions
- o Pressurizer and Hot Leg Nozzle Loads Acceptable
- o Piping Stress Within Code Limits
- o Pipe Movements to be Reviewed Against Clearance

Figure 2-23. Conclusions - Global Stress Analysis

d, c, e

Figure 2-24. Local Stress in Piping Due to Thermal Stratification

a, c, e



Figure 2-25. Independence of Local and Structural Thermal Stratification Stresses Permits Combination by Superposition

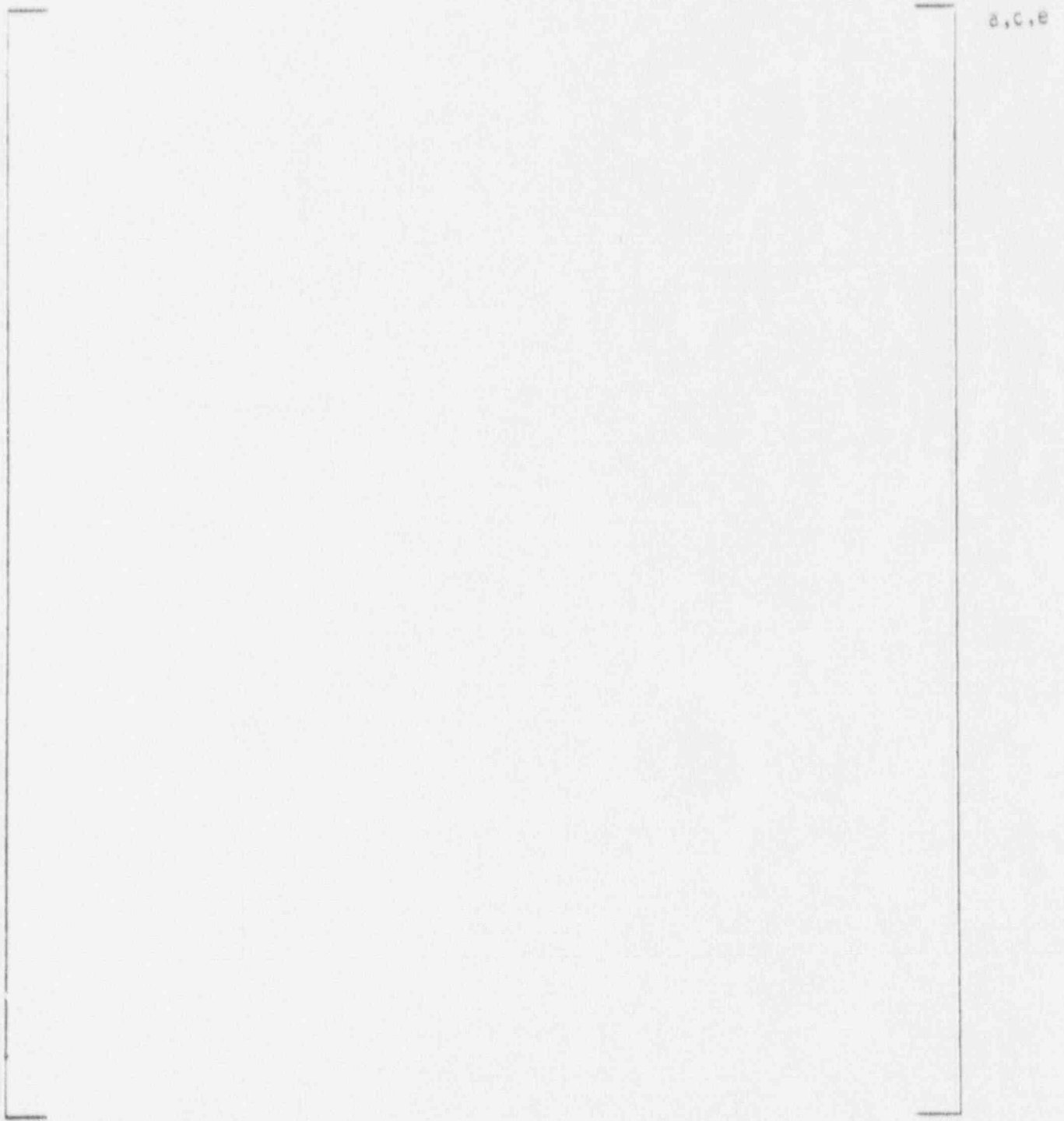


Figure 2-26. Test Case for Superposition of Local and Structural Stresses

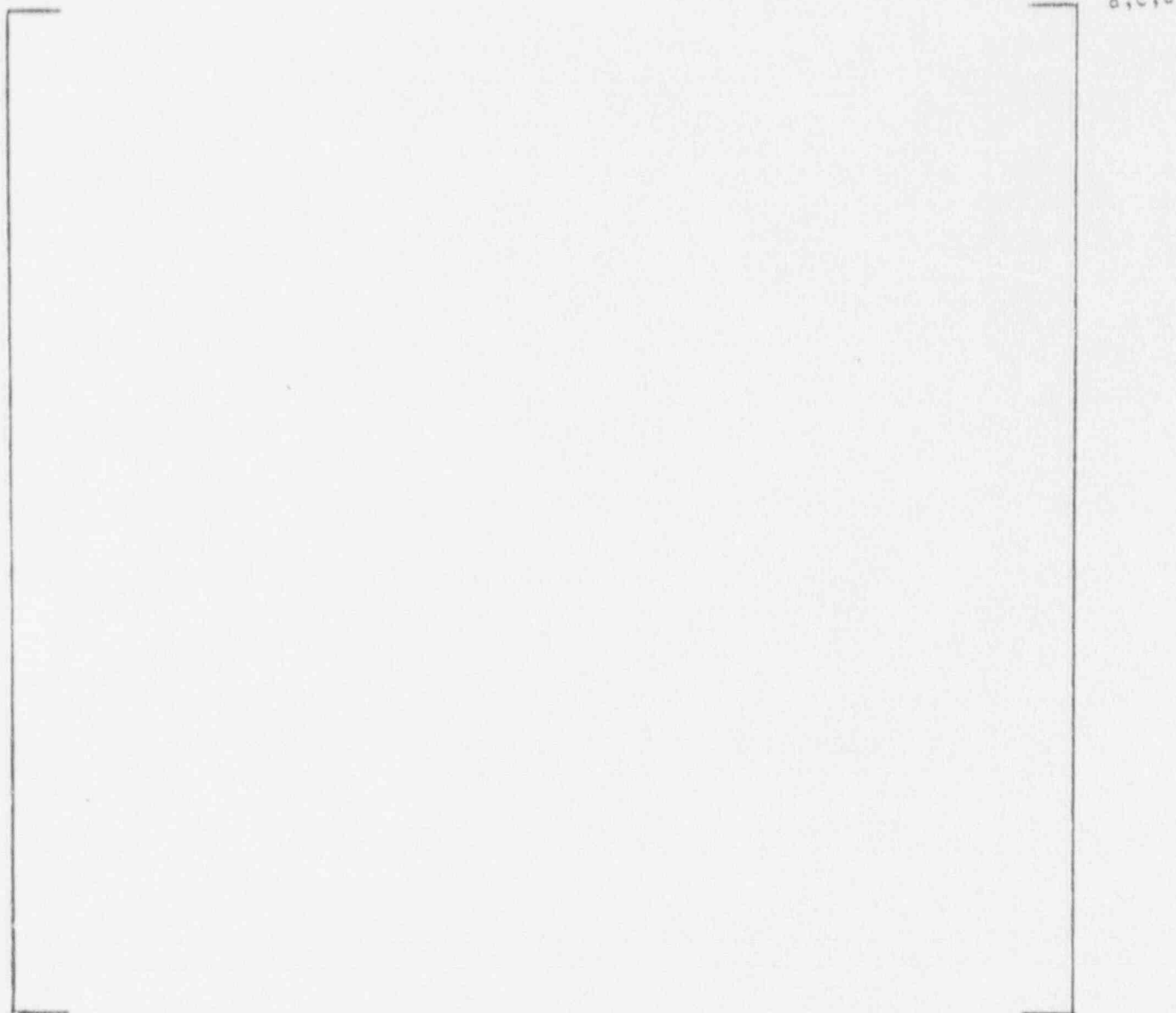


Figure 2-27. Local Stress - Finite Element Models/Loading

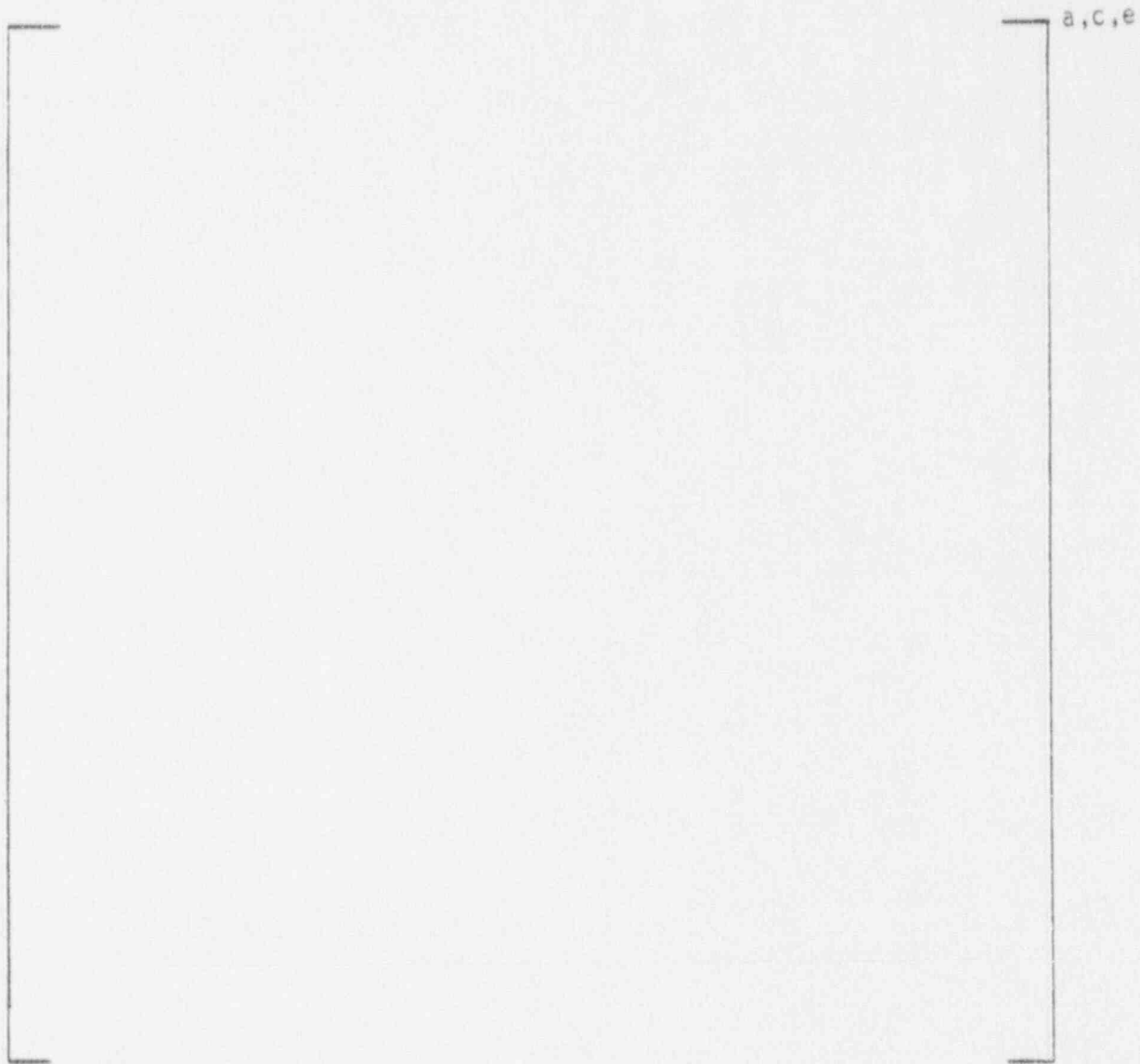


Figure 2-28. Piping Local Stress Model and Thermal Boundary Conditions

a,c,e

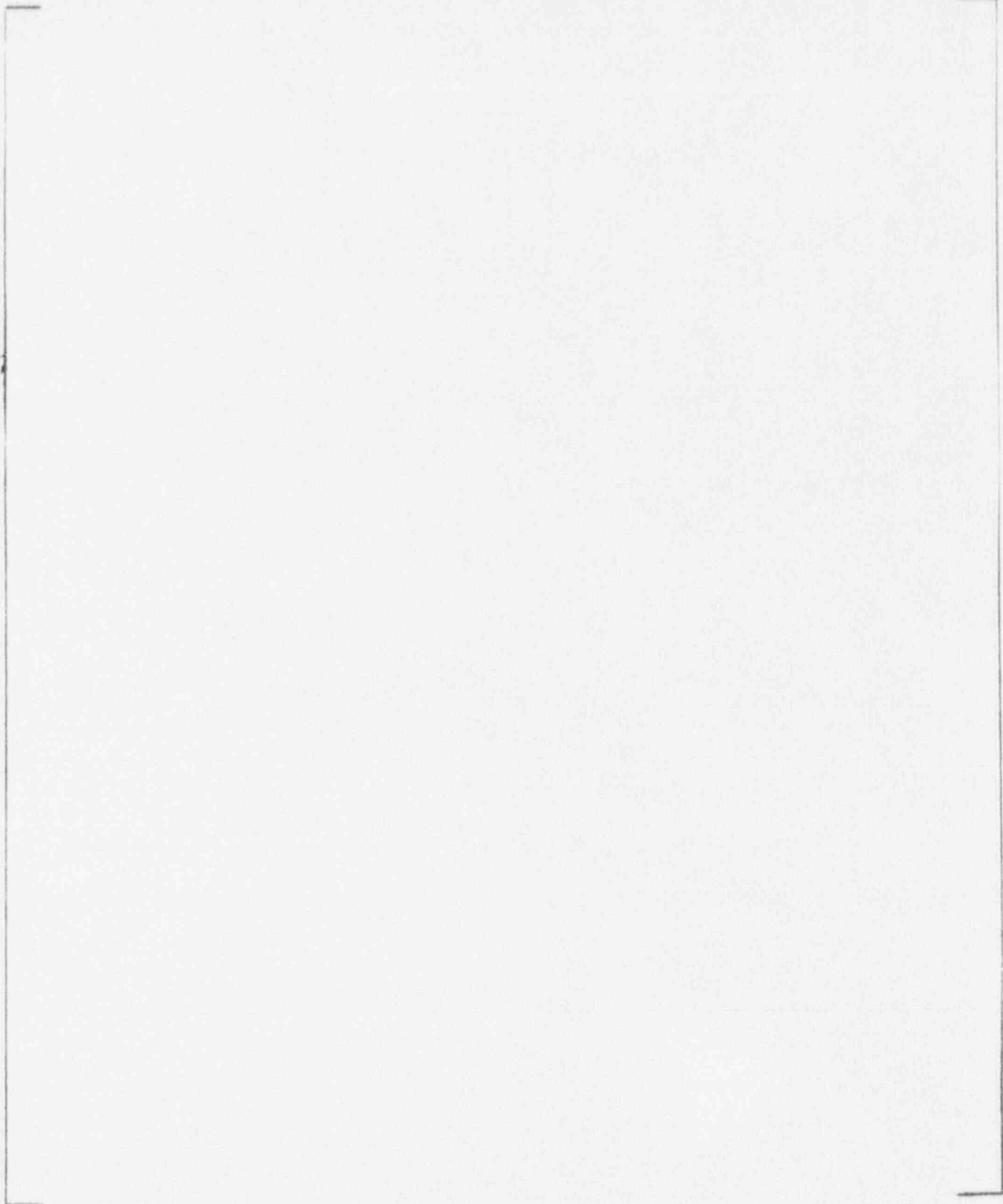


Figure 2-29. Surge Line Temperature Distribution at []^{a,c,e} Axial Locations

a,c,e

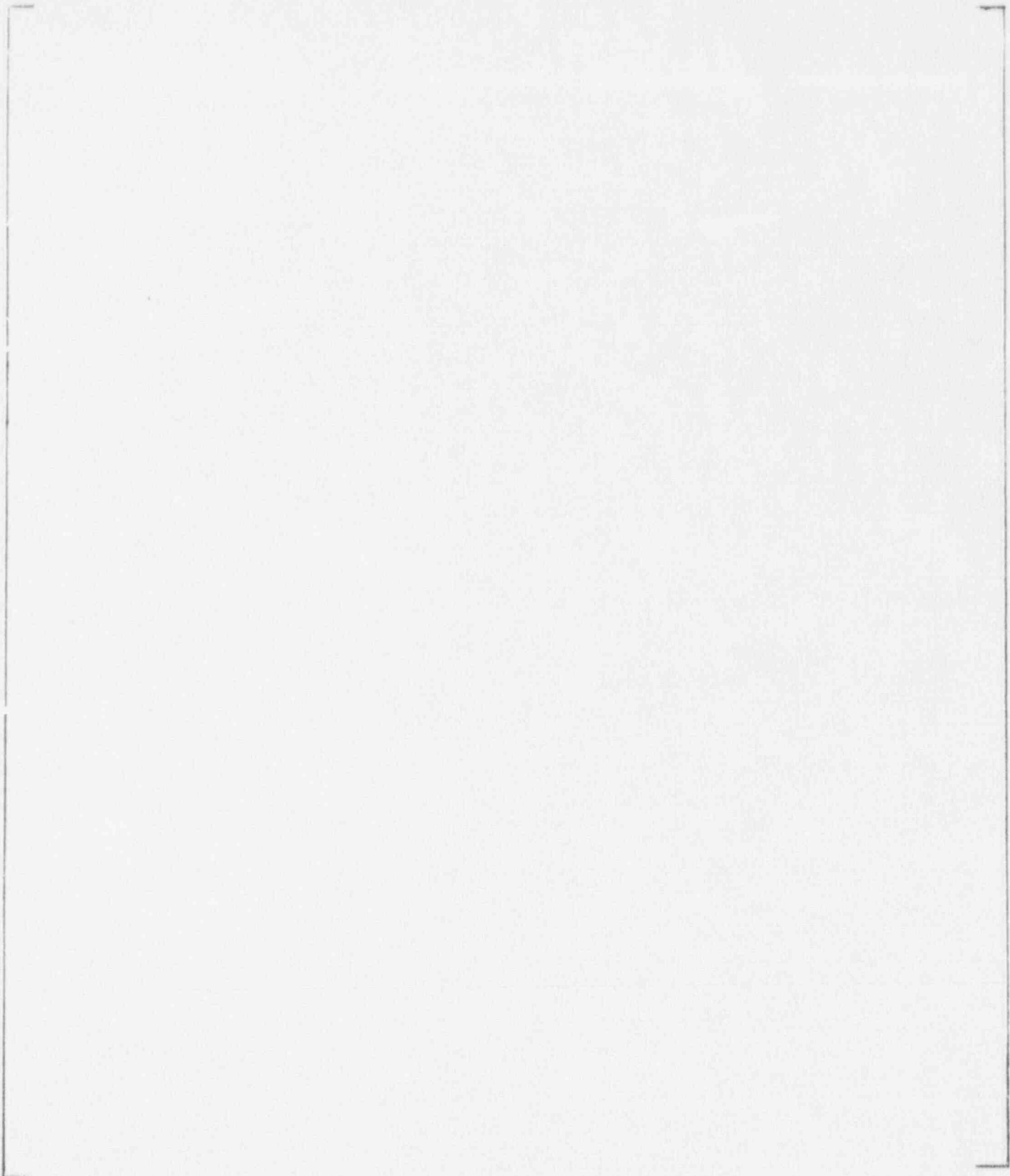


Figure 2-30. Surge Line Local Axial Stress Distribution at []^{a,c,e}
Axial Locations

a, c, e

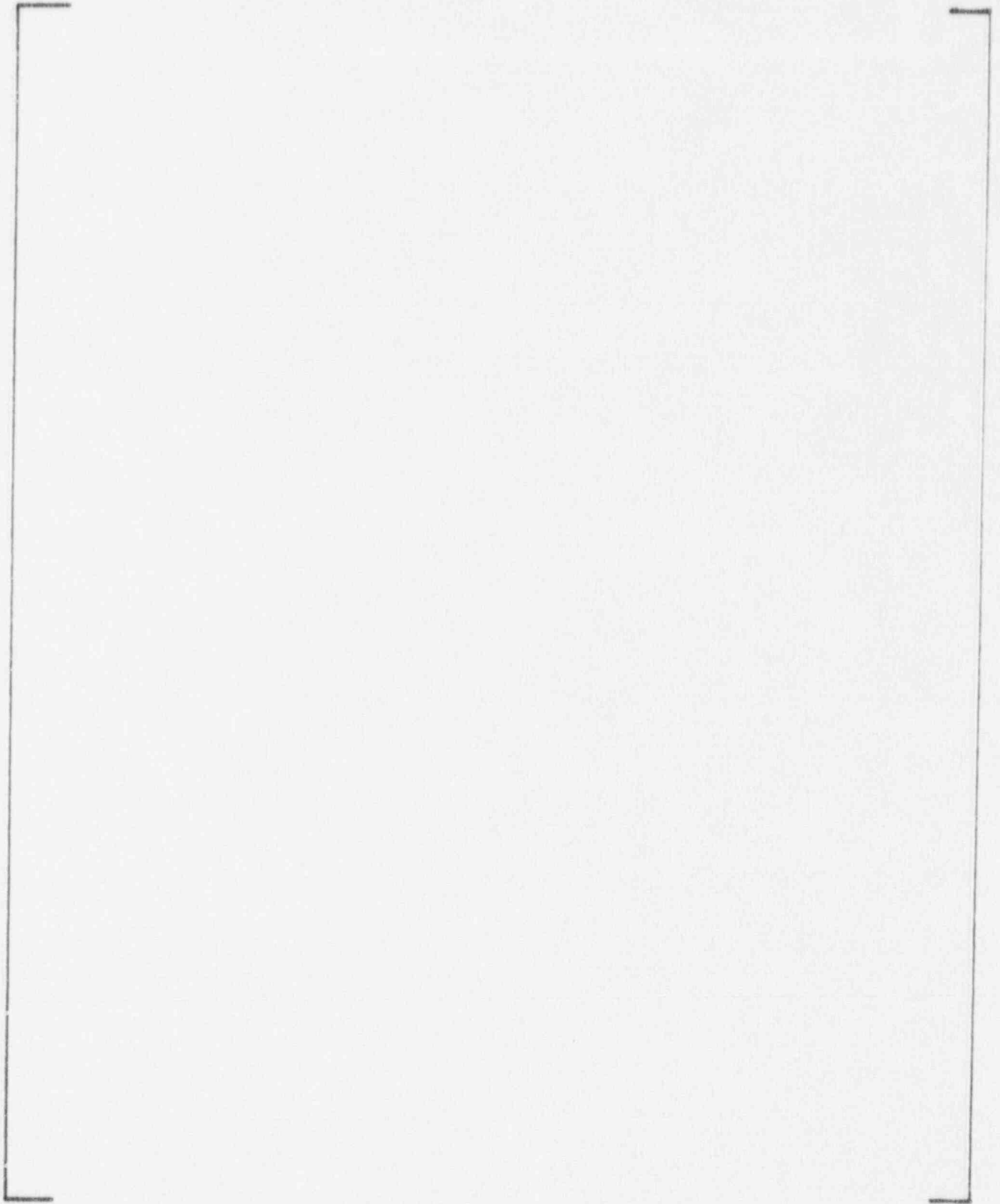


Figure 2-31. Surge Line Local Axial Stress on Inside Surface at
[]^{a, c, e} Axial Locations

a, c, e

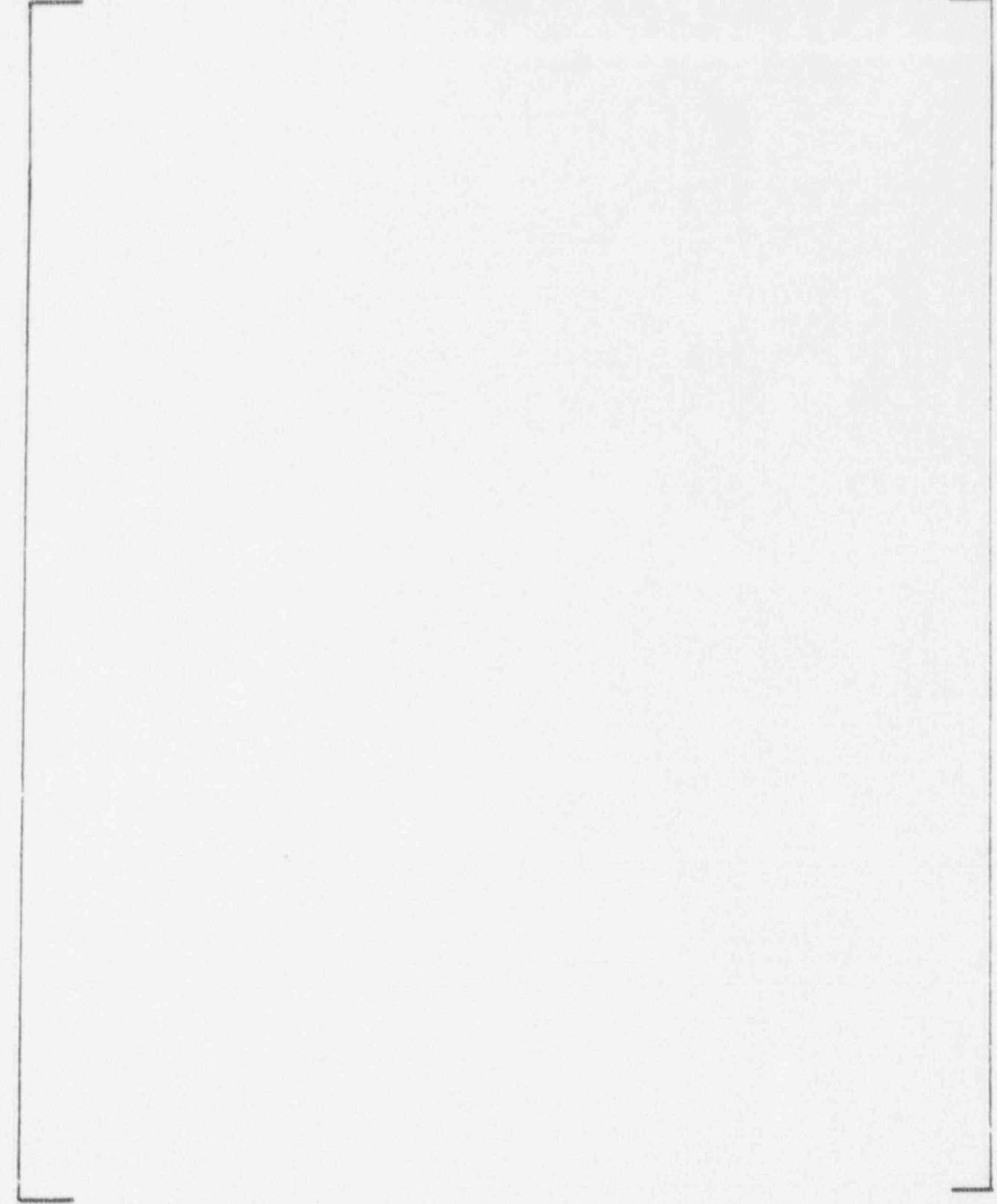


Figure 2-32. Surge Line Local Axial Stress on Outside Surface at []^{a, c, e} Axial Locations



Figure 2-33. Surge Line Temperature Distribution at Location []^{a,c,e}



Figure 2-34. Surge Line Local Axial Stress Distribution at Location []^{a,c,e}

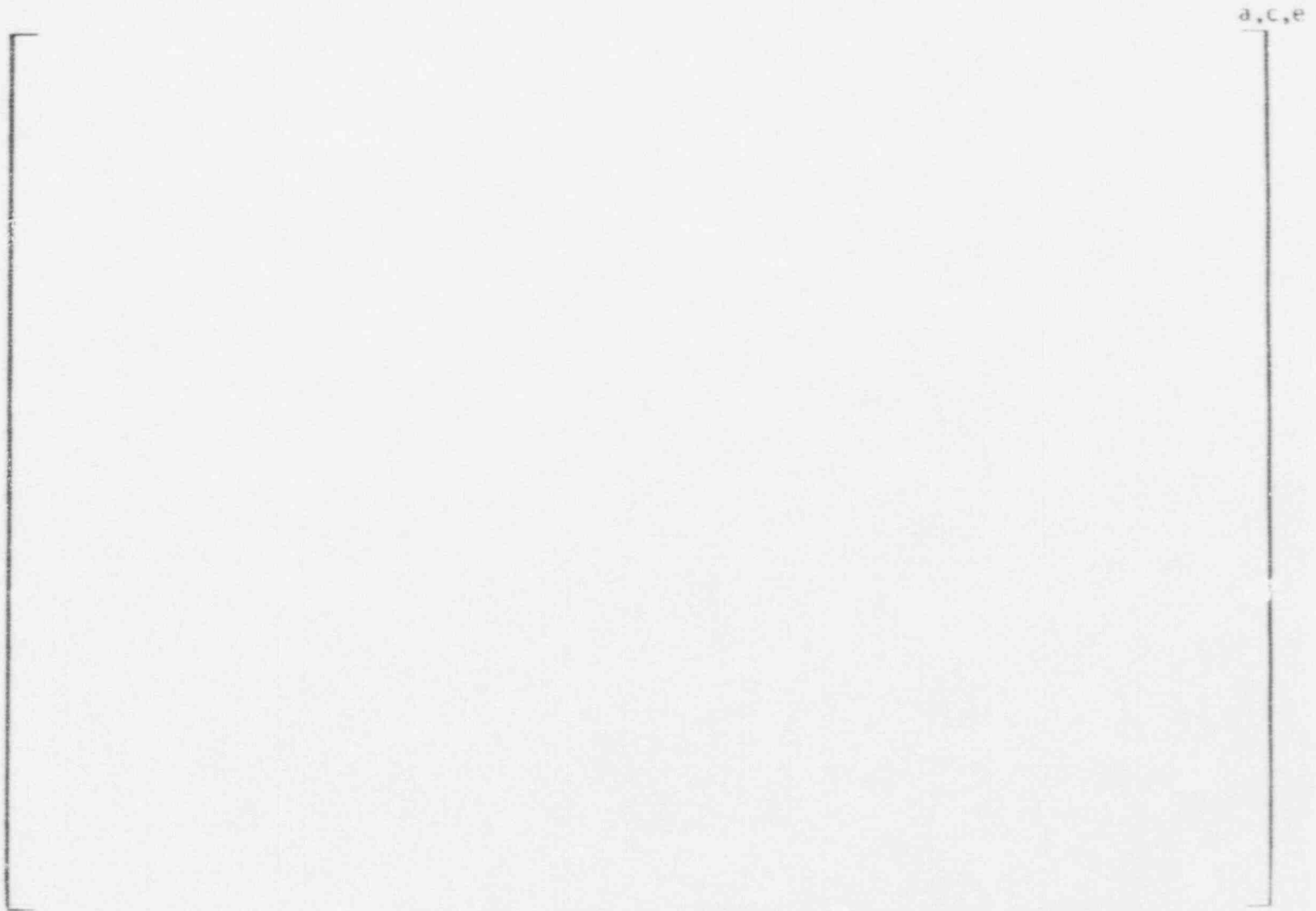


Figure 2-35. Surge Line Temperature Distribution at Location [] a,c,e

2-55



Figure 2-36. Surge Line Local Axial Stress Distribution at Location []^{a,c,e}



Figure 2-37. Surge Line Temperature Distribution at Location []^{a,c,e}

a,c,e



Figure 2-38. Surge Line Local Axial Stress Distribution at Location []^{a,c,e}

34915/121508 IC



Figure 2-39. Surge Line Temperature Distribution at Location []^{a,c,e}

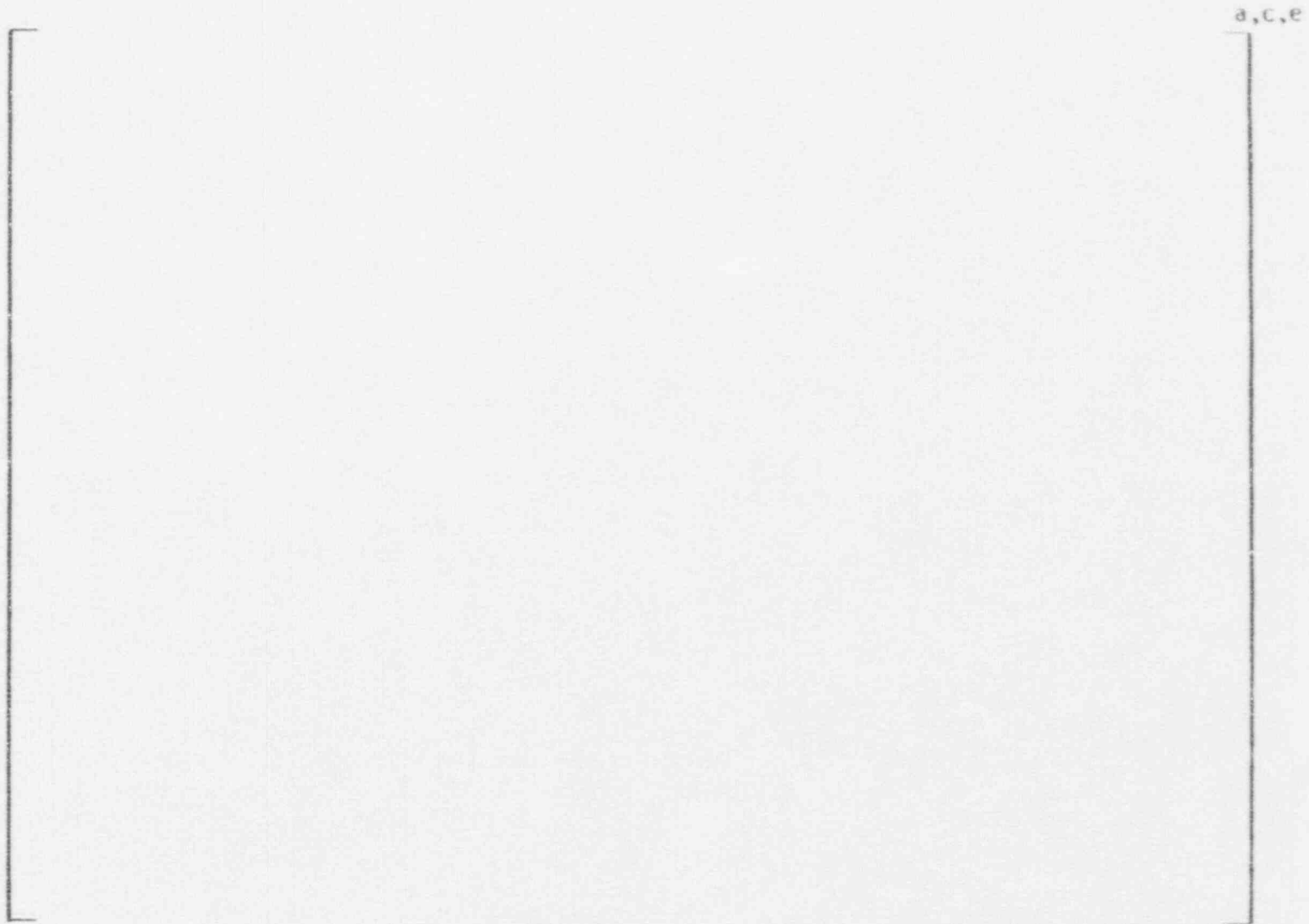


Figure 2-40. Surge Line Local Axial Stress Distribution at Location []^{a,c,e}

2-60



Figure 2-41. Surge Line Temperature Distribution at Location []^{a,c,e}

2-61



Figure 2-42. Surge Line Local Axial Stress Distribution at Location []^{a,c,e}

2-62



Figure 2-43. Surge Line RCL Nozzle 3-D WECAN Model #1

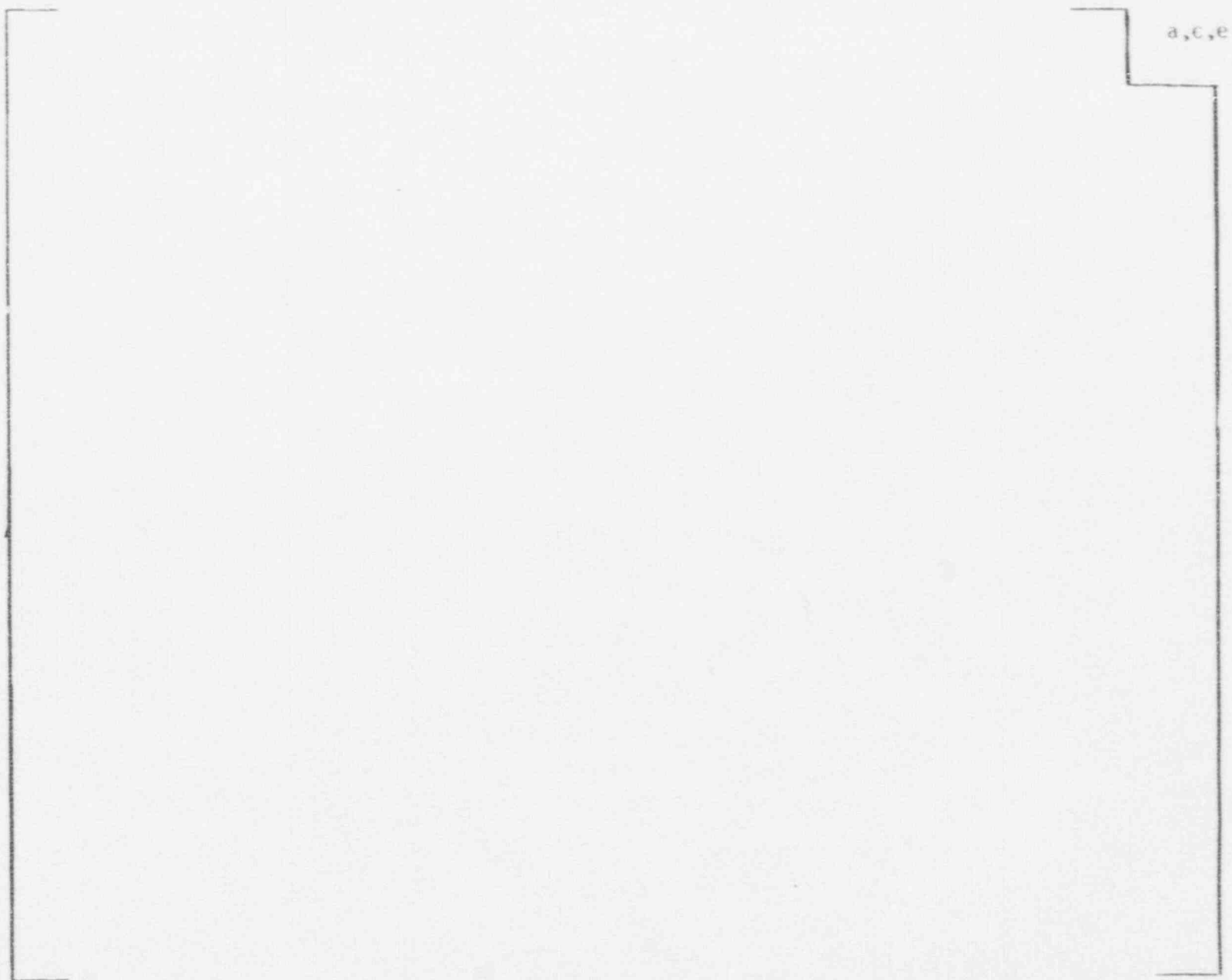


Figure 2-44. Surge Line RCL Nozzle 3-D WECAN Model #2

Figure 2-45. Hot Leg Nozzle Stress Analysis

- o **Two 3-Dimensional Models Developed**
- o **Loading Included**
 - **Pressure**
 - **Bending Moments**
 - **Stratification**
- o **Stratification Profile Based on Observation During RCP Trip**

2-65

a,c,e

Figure 2-46. Surge Line Nozzle Temperature Profile Due to Thermal Stratification

2-66

a,c,e

Figure 2-47. Surge Line Nozzle Stress Intensity Due to Thermal Stratification

a, c, e



Figure 2-48. Surge Line Nozzle Stress in Direction Axial to Surge Line Due to Thermal Stratification

34915/121588 10

a, c, e

Figure 2-49. Surge Line Nozzle Stress Intensity Due to Pressure

$a_3 C_3 e$



Figure 2-50. Surge Line Nozzle Stress Intensity Due to Pressure



Figure 2-51. Surge Line Nozzle Stress Intensity Due to Bending

2-71

Figure 2-52. Surge Line Nozzle Stress in Direction Axial to Surge Line Due to Bending Showing Magnified Displacement

34916/121588 10

Figure 2-53. Surge Line Nozzle Stress Intensity Due to Bending Showing Showing Magnified Displacement



Figure 2-54. Surge Line Nozzle Stress Intensity Due to Bending

Figure 2-55. Results

- o [^{a, c, e}] Stress Profiles Developed for Pipe Cross-Section
- o Maximum Stresses Occur on Inside Surface Near Interface
- o Results Consistent with Theory
- o Stresses to be Combined with Structural Bending

Figure 2-56. Local Stress Conservatism

- o **The Hot/Cold Fluid Interface Is Assumed To Have Zero Width. A More Gradual Change From Hot To Cold Would Significantly Decrease Local Stresses.**

- o **Stresses Are Based On Linear Elastic Analysis Even Though Stress Levels Exceed Material Yield Point.**

**Feedwater Line in PWR's
Flow Tests For LMFBR**

Experimental Tests in Japan

- Mitsubishi Heavy Industries, Ltd.

Thermal Striping Affects ASME Fatigue Analysis

- Temperature Fluctuations at Boundary
- Thermal Discontinuity Stresses
- Usage Factor for Fatigue Life

Figure 2-57. Background - Thermal Striping Analysis



Figure 2-58. Thermal Striping Fluctuation

2-78



Figure 2-59. Stratification and Striping Test Models



Figure 2-60. Thermal Striping Temperature Distribution





Figure 2-61. Striping Finite Element Model

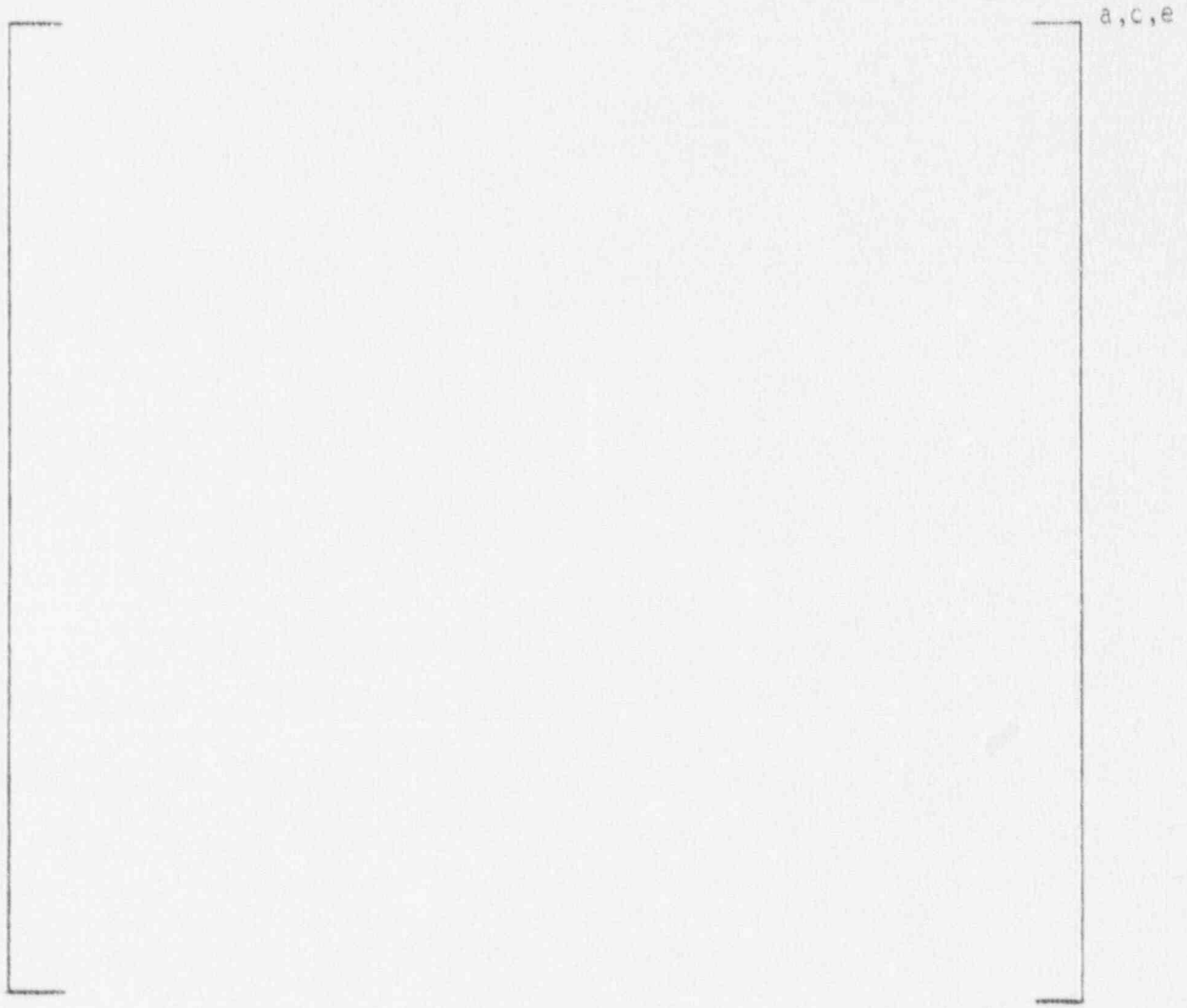


Figure 2-62. Thermal Striping Stresses



Figure 2-63. Factors Affecting Thermal Striping Stress



Figure 2-64. Attenuation of Thermal Striping Potential by Molecular
Conduction (Interface Wave Height of [λ]^{a, c, e})



Figure 2-65. Conservatism in Thermal Striping Analysis

SECTION 3.0
ASME SECTION III FATIGUE USAGE FACTOR EVALUATION

3.1 Code and Criteria

Fatigue usage factors for the Beaver Valley Unit 1 surge line were evaluated based on the requirements of the ASME B & PV Code, Section III [1], Subsection NB-3600, for piping components. The more detailed techniques of NB-3200 were employed, as allowed by NB-3611.2. The fatigue evaluation required for level A and B service limits in NB-3653 is summarized in table 3-1. ASME III fatigue usage factors were calculated for []^{a,c,e} points in the surge line piping using program WECEVAL[2]. The transient input data used in the fatigue analysis were provided in Section 1.0 with system ΔT in exceedance of 320°F reconciled.

3.2 Analysis for Thermal Stratification

With thermal transients redefined to account for thermal stratification as described in section 1.0, the stresses in the piping components were established (section 2) and fatigue usage factors were calculated. Due to the non-axisymmetric nature of the stratification loading, stresses due to all loadings were obtained from finite element analysis and then combined on a stress component basis.

3.2.1 Stress Input

Stresses in the pipe wall due to internal pressure, moments and thermal stratification loading were obtained from the WECAN 2-D analysis of a 14 inch, schedule 160 pipe. []

] ^{a,c,e}

[

]a,c,e

3.2.2 Classification and Combination of Stresses

As described in 3.3.1 the total stress in the pipe wall was determined for each transient load case. Two types of stress were calculated - S_n (Eq 10), to determine elastic-plastic penalty factors, K_e , and S_p (Eq 11) - peak stress. For most components in the surge line (girth butt welds, elbows, bends) no gross structural discontinuities are present. As a result, the code-defined "Q" stress (NB-3200), or $C_3 E | \alpha \Delta T_a - \alpha b T_b |$ in Eq (10) of NB-3600 is zero. Therefore, for these components, the Eq. (10) stresses are due to pressure and moment.

For the RCL hot leg nozzle, the results of the 3-D finite element WECAN analysis of the nozzle were used to determine "Q" stress for transients with stratification in the nozzle. Note also that the Eq. (10) stresses included appropriate stress intensification using the secondary stress indices from NB-3681.

Peak stresses, including the total surface stress from all loadings - pressure, moment, stratification - were then calculated for each transient.

[

]a,c,e

3.2.3 Cumulative Fatigue Usage Factor Evaluation

Program WECEVAL uses the S_n and S_p stresses calculated for each transient to determine usage factors at selected locations in the pipe cross section. Using a standard ASME method, the cumulative damage calculation is performed according to NB-3222.4(e)(5). The inside and outside pipe wall usage factors

were evaluated at [$j^{a,c,e}$] through the pipe wall of the 2-D WECAN model (figure 2-28).

This includes:

- 1) Calculating the S_n and S_p ranges, K_e , and S_{alt} for every possible combination of the [$j^{a,c,e}$] transient load sets.
- 2) For each value of S_{alt} , use the design fatigue curve to determine the maximum number of cycles which would be allowable if this type of cycle were the only one acting. These values, $N_1, N_2 \dots N_n$, were determined from Code figures I-9.2.1 and I-9.2.2, curve C, for austenitic stainless steels.
- 3) Using the actual cycles of each transient loadset supplied to WECAN, n_1, n_2, \dots, n_n , calculate the usage factors $U_1, U_2 \dots U_n$ from $U_i = n_i/N_i$. This is done for all possible combinations. If N_i is greater than 10^{11} cycles, the value of U_i is taken as zero.

[

$j^{a,c,e}$

- 4) The cumulative usage factor, U_{cum} , is calculated as $U_{cum} = U_1 + U_2 + \dots + U_n$. The code allowable value is 1.0.

3.2.4 Simplified Elastic-Plastic Analysis

When code Eq. (10), S_n , exceeded the $3S_m$ limit, a simplified elastic-plastic analysis was performed per NB-3653.6. This required separate checks of expansion stress, Eq. (12), and Primary Plus Secondary Excluding Thermal Bending Stress, Eq. (13), Thermal Stress Ratchet, and calculation of the elastic-plastic penalty factor,

K_e , which affects the alternating stress by $S_{alt} = K_e S_p / 2$. The K_e values for all combinations were automatically calculated by WECEVAL. Thermal stress ratchet was also checked. Eq. (13) is not affected by thermal stratification in the pipe where no gross structural discontinuities exist, but is required to be verified at the nozzle. Eq. (12) was evaluated in the Global ANSYS analysis by checking the worst possible range of stress due to the expansion bending moments (section 2).

3.2.5 Fatigue Usage Results

The maximum usage factors were []^{a,c,e} at the elbow (nodes 192 to 194, figure 1-16) and []^{a,c,e} at the RCL nozzle safe end (node 171, figure 1-16).

The above usage factors do not include the effects of striping. Because the nature of striping damage is at a much higher frequency, varies in location due to fluid level changes and is maximized at a different location than the ASME usage factor, it was assumed to be more appropriate to determine a total usage factor by conservatively adding the above calculated and striping usage factors. This results in a total U_{cum} of []^{a,c,e}, less than the Code allowable of 1.0.

3.3 Conservatism in Fatigue Usage Calculation

The above calculated ASME usage factors contain the inherent conservatism known to be in the ASME Code methods. These include the conservatism in the elastic-plastic penalty factor, K_e , the method of combining loadsets based on descending S_{alt} , and the factor of 2 on stress and 20 on cycles in the design fatigue curve.

Also, due to input limitations in program WECEVAL, the maximum value of peak stress intensification for all loading types was used. This was conservative at girth butt welds, since $K_1 = 1.2$, $K_2 = 1.8$, $K_3 = 1.7$ in NB-3681 and $K=1.8$ was used in WECEVAL for all stresses.

3.4 References

3-1. ASME Boiler and Pressure Vessel Code, Section III, 1986 Edition.

3-2. WCAP-9376, WECEVAL, Computer Code to Perform ASME BPVC Evaluations Using Finite Element Models, Generated Stress States, April, 1985. [Proprietary]

3-3. []^{a,c,e}

3-4. []^{a,c,e}

TABLE 3-1
CODE/CRITERIA

- o ASME B&PV Code, Sec. III, 1986 Edition
 - NB3600
 - NB3200

- o Level A/B Service Limits
 - Primary Plus Secondary Stress Intensity $\leq 3S_m$ (Eq. 10)

 - Simplified Elastic-Plastic Analysis
 - Expansion Stress, $S_e \leq 3S_m$ (Eq. 12) - Global Analysis
 - Primary Plus Secondary Excluding Thermal Bending $< 3S_m$ (Eq. 13)
 - Elastic-Plastic Penalty Factor $1.0 \leq K_e \leq 3.333$

 - Peak Stress (Eq. 11)/Cumulative Usage Factor (U_{cum})
 - $S_{alt} = K_e S_p / 2$ (Eq. 14)
 - Design Fatigue Curve
 - $U_{cum} \leq 1.0$

SECTION 4.0 FATIGUE CRACK GROWTH EVALUATION

4.1 Introduction

To determine the sensitivity of the pressurizer surge line to the presence of small cracks when subjected to the transients discussed in section 1.0, fatigue crack growth analyses were performed. The transients exceeding a system ΔT of 320°F were included. This section summarizes the analyses and results.

Figure 4-1 presents a general flow diagram of the overall process. The methodology consists of seven basic steps as shown in figure 4-2. Steps 1 thru 4 are discussed in sections 1 and 2 of this report. Steps 5 thru 7 are specific to fatigue crack growth and are discussed in this section and summarized in figure 4-3.

There is presently no fatigue crack growth rate curve in the ASME Code for austenitic stainless steels in a water environment. However, a great deal of work has been done recently which supports the development of such a curve. An extensive study was performed by the Materials Property Council Working Group on Reference Fatigue Crack Growth concerning the crack growth behavior of these steels in air environments, published in reference 4-1. A reference curve for stainless steels in air environments, based on this work, is in the 1989 Edition of Section XI of the ASME Code. This curve is shown in figure 4-4.

A compilation of data for austenitic stainless steels in a PWR water environment was made by Bamford (reference 4-2), and it was found that the effect of the environment on the crack growth rate was very small. For this reason it was estimated that the environmental factor should be set at 1.0 in the crack growth rate equation from reference 4-1. Based on these works (references 4-1 and 4-2) the fatigue crack growth law used in the analyses is as shown in figure 4-5.

4.2 Initial Flaw Size

Various initial surface flaws were assumed to exist. The flaws were assumed to be semi-elliptical with a six-to-one aspect ratio. The largest initial flaw assumed to exist was one with a depth equal to 10% of the wall thickness, the maximum flaw size that could be found acceptable by Section XI of the ASME code.

4.3 Critical Locations for FCG

All five locations (as referred to in section 1.2.5), representing all cross sections of the surge line where thermal stratification could occur, were evaluated for fatigue crack growth. Figure 4-6 identifies the five locations. The location []^{a,c,e} stratification profile exists at the surge line RCL nozzle when the RCP pump is not running and, therefore, turbulent mixing caused by flow in the main RCL piping is not occurring. This effect was observed in the surge line monitoring programs (section 1.2.3.) This temperature profile develops a lower inside-wall local axial tensile stress than developed at other locations (see table 2-4 in section 2.0). Based upon the above discussion, location []^{a,c,e} is not a critical location for fatigue crack growth. For completeness, however, fatigue crack growth calculations were performed at location []^{a,c,e}.

Figure 4-7 identifies the positions at each location where fatigue crack growth was checked. These positions []^{a,c,e} are controlling positions because the global structural bending stress is maximum at positions []^{a,c,e} while the local axial stress on the inside surface is maximum at positions []^{a,c,e}.

4.4 Results of FCG Analysis

Results of the fatigue crack growth analysis are presented in table 4-1 for a 10% wall initial flaw. The maximum depth for full service life was less than 25% of the wall. The transients exceeding a system Δt of 320°F had almost no impact on the results.

Conservatism existing in the fatigue crack growth analysis are listed in figure 4-8.

4.5 References

- 4-1. James, L. A. and Jones, D. P., "Fatigue Crack Growth Correlations for Austenitic Stainless Steel in Air," in Predictive Capabilities in Environmentally Assisted Cracking, ASME publication PVP-99, December 1985.
- 4-2. Bamford, W. H., "Fatigue Crack Growth of Stainless Steel Reactor Coolant Piping in a Pressurized Water Reactor Environment," ASME Trans. Journal of Pressure Vessel Technology, Feb. 1979.

TABLE 4-1
 FATIGUE CRACK GROWTH RESULTS FOR 10% WALL INITIAL FLAW SIZE

Location	Position	Initial Size (in)	Initial (% Wall)	Final (40 yr) Size (in)	Final Flaw (% Wall)
----------	----------	----------------------	---------------------	----------------------------	------------------------

a, c, e

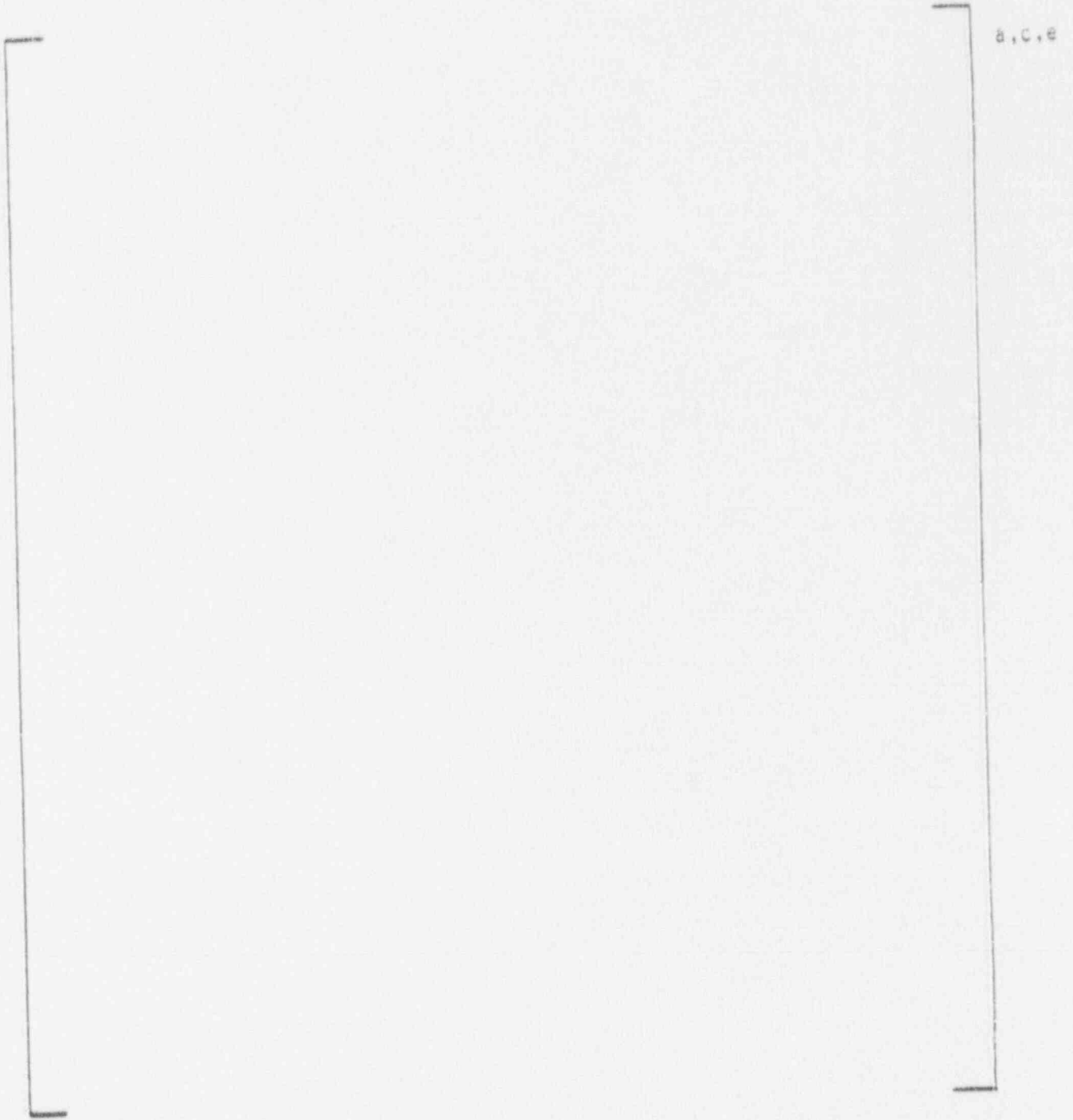


Figure 4-1. Determination of the Effects of Thermal Stratification on Fatigue Crack Growth



a.c.e

Figure 4-2. Fatigue Crack Growth Methodology

- o Standard ASME Section XI Methods Used
- o Crack Growth Law Based on Curve for Austenitic Stainless Steel in Air Environment (Section XI of the 1989 ASME Code)
- o Initial Flaw Sizes Selected Based on Section XI Inspection Detection Tolerances
- o All Locations Checked for FCG
- o Results: Crack Growth at All Locations Must Remain Within six tenths of the thickness ($0.6t$)

Figure 4-3. Aspects of the Fatigue Crack Growth Evaluation

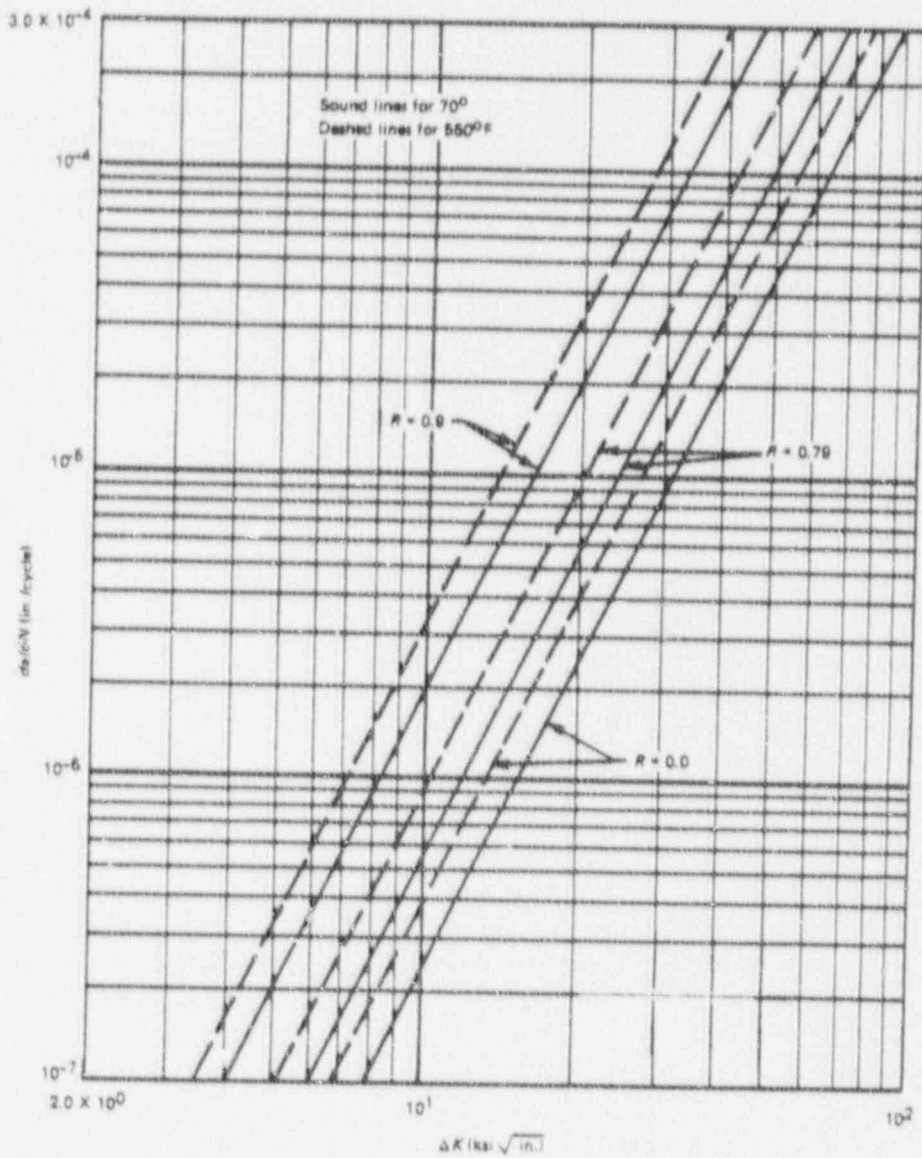


Figure 4-4. Fatigue Crack Growth Rate Curve for Austenitic Stainless Steel

$$\frac{da}{dn} = C F S E \Delta K^{3.30}$$

where

$\frac{da}{dn}$ = Crack Growth Rate in inches/cycle

C = 2.42×10^{-20}

F = Frequency factor (F = 1.0 for temperature below 800°F)

S = R ratio correction (S = 1.0 for R = 0; S = 1 + 1.8R for 0 < R < .8; and S = -43.35 + 57.97R for R > 0.8)

E = Environmental Factor (E = 1.0 for PWR)

ΔK = Range of stress intensity factor, in psi $\sqrt{\text{in}}$

R = The ratio of the minimum K_I (K_{Imin}) to the maximum K_I (K_{Imax}).

Figure 4-5. Fatigue Crack Growth Equation for Austenitic Stainless Steel



Figure 4-6. Fatigue Crack Growth Critical Locations

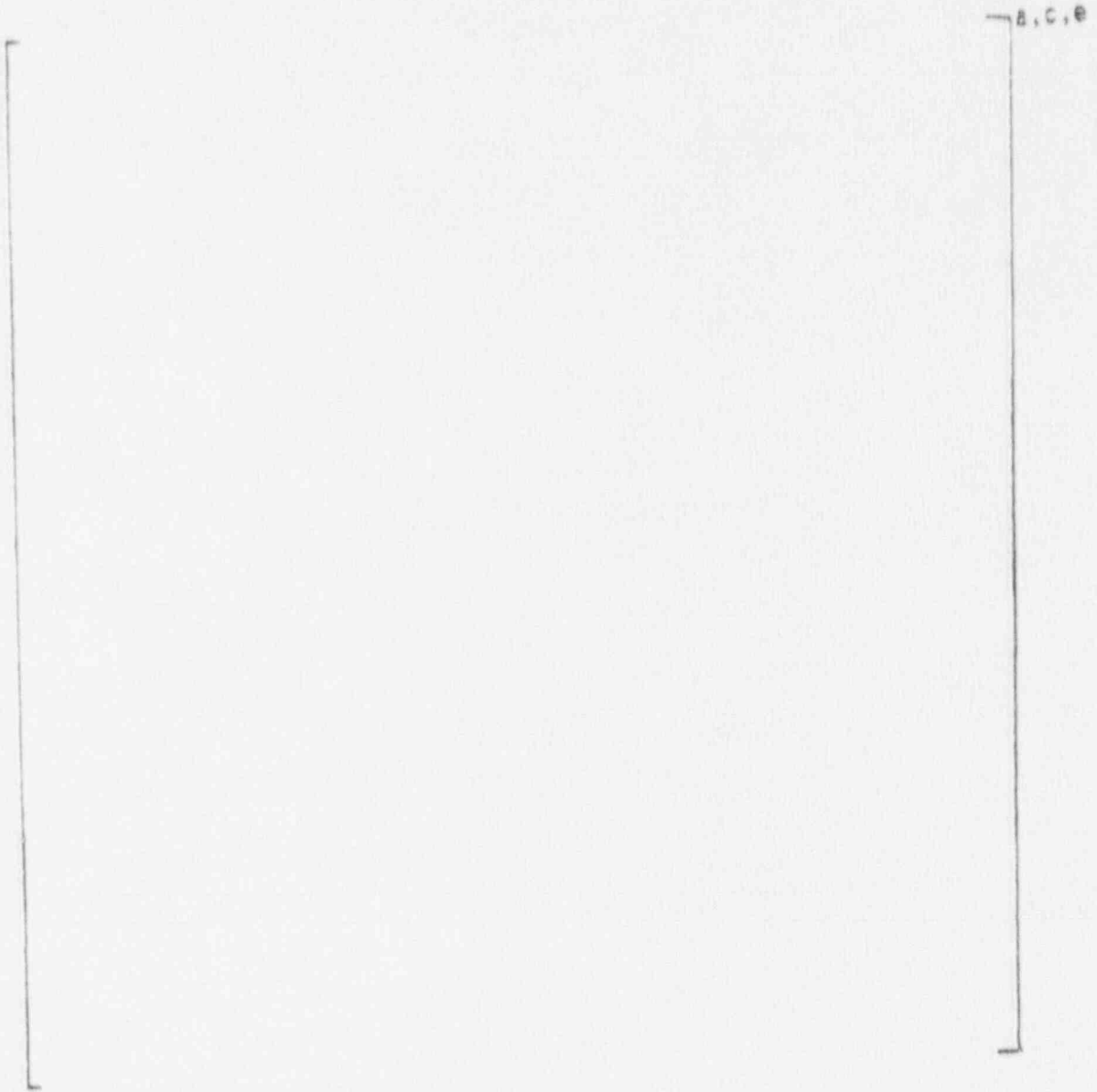


Figure 4-7. Fatigue Crack Growth Controlling Positions at Each Location

- o Plant operational transient data have shown that the conventional design transients contain significant conservatisms

[

] a,c,e

- o FCG analysis assumes crack growth on every cycle

Figure 4-8. Fatigue Crack Growth Conservatisms

SECTION 5.0 ASSESSMENT OF LEAK-BEFORE-BREAK

5.1 Background

The recent concern for thermal stratification in pressurizer surge lines has prompted the analyses presented in previous sections. Specifically, thermal stratification has been shown to impact normal operating loads and to have the potential for imposing large thermal bending loads during the heatup and cooldown transients. Also under the current surge line configuration, the normal operating loads are identical to those of Beaver Valley Unit 2 as reported in Reference 1. The discussion of section 1.0 concludes that prior thermal stratification transients used in the evaluation of Beaver Valley Unit 2 (see Reference 1) are also applicable to Beaver Valley Unit 1 with the exception of plant specific transients which exceeded a system ΔT of 320°F. These transients are accounted for in the analyses of sections 3.0 and 4.0.

In this section, leak-before-break for the pressurizer surge line is assessed taking into account thermal stratification. The leak-before-break methodology is reviewed and the analyses are summarized. Conclusions are drawn.

5.2 Methodology

The steps of the leak-before-break methodology are reviewed in table 5-1. Items 2, 3 and 8 are addressed in sections 2, 1 and 4 of this report, respectively. This section addresses items 1, and 4 through 7. The conservatisms used in this section are listed in table 5-2.

5.3 Material and Fracture Toughness Properties

Applicable material properties were obtained from the Certified Materials Test Report and are given in table 5-3. The material is SA376 TP316, a wrought product form, or its worked equivalent. The ASME code minimum properties are

also given in table 5-3. It is seen that the measured properties well exceed those of the code. As seen later, properties at 653°F and 135°F are required for the leak rate and stability analyses. Industry data at room temperature and 650°F were used as a basis for determining tensile properties at the required temperatures. The required average and minimum properties are given in table 5-4 along with the modulus of elasticity. The stress strain curves required for the stability analyses are given in figures 5-1 and 5-2. The curve at 653°F was obtained by application of the Nuclear Systems Materials Handbook (reference 2). The curve for 135°F was obtained from experimental data. Fracture toughness properties are given in table 5-5 taken from references 3 through 6. Conservative estimates of toughness were chosen by using the material footnoted by d.

5.4 Loading Conditions

Because thermal stratification can cause large stresses at heatup and cooldown temperatures in the range of 455°F, a review of stresses was used to identify the worst situations for LBB applications. The loadings states so identified are given in table 5-6. Two locations, nodes 171 and 196, as shown in figure 5-3, are the most critical for LBB evaluation. Node 196 at the pressurizer nozzle is the critical location for normal operation at 653°F while node 171 at the hot leg junction is the critical location during heatup and cooldown with the pressurizer nominally at 455°F. There are field welds at both locations being SMAW following a GTAW root pass.

Seven loading cases were identified for LBB evaluations as given in table 5-7. Cases A and B are normal operating conditions with a [

j a, c, e

j^{a,c,e}

Thus, there are seven LBB analyses to be performed as outlined in table 5-8. The loads appropriate for these cases are given in table 5-9. The stresses are also given. The minimum wall thickness is 1.246 in. The seven cases for analyses as associated with location and temperatures are given in table 5-10.

5.5 Results

Beaver Valley Unit 1 employs a shutdown specification of 1.0 gpm unidentified leakage in response to Regulatory Guide 1.45. The leakage size flaw then is the one giving 10 gpm. Leakage flaws were calculated for the seven cases using the methodology of section 5.0 of reference 7. The results are given in table 5-11.

J-integral stability evaluations were made for each of the cases for faulted loads and a flaw size twice the leakage flaw. Since the absolute sum method was used in combining the load components for determining the faulted loads, a margin on load is not required. The J-integral analyses were made using the EPRI Handbook procedure (reference 8). The stability results are given in table 5-12. Significantly, the calculated J values are all less than the J_{max} of 3000 in-lb/in².

Critical flaw sizes were obtained using the limit load procedure as outlined in SRP 3.6.3 (reference 9), accounting for the SMAW weld by using the appropriate Z-formula. The instability flaw sizes so determined are also given in table 5-12. Stability margins on leakage flaws in excess of 2 are again demonstrated.

5.6 Conclusions

Considering the results of the prior sections and this section, the LBB criteria outlined in table 5-1 have been met and thus LBB has been demonstrated for the Beaver Valley Unit 1 pressurizer surge line considering thermal stratification; specifically,

- o LBB exists at operating temperature without stratification.
- o LBB exists at operating temperature with stratification.
- o LBB exists for forced cooldown due to leakage.
- o LBB exists for extended stratification.

5.7 References

1. Brice-Nash, R. L. et. al., Evaluation of Thermal Stratification for the Beaver Valley Unit 2 Pressurizer Surge Line, WCAP-12093, December 1988 and Supplements:
 - Supplement 1 - Additional information in support of the Evaluation of Thermal Stratification for the Beaver Valley Unit 2 Pressurizer Surge Line, February 1989.
 - Supplement 2 - Additional information in support of the Evaluation of Thermal Stratification for the Beaver Valley Unit 2 Pressurizer Surge Line, August 1989.
 - Supplement 3 - Evaluation of Pressurizer Surge Line Transients Exceeding 320°F for Beaver Valley Unit 2, July 1990.
2. Nuclear Systems Materials Handbook, Part I - Structural Materials, Group 1 - High Alloy Steels, Section 4, ERDA Report TID 26666, November 1975 Revision.
3. Palusamy, S. S. and Hartmann, A. J., Mechanistic Fracture Evaluation of Reactor Coolant Pipe Containing a Postulated Circumferential Through-Wall Crack, WCAP 9558, Rev. 2, May 1981 (Westinghouse Proprietary Class 2).

4. Landes, J. D. and McCabe, D. E., Elastic-Plastic Methodology to Establish R-Curves and Instability Criteria - Topical Report on Toughness Characterization of Austenitic Stainless Steel Pipe Weldments, R&D Document No. 86-2D/-PSALE-R1, Westinghouse R&D Center, February 13, 1986.
5. Palusamy, S. S., Tensile and Toughness Properties of Primary Piping Weld Metal for Use in Mechanistic Fracture Evaluation, WCAP-9787, May, 1981 (Westinghouse Proprietary Class 2).
6. Bamford, et. al., The Effects of Thermal Aging on the Structural Integrity of Cast Stainless Steel Piping for Westinghouse Nuclear Steam Supply Systems, WCAP-10456, November, 1983 (Westinghouse Proprietary Class 2).
7. Roarty, D. H. et. al., Technical Justification for Eliminating Primary Loop Pipe Rupture as the structural design basis for Beaver Valley Unit 1, WCAP-11317, March 1987 (Westinghouse Proprietary Class 2).
8. Kumar, V., German, M. D. and Shih, C. P., "An Engineering Approach for Elastic-Plastic Fracture Analysis," EPRI Report NP-1931, Project 1237-1, Electric Power Research Institute, July 1981.
9. USNRC Standard Review Plan 3.6.3, Leak-Before-Break Evaluation Procedures, NUREG-0800.

TABLE 5-1
STEPS IN A LEAK-BEFORE-BREAK ANALYSIS

- (1) Establish material properties including fracture toughness values
- (2) Perform stress analysis of the structure
- (3) Review operating history of the structure
- (4) Select locations for postulating flaws
- (5) Determine a flaw size giving a detectable leak rate
- (6) Establish stability of the selected flaw
- (7) Establish adequate margins in terms of leak rate detection, flaw size and load.
- (8) Show that a flaw indication acceptable by inspection remains small throughout service life.

TABLE 5-2
LBB CONSERVATISMS

- o Factor of 10 on Leak Rate
- o Factor of 2 on Leakage Flow
- o Algebraic Sum of Loads for Leakage
- o Absolute Sum of Loads for Stability
- o Average Material Properties for Leakage
- o Minimum Material Properties for Stability
- o Lower Bound Fracture Toughness Properties
- o Conservative EPFM J Analyses
- o Conservative Limit Load Analyses

TABLE 5-3
 ROOM TEMPERATURE MECHANICAL PROPERTIES OF THE PRESSURIZER
 SURGE LINE MATERIALS AND WELDS OF THE BEAVER VALLEY UNIT 1 PLANT

Heat No./ Serial No.	Product	Form	0.2% Offset Yield Stress (psi)	Ultimate Strength (psi)
a, c, e				

ASME Code Minimum Requirements

Pipe, Pipe Bend, Elbow	SA376 TP316	30,000	75,000
Weld	ER308	N.A. ^a	80,000

^a N.A. - not applicable

TABLE 5-4
 TENSILE PROPERTIES FOR THE SURGE LINE MATERIAL
 AT 135°F and 653°F

Temperature (°F)	Yield Stress (psi)		Ultimate Strength (psi)		Modulus of Elasticity (psi x 10 ⁶)
	Average	Minimum	Average	Minimum	

[

]

a, c, e

TABLE 5-5
 FRACTURE TOUGHNESS PROPERTIES FOR 316 STAINLESS STEELS AND WELDS

Material	Test Temperature (°F)	J_{Ic} (in-lb/in ²)	T_{mat}	Reference
SA376 TP316	[]	[]	a, c, e	3
SA376 TP316			4	
Weld			5	
Weld ^d			6	

TABLE 5-6
TYPES OF LOADINGS

Pressure (P)

Dead Weight (DW)

Normal Operating Thermal Expansion (TH)

Safe Shutdown Earthquake and Seismic Anchor Motion (SSE)^a

[a, c, e
---	---------

^aSSE is used to refer to the absolute sum of these loadings.

TABLE 5-7
NORMAL AND FAULTED LOADING CASES FOR LBB EVALUATIONS

CASE A: This is the normal operating case at 653°F consisting of the algebraic sum of the loading components due to P, DW and TH.

[] a,c,e

CASE D: This is the faulted operating case at 653°F consisting of the absolute sum (every component load is taken as positive) of P, DW, TH and SSE.

[] a,c,e

TABLE 5-8
ASSOCIATED LOAD CASES FOR ANALYSES

A/D This is here-to-fore standard leak-before-break evaluation.

a,c,e

TABLE 5-9
SUMMARY OF LOADS AND STRESSES AT THE CRITICAL LOCATIONS

OD = 14 in., Minimum Wall Thickness = 1.246 in.

Node	Case	Force F (lbs)	Stress σ_F (psi)	Moment M (in-lbs)	Stress σ_M (psi)	Total Stress (psi)	
[a,c,e
196	A	233208	4674	1996626	13638	18312	a,c,e
196	D	242850	4867	2478764	16931	21798	a,c,e

TABLE 5-10
 LOAD CASES, LOCATION AND TEMPERATURES CONSIDERED FOR
 LEAK-BEFORE-BREAK EVALUATIONS

Case	Node	Temperature (°F)	
		Leak Rate	Stability
A/D	196	653	653 a,c,e

TABLE 5-11
LEAKAGE FLAWS FOR THE LEAK-BEFORE-BREAK ANALYSES

Case	Node Location	Leakage Flow (in.)
A/D	196	3.36

[a,c,e]

TABLE 5-12
RESULTS OF STABILITY EVALUATION

J-INTEGRAL ANALYSES

Case	Criteria						
	Node	J_{Ic} (in-lb/in ²)	T_{mat}	J_{max} (in-lb/in ²)	Crack Length (in)	J_{app} (in-lb/in ²)	T_{app}
A/D				a,c,e	6.72		a,c,e

LIMIT LOAD ANALYSES (SMAW)

Faulted Load Case	Node	Critical Flaw Size (in.)
D		13.3 a,c,e

^aN.A. - Not Applicable, $J_{app} < J_{Ic}$

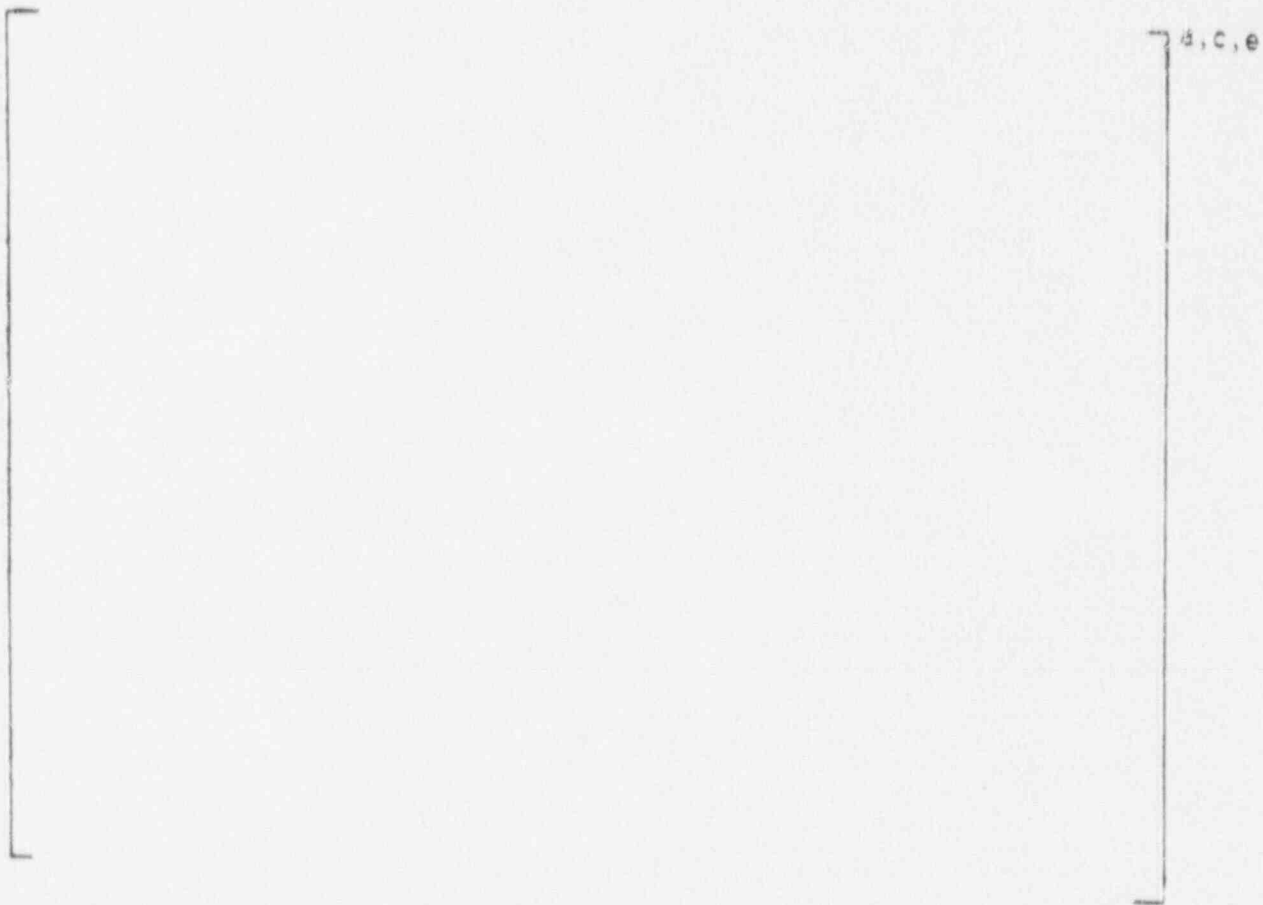


Figure 5-1. Minimum True Stress-True Strain Curve for 316 Stainless Steel at 653°F

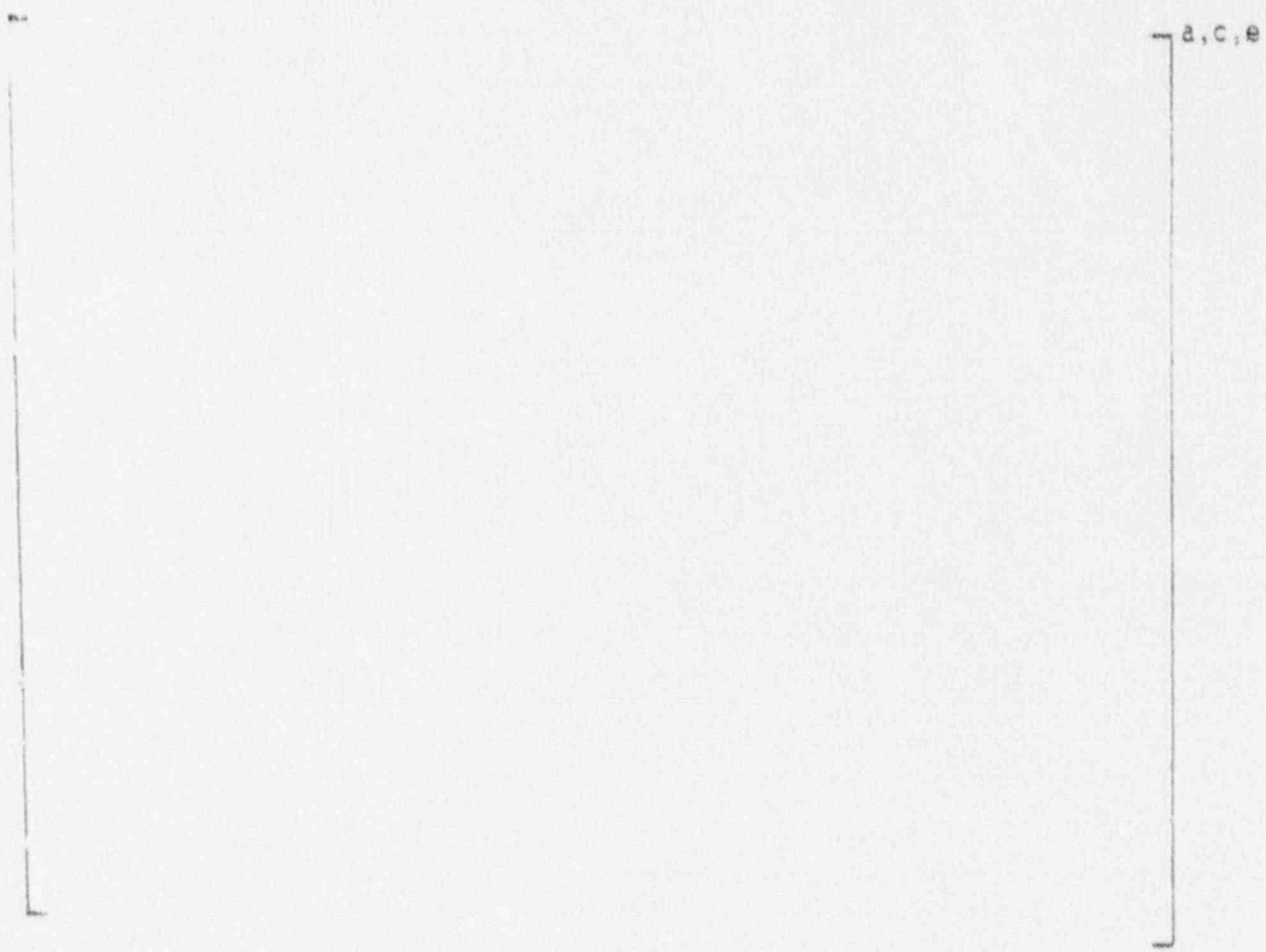


Figure 5-2. Minimum True Stress-True Strain Curve for 316 Stainless Steel at 135°F

a, c, e

Figure 5-3. Sketch of Analysis Model for Beaver Valley Unit 1 Pressurizer Surge Line Showing Node Points, Critical Locations, Weld Locations and Type of Welds

6.0 CONCLUSIONS

Extensive generic and plant specific data evaluations have been performed and design transients have been updated for thermal stratification. Finite element stress analyses have been performed and ASME Code stress limits are met. The total fatigue usage factor including the effect of thermal striping is less than the ASME Code requirement of 1. Fatigue crack growth is limited with a hypothesized flaw 10% through the wall estimated to grow to about 25% through the wall for full service life. In these fatigue analyses, transients to date which exceeded a system ΔT of 320°F are included. Leak-before-break was established for operating conditions and for bounding high load thermal stratification conditions.

Based on the current understanding of the thermal stratification phenomenon, it is concluded that thermal stratification has very limited impact on integrity of the pressurizer surge line of the Beaver Valley Unit 1 nuclear power plant. The forty year design life is not impacted. The surge line has been demonstrated to exhibit leak-before-break.

APPENDIX A
LIST OF COMPUTER PROGRAMS

This appendix lists and summarizes the computer codes used in the analysis of stratification in the Beaver Valley Unit 1 pressurized surge line. The codes are:

1. WECAN
2. WECEVAL
3. STRFAT2
4. ANSYS
5. FCG

A.1 WECAN

A.1.1 Description

WECAN is a Westinghouse-developed, general purpose finite element program. It contains universally accepted two-dimensional and three-dimensional isoparametric elements that can be used in many different types of finite element analyses. Quadrilateral and triangular structural elements are used for plane strain, plane stress, and axisymmetric analyses. Brick and wedge structural elements are used for three-dimensional analyses. Companion heat conduction elements are used for steady state heat conduction analyses and transient heat conduction analyses.

A.1.2 Feature Used

The temperatures obtained from a static heat conduction analysis, or at a specific time in a transient heat conduction analysis, can be automatically input to a static structural analysis where the heat conduction elements are replaced by corresponding structural elements. Pressure and external loads can also be include in the WECAN structural analysis. Such coupled thermal-stress analyses are a standard application used extensively on an industry wide basis.

A.1.3 Program Verification

Both the WECAN program and input for the WECAN verification problems, currently numbering over four hundred, are maintained under configuration control. Verification problems include coupled thermal-stress analyses for the quadrilateral, triangular, brick, and wedge isoparametric elements. These problems are an integral part of the WECAN quality assurance procedures. When a change is made to WECAN, as part of the reverification process, the configured inputs for the coupled thermal-stress verification problems are used to reverify WECAN for coupled thermal-stress analyses.

A.2 WECEVAL

A.2.1 Description

WECEVAL is a multi-purpose program which processes stress input to calculate ASME Section III, Subsection NB equations and usage factors. Specifically, the program performs primary stress evaluations, primary plus secondary stress intensity range analysis, and fatigue analysis for finite element models generated and run using the WECAN computer program. Input to WECEVAL consists of card image data and data extracted from the output TAPE12's generated by WECAN's stress elements. The program reads the input data, performs the necessary calculations, and produces summary sheets of the results.

The required stresses are read from the WECAN TAPE12's and placed onto intermediate or restart files. The user may then catalog these files for use in later evaluations. The stress state for a particular loading condition is obtained by a ratio-superposition technique. This optimal stress state is formed by manipulating the signs of the applied loads to generate the largest possible stress magnitude.

A.2.2 Feature Used

WECEVAL has many options and features which enhance its versatility. Among those used for this evaluation were:

1. The ability to perform simplified elastic-plastic analysis per NB-3228.5, including the automatic calculation of K_e factors and removal of thermal bending stresses from the maximum range of stress intensity evaluations.
2. Built-in ASME fatigue curves plus provisions for accepting user-defined fatigue curves.
3. Equivalent moment linearization technique, along with the ability to correct for the radius effects in cylindrical and spherical geometries.
4. The ability to limit the interactions among load conditions during the fatigue analysis.
5. Generating input for the fatigue crack growth program FCG.

A.2.3 Program Verification

WECEVAL is verified to Westinghouse procedures by independent calculations of ASME III NB Code equations and comparison to WECEVAL results.

A.3 STRFAT2

A.3.1 Description

STRFAT2 is a program which computes the alternating peak stress on the inside surface of a flat plate and the usage factor due to striping on the surface. The program is applicable to be used for striping on the inside surface of a pipe if the program assumptions are considered to apply for the particular pipe being evaluated.

For striping the fluid temperature is a sinusoidal variation with numerous cycles.

The frequency, convection film coefficient, and pipe material properties are input.

The program computes maximum alternating stress based on the maximum difference between inside surface skin temperature and the average through wall temperature.

A.3.2 Feature Used

The program is used to calculate striping usage factor based on a ratio of actual cycles of stress for a specified length of time divided by allowable cycles of stress at maximum the alternating stress level. Design fatigue curves for several materials are contained into the program. However, the user has the option to input any other fatigue design curve, by designating that the fatigue curve is to be user defined.

A.3.3 Program Verification

STRFAT2 is verified to Westinghouse procedures by independent review of the stress equations and calculations.

A.4 ANSYS

A.4.1 Description

ANSYS is a public domain, general purpose finite element code.

A.4.2 Feature Used

The ANSYS elements used for the analysis of stratification effects in the surge and RHR lines are STIF 20 (straight pipe), STIF 60 (elbow and bends) and STIF14 (spring-damper for supports).

A.4.3 Program Verification

As described in section 2.1, the application of ANSYS for stratification has been independently verified by comparison to WESTDYN (Westinghouse piping]

analysis code) and WECAN (finite element code, section 8.1). The results from ANSYS are also verified against closed form solutions for simple beam configurations.

A.5 FCG

A.5.1 Description

The FCG computer program models fatigue crack growth using linear elastic fracture mechanics methods. In order to provide a realistic model of crack growth the design transients which are input are automatically scheduled evenly over the life of the system or component.

A.5.2 Features Used

The program options enable calculation of crack tip stress intensity factors (K_I) for surface flaws and embedded flaws in a large number of geometries, under any loading condition. Crack growth results are determined for each year of operation, and summarized in tabular form at the end of the output, at 10 year intervals.

A.5.3 Program Verification

The program has been verified by performing alternate calculations and placed under Westinghouse configuration control. The calculations using this program were presented and approved by the NRC staff in connection with several applications.

APPENDIX B
FATIGUE CYCLE APPROACH VS. DESIGN TRANSIENTS

The fatigue cycle approach is acceptable based on the following:

The mean stress is more than accounted for by the relative severity of the heatup/cooldown design transients. Figure B-1 (plant A) shows the actual worst case transient distribution observed with a maximum operating system ΔT of 275°F. Figure B-2 shows the heatup/cooldown design transients distribution applied to an operating system ΔT of 275°F. Note that the relative magnitude and number of cycles considered in the design transients is considerably more severe than those observed. Furthermore, since stress is proportional to ΔT and the average ΔT in the design transients is considerably higher than the average ΔT of the observed transients, it can be concluded that the mean stress effect not considered in the fatigue cycle approach is more than accounted for by the relative severity of the design transients. Figure B-3 shows the heatup design transient distribution superimposed on the worst case distribution observed.

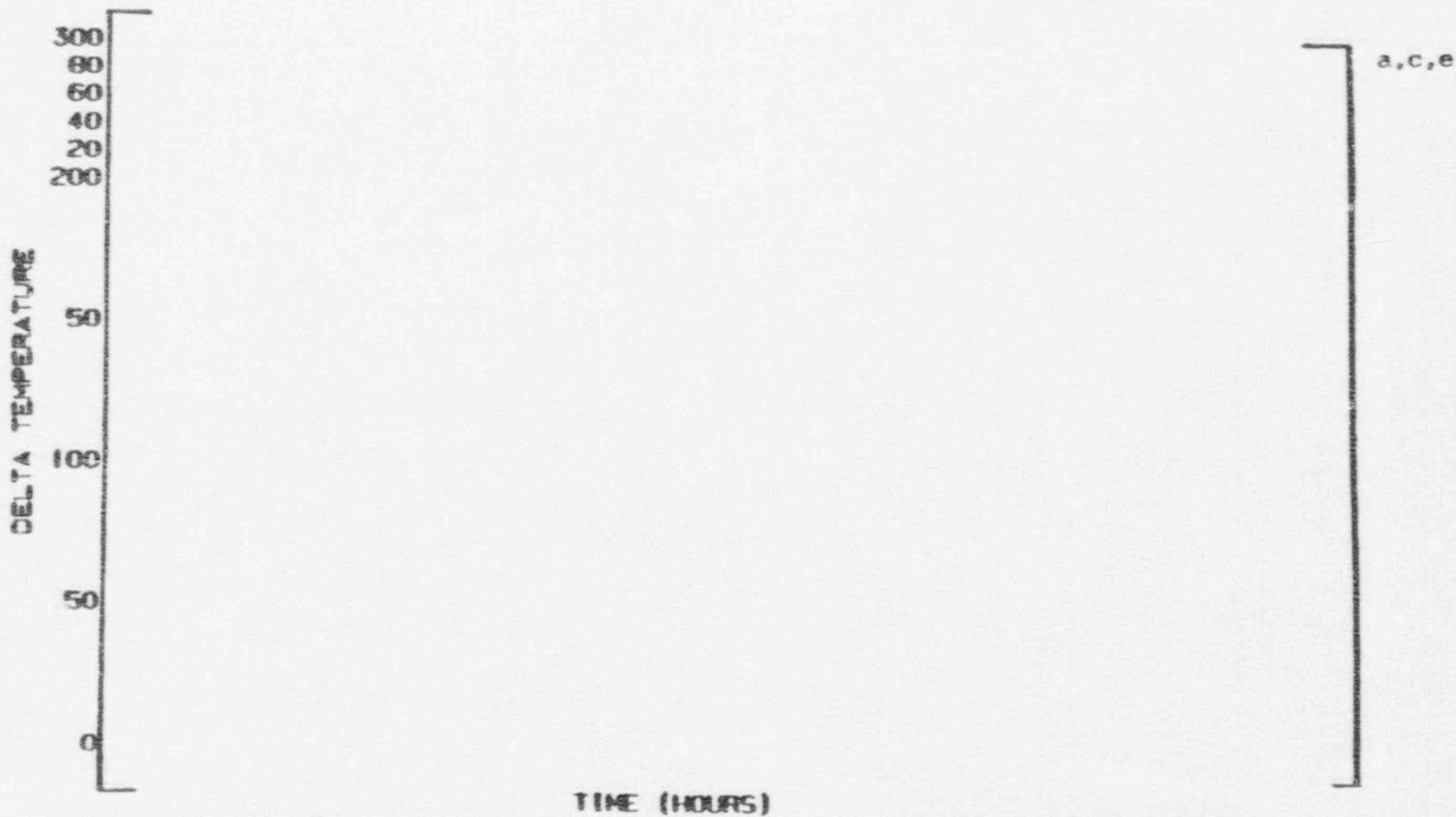


Figure B-1. []^{a,c,e} Location 1 - Observed Transients

a,c,e

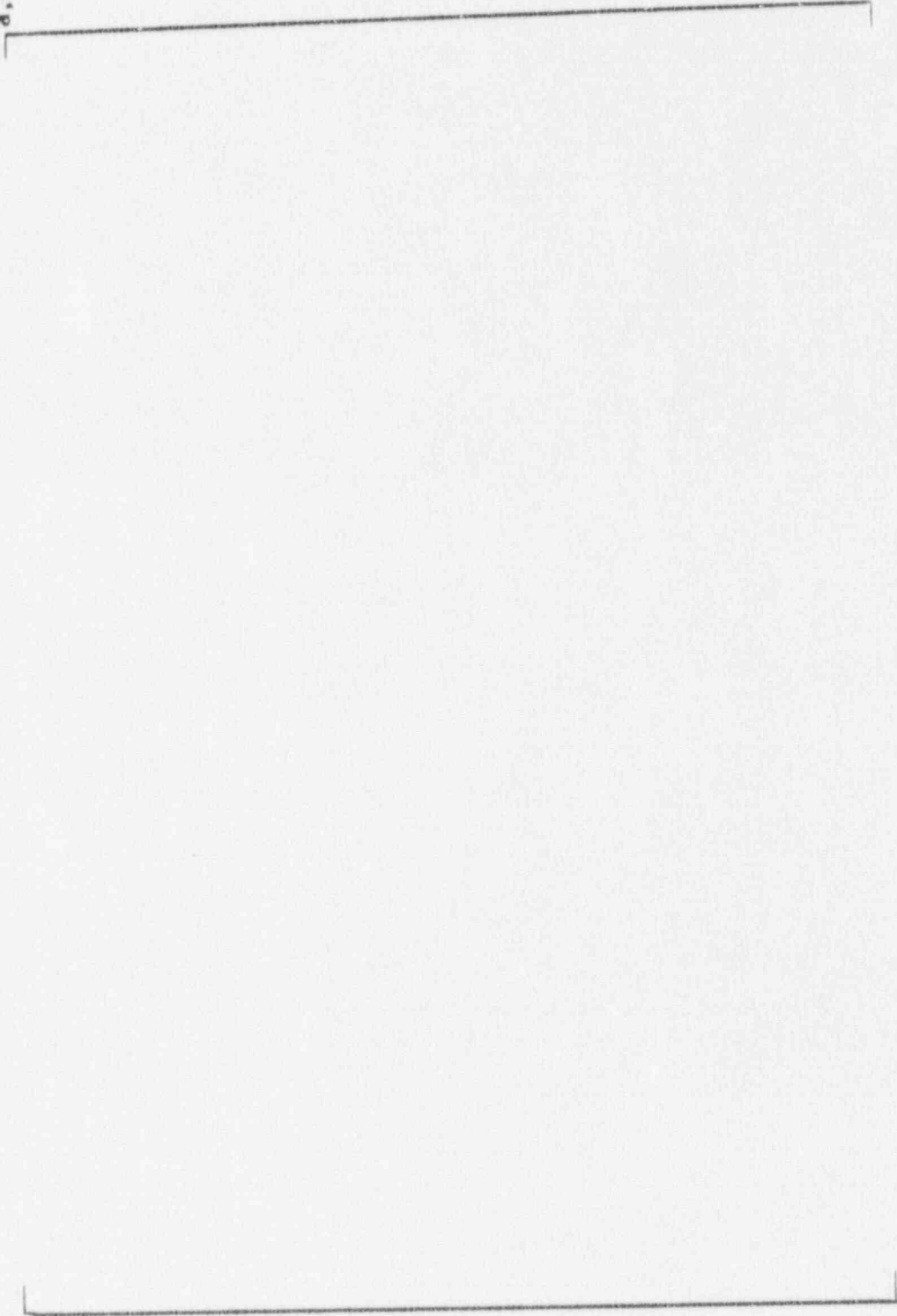
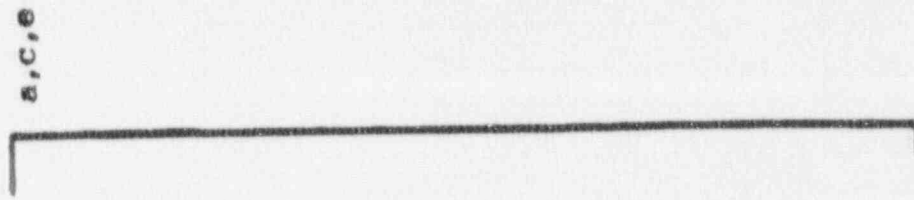
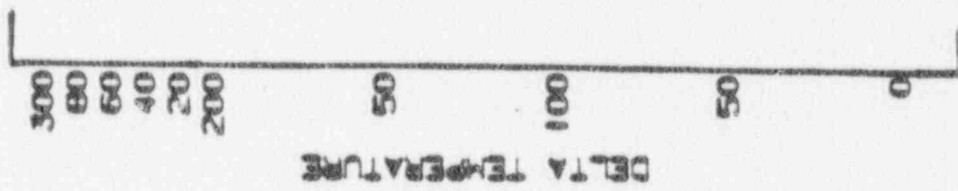


Figure B-2. Typical Heatup Design Transient Distribution Applied to One Heatup Cycle

3462s/122786 10



TIME (HOURS)

a,c,e

Figure B-3. [

34826/122788 10